Performance Analysis for IEEE 802.11 String-Topology Multi-hop Networks

July 2015

Kosuke Sanada

Graduate School of Advanced Integration Science
CHIBA UNIVERSITY

(千葉大学審査学位論文)

Performance Analysis for IEEE 802.11 String-Topology Multi-hop Networks

July 2015

Kosuke Sanada

Graduate School of Advanced Integration Science
CHIBA UNIVERSITY

This thesis is dedicated to my beloved family...

Contents

Acknowledgment **1**

Chapter 1 General Introduction **2**

1.1 General Background 2

1.2 Research Works 6

1.3 Outline of Thesis 8

Chapter 2 Analysis for IEEE 802.11 networks **14**

2.1 IEEE 802.11 DCF 15

2.2 Single-hop Networks 16

2.2.1 Saturated Throughput Analysis based on Bianchi's Markov-Chain model 16

2.2.2 Bianchi's Markov-chain model considering Non-saturated Condition 18

2.3 Multi-hop Networks 19

2.3.1 Hidden Node Problem in the String-Topology Multi-hop Networks . 19

2.3.2 Maximum Throughput Analysis for IEEE 802.11 String-Topology Multi-hop Networks using Airtime Expression 20

2.3.2.1 Airtime 21

2.3.2.2 Collision Probability 22

2.3.2.3 Flow Constraint in Multi-hop Networks 23

2.3.2.4 Link Capacity Equation 23

Chapter 3 Backoff-Stage Synchronization (BSS) in Multi-hop Networks 33

3.1 Backoff-Stage Synchronization (BSS) in IEEE 802.11 Multi-hop Networks . 34

3.1.1 Unexpected Phenomenon in IEEE 802.11 Multi-hop Networks . . . 34

3.1.2 The occurrence mechanism of BSS 35

3.1.3 Sufficient Conditions for BSS Occurrence 37

3.1.4 BSS in Chain Topology Multi-hop Network with One-Way Flow: Another Example of BSS 39

3.2 Impact on Communication 39

3.2.1 Short-Time-Range Unfairness and Long-Time-Range Fairness . . . 39

3.2.2 Network Dynamics with Request To Send / Clear To Send Handshake 41

3.3 BSS Detection 42

3.4 Conclusion 44

Chapter 4 Analytical Expressions for IEEE 802.11 Multi-hop Network with Backoff-Stage Synchronization 57

4.1 Maximum Throughput Analysis taking into account BSS 58

4.1.1 Derivation of Maximum Throughput 58

4.1.2 Frame-collision probability and transmission probability: The analytical expression of BSS in three-hop network 60

4.1.2.1 Nodes 1 and 2 61

4.1.2.2 Nodes 0 and 3 63

4.2 Simulation and Experiment Verifications 69

4.3 Conclusion 70

Chapter 5 End-to-End Delay Analysis for IEEE 802.11 String-Topology Multi-hop Networks 80

5.1 End-to-End throughput and Delay Analysis 81

5.1.1 MAC-Layer Operations of Individual Node 82
5.1.1.1 Airtime 82
5.1.1.2 Collision Probability 82
5.1.1.3 Frame-Transmission Probability and Frame-Existence Probability 83
5.1.2 Flow Constraint in Multi-hop Networks 84
5.1.3 Comparison with Maximum Throughput Analysis 85
5.1.4 End-to-End Delay 86
5.2 Simulation Verification 89
5.3 Conclusion 93

Chapter 6 Analytical Expressions of End-to-End Throughput for IEEE 802.11 Multi-hop Networks 104

6.1 Analytical expressions of end-to-end throughput for IEEE 802.11 multi-hop networks 105
6.1.1 Airtime and Throughput 106
6.1.2 Transmission Probability and Collision Probability: Markov Chain Model for Two-way Flows 107
6.1.2.1 Transmission Probability 107
6.1.2.2 Collision Probability 110
6.1.3 Flow Constraint in Multi-hop Networks 111
6.1.4 Buffer-Blocking Probability 114
6.2 Simulation Verification 117
6.2.1 One-way flow 118
6.2.2 Two-way flow 118

Chapter 7 Overall Conclusion and Future Problems 129

7.1 Overall Conclusion 129

7.2 Future Problems 131

Research Achievements **133**

Figure Contents

1.1 Outline of this thesis. 9

2.1 (α) String topology two-hop networks and (β) a time-series example of the channel access of the IEEE 802.11 DCF 26

2.2 Bianchi's Markov-chain model for BT-decrement state. 27

2.3 (α) String topology two-hop networks and (β) a timeline example of the channel access of the IEEE 802.11 DCF 28

2.4 Network topology used for analysis. 29

3.1 Maximum throughput versus number of hop in a string topology multi-hop network with two-way flows. 46

3.2 Three-hops network topology with two-way flows. 46

3.3 Timeline of transmission attempts for each node in the three-hop network. 47

3.4 Channel-access example of Nodes 0 and 3. 47

3.5 Relationship between backoff-stage number and collision probability. 48

3.6 String-topology five-hops network with two-way flows. 48

3.7 Chain-topology five-hop network with one-way flow 49

3.8 Timeline of transmission attempts for each node in the chain-topology five-hop network topology. 50

3.9 Window-fairness-index calculation for $d = 4$. 50

3.10 Window fairness index between the Nodes 0 and 3 transmissions versus the window size for fixed offered load in the three-hop network. 51
3.11 Window fairness index between the Nodes 0 and 3 versus window size for fixed h in the three-hop network. 52
3.12 Maximum throughput versus number of hop in a string topology multi-hop network with and without RTS/CTS. 53
3.13 The example of timelines of successful transmission, failed transmission and their backoff-stage number. 53
3.14 The fairness index for the BSS detection with respect to Node 0 versus the data sequence time T_s 54

4.1 Markov chain model considering two-way flows. 74
4.2 Markov-chain model for Nodes 0 and 3 with front part and rear part. . . . 75
4.3 Markov-chain model of Node 0 and 3 expressing (a) WIN state and (b) DEFEAT state. 75
4.4 Mesh access point (MAP) for experiment. 76
4.5 String-topology three-hop network for experiment. 76
4.6 Experiment environment. 77
4.7 Maximum throughput as a function of payload size. 77

5.1 Buffer-queueing model of Node i. 95
5.2 Maximum throughput versus number of hops. 95
5.3 Frame-existence probabilities of analytical (lines) and simulation (plots) results versus the offered load for fixed node numbers in nine-hop network. 96
5.4 Collision probabilities of analytical (lines) and simulation (plots) results versus offered load for fixed node numbers in nine-hop network. 96

5.5 Transmission delays of analytical results (lines) and simulation ones (plots) versus offered load for fixed node numbers in nine-hop network. 97
5.6 End-to-end delays of analytical results (lines) and simulation ones (plots) versus offered load for fixed hop numbers. 98
5.7 End-to-end delays of analytical results (lines) and simulation ones (plots) versus offered load for one-hop network. 99
5.8 End-to-end delay of nine-hop network versus offered load. 99

6.1 H-hop string-topology network with two-way flow. 121
6.2 Markov-chain model for BT-decrement and transmission state model of Node i. 121
6.3 Buffer-queueing model of Node i. 122
6.4 End-to-end throughputs of six-hop network with one-way flow versus offered load of Flow 1 for $O_2 = 0$ Mbps and $P = 200$ bytes. 122
6.5 Maximum throughputs with one-way flow versus payload size for eight hop network. 123
6.6 End-to-end throughputs of six-hop network with two-way flow as a function of offered load of Flow 1 for $O_2 = 0.8$ Mbps and $P = 200$ bytes. 124

Table Contents

3.1 System Parameters 45

4.1 Relationship between backoff stage and state of nodes 71

4.2 System Parameters 72

4.3 Specifications of WLAN node 73

5.1 System Parameters 94

6.1 System Parameters 120

Acknowledgment

I would first like to thank my research supervisor Associate Professor Hiroo Sekiya, for his guidance and encouragement throughout my study and research. I have benefited from his vast wealth of knowledge and his constructive comments during my research.

I owe a great deal of thanks to the members of my thesis committee, Professor Shingo Kuroiwa, Professor Shigeo Shioda, Professor Noritaka Osawa, Associate Professor Hiroo Sekiya and Research Associate Nobuyoshi Komuro from Chiba University, Japan for their many helpful comments and suggestions.

I also gratefully appreciate the financial support of Japan Society for the Promotion of Science (JSPS) that made it possible to complete my thesis.

I also would like to thank the members and staff who encouraged and helped me to complete my research at Sekiya-Komuro Laboratory.

Special thanks to my family, especially to my parents, for their constant encouragement, endless love and support.

Graduate School of Advanced Integration Science

Chiba University

Kosuke Sanada

Chapter 1

General Introduction

1.1 General Background

Recently, Wireless Multi-hop Networks (WMHNs) have attracted considerable attention. WMHNs consist of collection of mobile nodes. Because the nodes act as both sources and routers, WMHNs do not need central control terminals, such as Access Points (APs). Each node can send a message to its destination no matter if the node cannot communicate directly. This is because each node operates as routers and relays the message to destination. In this sense, WMHNs are economical and have good scalability. Originally, the WMHNs have been intended to use in battlefields or disaster sites. In recent years, various applications with WMHNs have been studied in various research fields. For example, WMHNs are suitable for various networks such as wireless sensor networks [1]-[2], Vehicle Ad-hoc NETworks (VANETs) in Intelligent Transport System (ITS) [3]-[6], wireless mesh networks for smart grid [7]-[8], home networks, and Wireless Local Area Networks (WLANs). The WMHNs are of great importance in many key applications for their promising features of rapid deployment and robustness. In this sense, WMHNs technology is important and fundamental for achieving ubiquitous society.

In WMHNs, however, the absence of central control terminals makes the network construction and maintenance complicated. Each node should operate autonomously and

the routing and resource management are done and all nodes coordinate to enable communications among themselves. For achieving high performances under the distributed manner, Medium Access Control (MAC) protocol is important. As the MAC layer protocol, IEEE 802.11 Distributed Coordination Function (DCF) has been used in WMHNs. The operations of autonomous distributed control are described in IEEE 802.11 DCF. IEEE 802.11 DCF initially defines MAC and PHYsical (PHY) layers specifications for WLAN. In WMHNs with IEEE 802.11 DCF, therefore, various problems such as the hidden node problem and the exposed problem occur [9]-[12]. For avoiding them, various MAC protocols for WMHNs have been proposed in recent years. The validity and effectiveness of theses protocols are often confirmed by using network simulator. However, it takes much computation cost for obtaining the statistical data for evaluations. As another approach to comprehend the network performances for WMHNs with low computation cost, there is the method by using analytical models.

The analytical models are effective for comprehending the essence of network dynamics. This is because effects of systems parameters to network and performance can be obtained explicitly from the mathematical models. Even though the quantitative accuracy decreases due to some idealizations and approximations, it is important to obtain the qualitative evaluations of the network performances as functions of system parameters. A network-simulator usage is the major method for the performance evaluations. The network simulators, however, provide network dynamics at a fixed parameter set. Therefore, it takes much computation cost when statistical data, such as throughput and collision probability and/or the system evaluations in wide-parameter region are needed for evaluations. It is possible to derive the statistical performance easily with low computation cost by using analytical expressions. In this sense, the analytical expressions of network performance are applicable to system designs. Especially, the analytical expressions are powerful tool of the system optimization.

Analyses for WMHNs have been paid attention by many researchers [9]-[28]. The operations and problems in WMHNs are often considered analytically by using some simple network topologies such as star topology, mesh topology, tree topology and string topology. For taking into account the operation in WMHNs, the string-topology network is often used. This is because it is one of the fundamental and simple multi-hop network topologies. The string-topology networks are important and often considered in VANETs [3]-[6]. The VANETs require the data frames to be relayed via multiple hops between vehicles on the spot [6]. IEEE 802.11p specifies the PHY- and MAC-layer features such that IEEE 802.11 could work in a vehicular environment. Because multi-hop vehicles are in line on the road, the vehicle-to-vehicle communications are often modeled by communications on string-topology multi-hop networks [3]. Though the string-topology network is a simple network topology, it is not easy to comprehend a network behavior. In this sense, it can be stated that analytical expressions of string-topology multi-hop network performances are useful and valuable.

For evaluating network performances, the end-to-end throughput is an important factor. The first purpose of the analyses in WMHNs was derivation of the end-to-end maximum throughput. For obtaining that, the expressions of two important operations in MAC layer, which are carrier sensing and the frame collisions due to hidden node problems, are key technologies. This is because the effect induced by two MAC-layer operations with respect to each node is different. It was proposed that the MAC-layer operations with respect to each node are expressed by using 'airtime' expressions [9]-[16]. The analytical procedure using airtime expressions is effective for consideration of the complex interferences among network nodes. Additionally, by associating the MAC-layer properties of network nodes with a network flow, the maximum end-to-end throughput can be obtained analytically.

In IEEE 802.11 multi-hop networks, each node decrements own BT individually. There-

fore, it is assumed in conventional multi-hop network analyses [9]-[17] that each node obtains transmission opportunity fairly and randomly. Analytical expression of the maximum throughput for IEEE 802.11 multi-hop network with two-way flows has been obtained in [17]. Following the conventional analyses, it is also assumed that each node obtains the transmission opportunities fairly and randomly. In [17], the analytical results are good agreement with simulation ones quantitatively. However, there is a difference between analytical result and simulation one only when hop number is three. It is supposed that special phenomenon, which is unexpected among the network designers, occurs in string-topology three-hop network. In addition, it is thought that this phenomenon collapses the assumptions in [9]-[16]. This consideration is obtained by comparing analytical results and simulation ones. It is necessary to clarify the impact of the unexpected phenomenon on WMHNs communication system.

For evaluating network in non-saturated state, the end-to-end delay is also an important evaluation factor. Delay analyses of wireless multi-hop network also have been carried out actively [21]-[28]. The end-to-end delay analyses until now have been carried out for evaluating MAC protocols. Therefore, it is assumed that the collision probabilities of all network nodes are identical. Namely, the heterogeneous network-node operations along a network flow have never been considered in multi-hop networks. Actually, network nodes have different collision in the network. Therefore, the conventional delay analyses are not suitable to comprehend the network performance. For obtaining the end-to-end delay in multi-hop network with high accuracy, it is necessary to consider individual states of network links, which are frame-transmission, carrier-sensing and channel-idle durations. It is considered that the individual node behavior can be expressed by using the individual states of network links.

1.2 Research Works

This thesis presents performance analysis for IEEE 802.11 string-topology multi-hop networks.

First, the occurrence of a special phenomenon in WMHNs is pointed out. This mutuality is named as "backoff-stage synchronization". The mechanisms and the sufficient conditions for backoff-stage synchronizaion occurrence are obtained from detail investigation. By using windows fairness index, the characteristic of this phenomenon, which is coexistence of fair transmission in long time range and unfair transmission in short time range, is extracted. The impact of this phenomenon on communication in IEEE 802.11 multi-hop network is discussed. By considering the characteristics, the detection method of this phenomenon is proposed. Under the BSS occurrence, each node can not work following design policy of the protocol even if each node operates following the description of the protocol. From the viewpoint of network science as well as communication, the BSS is interesting phenomenon.

Second, analytical expressions for IEEE 802.11 multi-hop network with backoff-stage synchronization are presented. For taking the features of the backoff-stage synchronization into account the analytical expressions, the modified Bianchi's Markov-chain models, which express the operation with respect to each network node, are proposed. Obtained analytical expressions are verified by the comparison with simulation and experimental results. By comparing the analytical result without the coupling effect, the occurrence of the coupling effect is shown analytically.

Third, analytical expression for end-to-end delay for IEEE 802.11 string-topology multi-hop networks is presented. For obtaining those expressions with high accuracy, frame-collision and carrier-sensing probabilities with respect to each node under the non-saturated condition are obtained. A new parameter, which is called as frame-existence probabil-

ity, is defined for expressing the operation in non-saturated condition. These expressions are associated as a network flow. The end-to-end delay of a string-topology multi-hop network can be derived as the sum of the transmission delays in the network flow. The analytical expressions are verified by comparing with simulation results.

Fourth, analytical expressions for end-to-end throughput of IEEE 802.11 string-topology multi-hop networks are presented. These analytical expressions are the enhanced version of the third proposed analytical model. The analytical expressions give throughput at any hop number, any frame length, and any offered load. For achieving that, the proposed analysis procedure includes two proposals for two problems, which are (i) analytical expressions in WMHNs until now are not valid for long frame communication such as video streaming [15], and (ii) there is no analytical expression, which is valid for asymmetric offered load in two-way flow situation. This analysis presents two proposals, which are: (i) a relationship between the backoff timer and frame length can be expressed by merging the Bianchi's Markov-chain model [29] and airtime expression [9]-[16], (ii) the Bianchi's Markov-chain models are modified for expressing the transmission process of two-way flows with asymmetric offered load individually. Obtained analytical expressions have been verified by the comparison with simulation results. Because it is possible to obtain the throughput with both symmetric and asymmetric two-way traffic flows, it is expected that the analytical expressions may be applied to maximum capacity derivation of VoIP, the TCP flow analysis, and more complicated network topology analyses.

These results enhance understanding for the essence of WMHNs. It is expected that the results in this thesis contribute to various applications, such as system optimization, network control and protocol design.

1.3 Outline of Thesis

Figure 1.1 shows an outline of this thesis and relationship among chapters and sections.

Chapter 2 introduces analysis for IEEE 802.11 networks. The operation about IEEE 802.11 DCF is explained. As an analysis model for single-hop network, Bianchi's Markov-chain model is introduced. In addition, Hidden node problem in the multi-hop network is explained. As analytical procedure for multi-hop networks, airtime expression is introduced.

Chapter 3 introduces the first work.

Chapter 4 introduces the second work.

Chapter 5 introduces the third work.

Chapter 6 introduces the fourth work.

Chapter 7 makes overall conclusions and gives future problems.

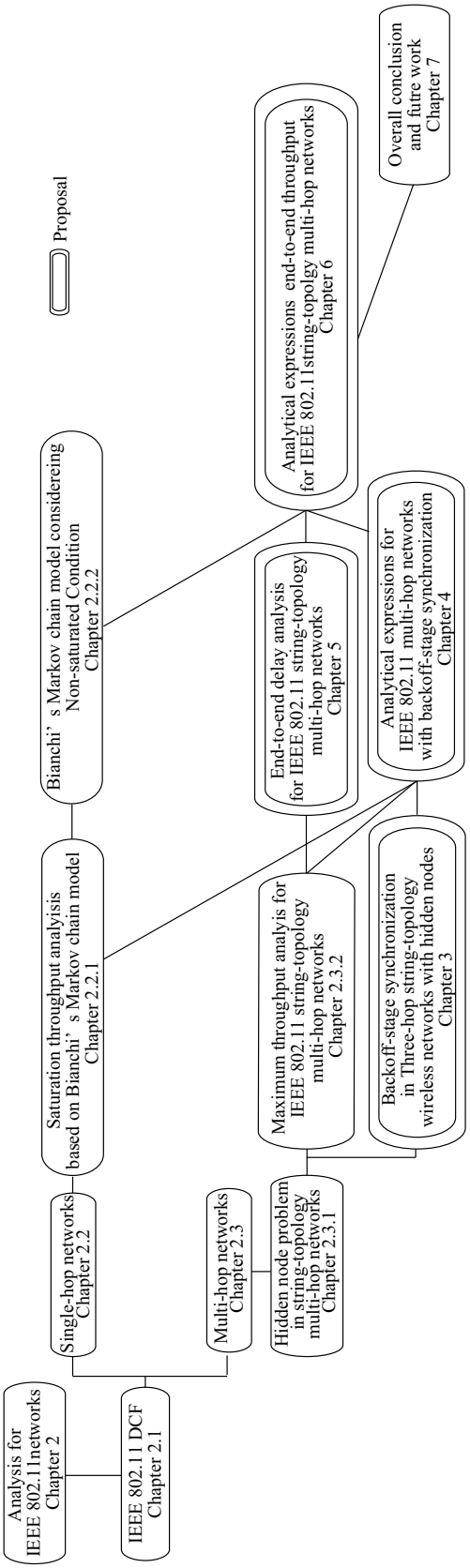

Figure 1.1: Outline of this thesis.

Reference

[1] I.F. Akyildiz, T. Melodia, and K. R. Chowdhury, "A survey on wireless multimedia sensor networks" *Computer networks*, vol. 51, no. 4 pp. 921-960, Mar. 2007

[2] Y. Wang, M.C. Vuran and S. Goddard, "Cross-layer analysis of the end-to-end delay distribution in wireless sensor networks" *IEEE/ACM Trans. Netw.* , vol. 20, no. 1 pp. 305-318, Feb. 2012

[3] B. Bellalta, E. Belyaev, M. Jonsson, and A. Vinel, "Performance evaluation of IEEE 802.11p-enabled vehicular video surveillance system",*IEEE Communications Letters.* vol. 18, no. 4, pp. 708-711, Apr. 2014.

[4] Lianghua Wu, Yuzhuo Fu, and Liang DongLianghua, "End-to-end throughput optimization in multi-hop wireless ad hoc networks", *the 15th Asia-Pacific Conference on Communication (APCC 2009)-010*, Shanghai, China, pp. 40-43, Oct. 2009.

[5] Wararkar, P, Dorle, S.S. "Vehicular adhoc networks handovers with metaheuristic algorithms", Electronic Systems, Signal Processing and Computing Technologies (ICESC), *2014 International Conference on*, pp. 160-165, Jan. 2014.

[6] G. Karagiannis, O. Altintas, E. Ekici, G. Hejenk, B. Jarupan, K. Line and T. Weil, "Vehicular networking: a survey and tutorial on requirements, architectures, challenges, standards and solutions", *IEEE trans.*, vol. 13, no. 4, pp. 584-615, Jul. 2011.

[7] L. Lei, J. Zhou, X. Chen and S. Cai, "Modelling and analysing medium access delay for differentiated services in IEEE 802.11s wireless mesh networks", *IET, Networks*, vol. 1, no. 2, pp. 91-99, June 2012.

[8] Yi. Xu and W. Wang, "Wireless mesh network in smart grid: modeling and analysis for time critical communications", IEEE trans. , vol. 12, no. 7, pp. 3360-3371, Jul. 2013.

[9] P. C. Ng and S. C. Liew, "Throughput analysis of IEEE 802.11 multi-hop ad hoc networks," *IEEE/ACM Trans. Networking*, vol. 15, no. 2, pp. 309-322, Apr. 2007.

[10] Zhao H, Garcia-Palacios E, Wang S, Wei J, Ma D. "Evaluating the impact of network density, hidden nodes and capture effect for throughput guarantee in multi-hop wireless networks". *Ad Hoc Networks*, vol. 11, no. 1, pp. 54-69. Jan. 2013.

[11] Y. Gao, D. Chui, and J. C. S. Lui, "The fundamental role of hop distance in IEEE 802.11 multi-hop ad-hoc networks," *IEEE International Conference on Network Protocol*, Boston, Massachusetts, USA, Nov. 2005.

[12] Y. Gao, D. Chui, and J. C. S. Lui, "Determining the end-to-end throughput capacity in multi-hop networks: methodology applications," *ACM Special Interest Group on Performance Evaluation 2006*, pp. 39–50, Jun. 2006.

[13] T. D. Senthilkumar, A. Krishnan, P. Kumar. "New approach for throughput analysis of IEEE 802.11 in adhoc networks". *IEEE International Conference on Control Communication and Automation*, Kanpur, India, pp. 148-153, Dec. 2008.

[14] H. Zhao, S. Wang, Y. Xi, Wei J, "Modeling intra-flow contention problem in wireless multi-hop networks", *IEEE Communications Letters* , vol. 14, no. 1, pp. 18-20, Jan. 2010.

[15] H. Sekiya, Y. Tsuchiya, N. Komuro, and S. Sakata, "Maximum throughput for long-frame communication in one-way string wireless multi-hop networks ," Wireless personal communications, vol. 60, no. 1, pp. 29-41, Mar. 2011.

[16] M. Inaba, Y. Tsuchiya, H. Sekiya, S. Sakata, and K. Yagyu "Analysis and expression of maximum throughput analysis in wireless multi-hop networks for VoIP Application," *IEICE Trans. Communications.*, vol. E92-B, no. 11, pp. 3422–3431, Nov. 2009.

[17] Y. Tsuchiya, M. Inaba, M. Matsumoto, H. Sekiya, S. Sakata and K. Yagyu, "Analysis of Maximum UDP Throughput of Short-hop String Networks for VoIP Applications," *Proc. WPMC*, Sept. 2009.

[18] T. Vanhatupa, M. Hannikainen, and T.D. Hamalainen "Multihop IEEE 802.11b WLAN performance for VoIP," *IEEE PIMRC 2005.*, vol. 3, pp. 1925–1930, Sept. 2005.

[19] G. R. Gupta and N. B. Shroff, "Delay analysis for multi-hop wireless networks," *IEEE INFOCOM*, Rio de Janeiro, Brazil, pp. 412-421, Apr. 2009.

[20] Y. Chen, Y. Tang, and I Darwazeh. "A Cross-layer analytical model of end-to-end delay performance for wireless multi-hop environments. *IEEE Global Telecommunication Conference 2010*, Miami, Florida, USA, pp. 1-6, Dec. 2010.

[21] X. Min and H. Martin, "Towards an end-to-end delay analysis of wireless multihop networks," *Ad Hoc Networks*, vol. 7, no. 5, pp. 849-861, Jul. 2009.

[22] A. Abdullah, F. Gebali, and L.Cai, "Modeling the throughput and delay in wireless multihop ad-hoc networks," *IEEE Global Telecommunication Conference*, Honolulu, Hawaii, USA, pp. 1-6, Nov. 2009.

[23] Khalaf, R. and Rubin, I. "Throughput and delay analysis single hop and multi hop IEEE 802.11 networks" *The Third International Conference on Broadband Communications* , Networks, and Systems, San Jose, California, USA, pp. 1-9, Oct. 2006.

[24] N. Bisnik and A. Abouzeid, "Queuing network models for delay analysis of multihop wireless ad hoc networks," *Ad Hoc Networking* , vol. 7, no.1, pp. 79-97, Jan. 2009.

[25] R. Khalaf, I. Rubin, J. Hsu, "Throughput and delay analysis of multihop IEEE 802.11 networks with capture", *IEEE International Conference on Communications*, pp. 3787-3792, Jun. 2007.

[26] H. Li, Y. Cheng, C. Zhou, and W. Zhuang. "Minimizing end-to-end delay: a novel routing metric for multi-radio wireless mesh networks" *IEEE International Conference on Communications* , Glasgow, Scotland, pp. 46-54, Apr. 2009.

[27] W. Jiao, M. Sheng, and K. S. Lui and Y. Shi "End-to-end delay distribution analysis for stochastic admission control in multi-hop wireless networks," *IEEE Trans. Wireless Communications*, vol. 13, no. 3, pp. 1308-1320, Mar. 2014.

[28] Ghadimi. E, Khonsari. A, Diyanat. A, Frarmani. M, Yazdani. N, "An analytical model of delay in multi-hop wireless ad hoc networks", *Wireless Networks* , vol. 17, no. 7, pp. 1679-1697, Oct. 2011.

[29] G. Bianchi,"Performance analysis of the IEEE 802.11 distributed coordination function," *IEEE J. Sel. Areas Commun*, vol. 18, no. 3, pp. 535-547, Mar. 2000.

Chapter 2

Analysis for IEEE 802.11 networks

●● ABSTRACT ●●

This chapter explains the operation of the IEEE 802.11 DCF and hidden node problem in multi-hop network. The operation about IEEE 802.11 DCF is explained. As an analysis model for single-hop network, Bianchi's Markov-chain model is introduced. By using Bianchi's Markov-chain model, the behavior of BT decrement for network node can be expressed explicitly. In addition, Hidden node problem in the multi-hop network is explained. As analytical procedure for multi-hop networks, airtime expression is introduced. Because the channel-access situation can be expressed by using network-node airtimes, frame-collision probabilities induced by hidden nodes can be expressed with simple form. The individual network-node operations are associated by "flow constraint" conditions, which express the Network-layer property.

2.1 IEEE 802.11 DCF

Figure 2.1 shows (α) two-hop string topology multi-hop networks and (β) a timeline example of the channel access of the IEEE 802.11 DCF [1]. In this network, Nodes 0 and 1 transmits a DATA frame to Nodes 1 and 2, respectively. In the IEEE 802.11 DCF, a transmitter senses the channel state before starting a frame-transmission process (a) in Fig 2.1. If transmitter senses no frame transmission during the Distributed InterFrame Space (DIFS), the transmitter starts the frame-transmission process. When the transmitter sense frame transmission of the nodes, which are in the carrier-sensing range of the transmitter, the transmitter defers the transmission.

As the first step of transmission process, each node decrements the BT before the frame transmission. The initial value of BT is randomly chosen between 0 and minimum value of Contention Window (CW) CW_{min} in (b) in Fig 2.1. Only when transmitter sense that the channel is idle, transmitter decreases the BT. If the transmitter senses the frame transmission of neighbor nodes, transmitter stops the BT decrement. The frame transmission is started when the BT is equal to 0 (c). When both transmitter and the neighbor nodes of the receiver transmit a frame simultaneously, the receiver cannot receive the frame because of the frame collision (e).

If the frame reception is succeeded, the receiver sends the ACKnowledgement (ACK) frame to the transmitter after waiting for the duration of the Short Inter Frame Space (SIFS). By receiving the ACK frame, the transmitter recognizes the transmission success (d). If the transmitter cannot receive the ACK frame from the receiver, the transmitter recognizes that the transmission is failed. In case of the transmission failure, the transmitter doubles the value of CW size, namely the value of BT for retransmission is randomly chosen from between 0 and $2CW_{min} - 1$ (f). The transmitter, if which CW is equal to maximum value of CW, keeps the value even if the transmission is failed. Namely, the

value of CW for s-th retransmission is expressed as

$$w_s = \begin{cases} 2^s(CW_{min}+1)-1 & 0 \le s \le L'-1 \\ 2^{L'}(CW_{min}+1)-1 = CW_{max} & L' \le s \le L \end{cases}, \tag{2.1}$$

where CW_{max} is the value of maximum CW, CW_{min} is the value of maximum CW, L is the number of retransmission limit and $L' = \log_2 \frac{CW_{max}+1}{CW_{min}+1}$. When the number of retransmission-attempt reaches L, the frame is dropped. After the frame-transmission success or the frame drop, the value of CW is reset to CW_{min}.

2.2 Single-hop Networks

2.2.1 Saturated Throughput Analysis based on Bianchi's Markov-Chain model

The case that a fixed number N of contending stations whose destination is a AP is considered. The analysis in this section is based on the following assumptions, which follow the assumptions in [2].

1. Each station has a single radio transceiver and all the network nodes use the same radio channel.

2. There are no hidden terminals. Namely, all the nodes in the network can sense the transmission of the other nodes.

3. Channel conditions of all the links are ideal. Namely, transmission failures occur only due to frame collisions.

4. Each station always has at least one frame in the transmission buffer.

Figure 2.2 shows Bianchi's Markov-chain model for BT-decrement state. In Fig. 2.2, frame drop because of re-transmission limit is considered. In Fig. 2.2, the transition

probabilities among the states are

$$\begin{aligned} &P\{[s,t-1]|[s,t]\} = 1, \\ &P\{[s,t]|[s-1,0]\} = \gamma/(w_s+1), \\ &P\{[0,t]|[s,0]\} = (1-\gamma)/(w_0+1), \\ &P\{[0,t]|[L,0]\} = 1/(w_0+1), \end{aligned} \tag{2.2}$$

where γ is collision probability of each station. $b[s,t]$ is defined as the stationary distribution of the Markov-chain model. The sum of the stationary distributions is equal to one, namely

$$\sum_{s=0}^{L}\sum_{t=0}^{W_s} b[s,t] = b[0,0]\sum_{s=0}^{L}\gamma^s\frac{w_s+2}{2} = 1, \tag{2.3}$$

from which

$$b[0,0] = \frac{1}{\sum_{s=0}^{L}\gamma^s\left(\frac{w_s+2}{2}\right)}. \tag{2.4}$$

Transmission probability in saturated condition is obtained as

$$\tau' = \sum_{s=0}^{L} b[s,0] = \frac{\sum_{s=0}^{L}\gamma^s}{\sum_{s=0}^{L}\frac{\gamma^s(w_s+2)}{2}}. \tag{2.5}$$

From the assumption 2, it is needed to consider the collisions among contending stations. This type of collisions occurs only when the BTs of multiple stations in the network are zero simultaneously. From the explanation of [2]-[11], the collision probability is obtained as

$$\gamma = 1-(1-\tau')^{N-1}. \tag{2.6}$$

From (2.5) and (2.6), there are two algebraic equations and two unknown values. Therefore, τ and γ can be fixed by using numerical method.

The maximum throughput of the network is obtained as

$$E = \frac{P_s P_{tr} P}{(1 - P_{tr})\sigma + P_s P_{tr} T + P_{tr}(1 - P_s) T_c}, \tag{2.7}$$

where $T_c = DIFS + FRAME$, P_{tr} is the probability that at lease one station transmits a DATA frame and P_s is the probability that a station successes the DATA transmission. From [2], the expressions of P_{tr} and P_s can be obtained as

$$P_{tr} = 1 - (1 - \tau')^N \tag{2.8}$$

and

$$P_s = \frac{N\tau(1 - \tau')^{N-1}}{P_{tr}}, \tag{2.9}$$

respectively.

2.2.2 Bianchi's Markov-chain model considering Non-saturated Condition

There are many analytical method for extending the Bianchi‘s model to non-saturated condition. In [4], In this subsection, the simplest one proposed in [8] is introduced.

τ is defined only in saturated condition. For expressing both in non-saturated and saturated condition, q is defined as the probability of a nonempty buffer. q is depends on network offered load. From (2.5), the transmission probability in both conditions is expressed as

$$\tau = q\tau' = \frac{q \sum_{s=0}^{L} \gamma^s}{\sum_{s=0}^{L} \frac{\gamma^s (w_s + 2)}{2}}. \tag{2.10}$$

By obtaining the expression of q, from (2.7), network throughput for any offered load can be obtained. Let θ is the mean service time (in slots) of a frame on the saturated

condition. Then, q is given by

$$q = P(\xi < \Theta) = \lambda\Theta, \tag{2.11}$$

where ξ is frame arrival interval and λ is frame-arrival rate. Obviously, λ is depends on network offered load. Because the average slot number of BT-decrement for one-frame transmission success is expressed as (2.23), the mean service time is expressed as

$$\Theta = \theta \times \sum_{i=0}^{L} \frac{w_s + 2}{2} \gamma^s, \tag{2.12}$$

where Ω is the mean time (in slots) that elapses for one decrement of the BT. Note that the one decrement of backoff timer contains channel idle slot and busy one. Therefore, we have

$$\theta = (1 - Ptr)\sigma + PtrPsT + Ptr(1 - Ps)Tc. \tag{2.13}$$

θ is expressed as a function of τ because both Ptr and Ps are a function of τ. From (2.6), (2.7), (2.10), (2.11), (2.12) and (2.13), the network throughput for given network offered load is obtained.

In the analytical procedure based on Bianchi model, however, it is assumed that collision probabilities of all the stations are identical. Therefore, the heterogeneous network-node operations along a network flow can not be considered.

2.3 Multi-hop Networks

2.3.1 Hidden Node Problem in the String-Topology Multi-hop Networks

Figure 2.3 shows (α) four-hop string topology multi-hop networks and (β) a timeline example of the channel access. In this network, Nodes 1 and 2 sense the transmission

of Node 0. However, Node 3 can not sense the transmission of Node 0 and vice versa. Therefore, there is a possibility that Nodes 0 and 3 transmit simultaneously. This relationship between Nodes 0 and 3 is called as "hidden node". In this case, Node 1 can not receive the DATA from Node 0 because of "hidden node collision". The hidden node problem provides high packet drop rates and throughput degradations [13]-[20]. Network nodes have different properties of hidden node collision because each node operates individually. Therefore, the consideration of hidden node problems let the multi-hop network throughput analysis be difficult. The description of hidden node collisions is a important ant key technique for wireless multi-hop networks.

2.3.2 Maximum Throughput Analysis for IEEE 802.11 String-Topology Multi-hop Networks using Airtime Expression

Figure 2.4 shows H-hop string-topology multi-hop network. The analysis in this section is based on the following assumptions [13]-[20].

1. Each node has a single radio transceiver and all the network nodes use the same radio channel.

2. Only the source node (Node 0) generates fixed sized UDP data frames following Poisson distribution. The destination of the frames is Node H.

3. Channel conditions of all the links are ideal. Namely, transmission failures occur only due to frame collisions.

4. Frame collisions between DATA and ACK frames and those among the ACK-frames transmissions can be ignored because ACK-frame length is shorter than DATA-frame length.

5. Node i can transmit DATA and ACK frame only to Nodes $i \pm 1$. Additionally, Nodes $i \pm 1$ and $i \pm 2$ can sense Node-i transmissions. Namely, Nodes i and $i+3$ are in the hidden node relationships [22].

2.3.2.1 Airtime

The 'airtime ' is time shares of the node states with respect to each node. The transmission airtime is the time share of frame transmissions, which includes both the successful- and the failure-transmission times. The transmission airtime of Node i is expressed by

$$X_i = \lim_{Time \to \infty} \frac{S_i}{Time}, \tag{2.14}$$

where S_i is the sum of the durations of the DATA frame transmission, ACK frame transmission, DIFS and SIFS in $Time$. S_i includes both the successful- and the failure-transmission durations. Therefore, X_i includes both the successful- and the failure-transmission times. By using the transmission airtime, MAC-layer properties can be considered in average time field.

The carrier-sensing airtime consists of the carrier-sensing durations. Therefore, the carrier-sensing airtime is regarded as the sum of frame-transmission durations in all the nodes in the carrier-sensing range. For expressing the carrier-sensing airtime, simultaneous frame-transmissions among carrier-sensing range nodes should be considered. There is a possibility that both Nodes i and $i+3$ can transmit frames because these two nodes are in the hidden node relationship. Both Nodes i and $i+3$ never transmit frames when common carrier-sensing range nodes of Nodes i and $i+3$ transmit a frame. Because the common carrier-sensing range nodes of Nodes i and $i+3$ are Nodes $i+1$ and $i+2$, the carrier-sensing airtime of Node i is

$$Y_i = \sum_{\substack{j=i-2 \\ j \neq i}}^{i+2} X_j - \sum_{j=i-2}^{i-1} \left(\frac{X_j X_{j+3}}{1 - X_{j+1} - X_{j+2}} \right) - \frac{X_{i-2} X_{i+2}}{1 - X_i}. \tag{2.15}$$

When a node is in neither transmission state nor carrier-sensing states, the channel related with the node is idle. Namely, the channel-idle airtime is expressed as

$$\begin{aligned} Z_i &= 1 - X_i - Y_i \\ &= 1 - X_i - \sum_{\substack{j=i-2 \\ j \neq i}}^{i+2} X_j + \sum_{j=i-2}^{i-1} \left(\frac{X_j X_{j+3}}{1 - X_{j+1} - X_{j+2}} \right) + \frac{X_{i-2} X_{i+2}}{1 - X_i}. \end{aligned} \tag{2.16}$$

By using transmission airtime of Node i X_i and collision probability of Node i γ_i, the throughput of Node i is expressed as

$$E_i = X_i(1 - \gamma_i)\frac{P}{T}, \tag{2.17}$$

where $T = DIFS + DATA + SIFS + ACK$, in which $DATA$ is the transmission time of the DATA frame, $DIFS$ is the duration of the DIFS, $SIFS$ is the duration of the SIFS, ACK is the transmission time of the ACK frame, and P is the payload size of DATA frame.

2.3.2.2 Collision Probability

By using airtime, the hidden node collision probability is expressed. A hidden node collision occurs when Node i starts to transmit a frame during the Node $i+3$ transmitting a DATA-frame. The collision probability of this type hidden node collision is expressed as

$$\gamma_{H_i}^{(1)} = \frac{aX_{i+3}}{1 - X_{i+1} - X_{i+2}}, \tag{2.18}$$

where $a = DATA/(DIFS + DATA + SIFS + ACK)$.

Additionally, a hidden node collision also occurs when the Node $i+3$ starts to transmit a frame during the Node-i transmitting a DATA frame. The collision probability that Node $i + 3$ starts to transmit a frame during the Node i transmits a DATA frame is

expressed as

$$\gamma_{H_i}^{(2)} = \frac{aX_i}{1 - X_{i+1} - X_{i+2}}. \tag{2.19}$$

Because the two types of hidden node collisions are disjoint events, the hidden node-collision probability of Node i is

$$\gamma_{H_i} = \gamma_{H_i}^{(1)} + \gamma_{H_i}^{(2)} = \frac{a(X_{i+3} + X_i)}{1 - X_{i+1} - X_{i+2}}. \tag{2.20}$$

2.3.2.3 Flow Constraint in Multi-hop Networks

The transmission airtimes of network nodes are fixed by taking into account Network-layer properties. Because each airtime depends on the states of neighbor nodes, transmission airtimes of network nodes are associated with Network-layer properties.

When the retransmission number reaches the retransmission limit L, the frame is dropped following the DCF policy. Therefore, the throughput of each node should satisfy

$$E_i = E_{i-1}. \tag{2.21}$$

The relationship in (2.21), which is called as the flow-constraint condition, expresses the network-layer property.

2.3.2.4 Link Capacity Equation

There are $H - 1$ equations with respect to H transmission airtimes from (2.21). It is necessary to obtain one more equation about transmission airtime for fixing the equations. We obtain the equation by considering which node limits the network capacity in three-hop network. When Node m is the link which limits the network capacity, from [18], Node m satisfies

$$X_m = Z_m G_m \frac{T}{\sigma}. \tag{2.22}$$

Equation (2.22) is called as "link capacity equation" [18]. Node-i transmission probability in channel idle state is expressed as

$$\begin{aligned} G_i &= \frac{R_i}{U_i} \\ &= \frac{1+\gamma_i+\gamma_i^2+\cdots+\gamma_i^L}{\frac{w_0+1+(w_1+1)\gamma_i+(w_2+1)\gamma_i^2+\cdots+(w_L+1)\gamma_i^L}{2}} \\ &= \frac{\sum_{s=0}^{L}\gamma_i^s}{\sum_{i=0}^{L}\frac{w_s+1}{2}\gamma_i^s}, \end{aligned} \tag{2.23}$$

where R_i is the average number of transmission attempts for Node i, U_i is the average slot number of BT-decrement for one-frame transmission success for Node i. G_i is defined based on the assumption that the network is in saturated condition [21]. From the expressions of (2.5) and (2.23), G_i is the same expression as τ'.

From (2.17), (2.20), (2.21) and (2.22), we have $2H$ algebraic equations which are

$$
\begin{cases}
X_m = \Bigg[1 - X_m - \sum\limits_{\substack{j=m-2 \\ j\neq m}}^{m+2} X_j \\
\qquad\qquad + \sum\limits_{j=m-2}^{i-1} \left(\dfrac{X_j X_{j+3}}{1 - X_{j+1} - X_{j+2}} \right) + \dfrac{X_{m-2} X_{m+2}}{1 - X_m} \Bigg] \times \dfrac{\sum\limits_{s=0}^{L} \gamma_i^s}{\sum\limits_{i=0}^{L} \dfrac{w_s + 1}{2} \gamma_i^s} \times \dfrac{T}{\sigma}, \\
X_0(1 - \gamma_0) = X_1(1 - \gamma_{(1,2)}), \\
X_1(1 - \gamma_1) = X_2(1 - \gamma_2), \\
\vdots \\
X_{H-2}(1 - \gamma_{H-2}) = x_{H-1}(1 - \gamma_{H-1}), \\
\gamma_0 = \dfrac{a(X_0 + X_3)}{1 - X_1 - X_2}, \\
\gamma_1 = \dfrac{a(X_1 + X_4)}{1 - X_2 - X_3}, \\
\vdots \\
\gamma_{H-4} = \dfrac{a(X_{H-4} + X_{H-1})}{1 - X_{H-3} - X_{H-2}}, \\
\gamma_{H-3} = \gamma_{H-2} = \gamma_{H-1} = 0
\end{cases}
\tag{2.24}
$$

When we consider $m = 0, 1, 2, \cdots, H-2, H-1$ in (2.24), we obtain H maximum network throughputs. The minimum value of them should be the maximum throughput in the network.

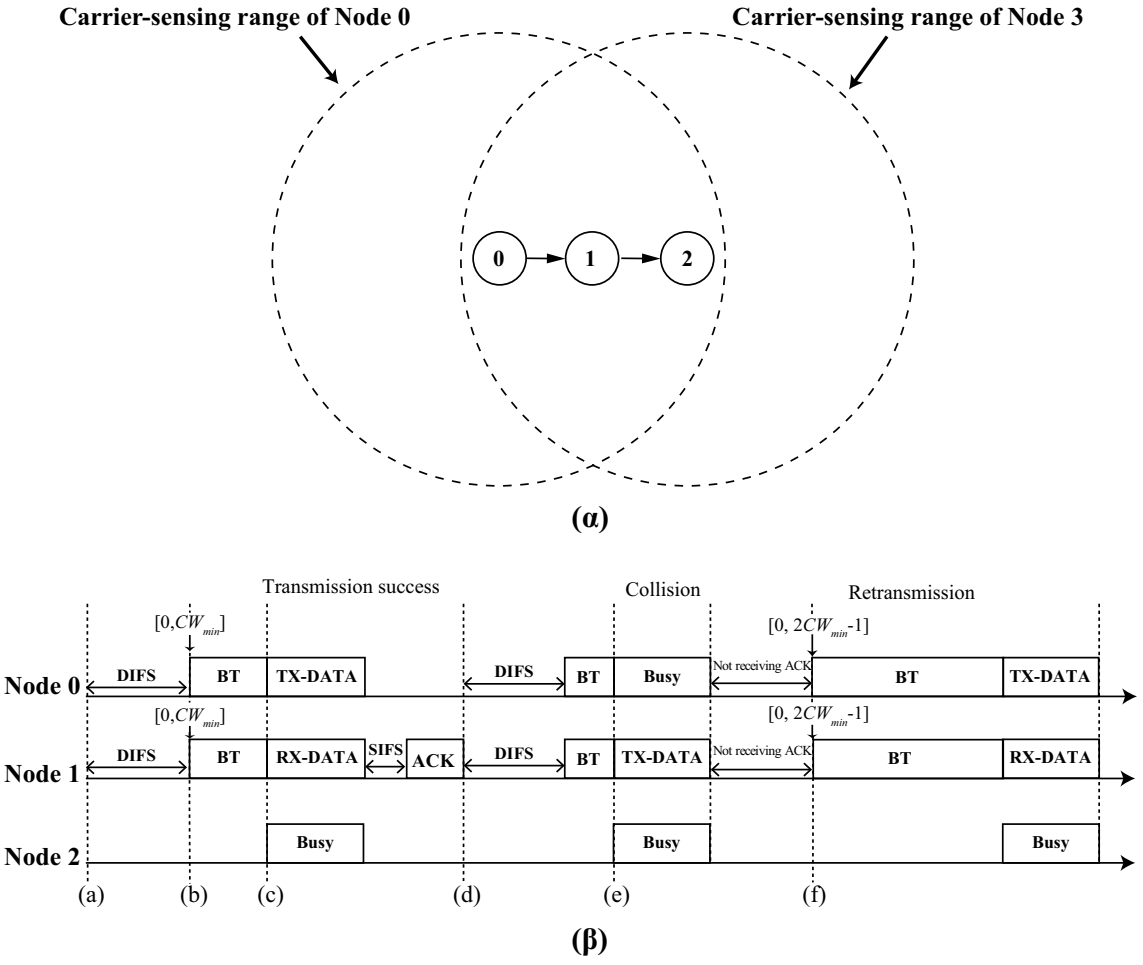

Figure 2.1: (α) String topology two-hop networks and (β) a time-series example of the channel access of the IEEE 802.11 DCF

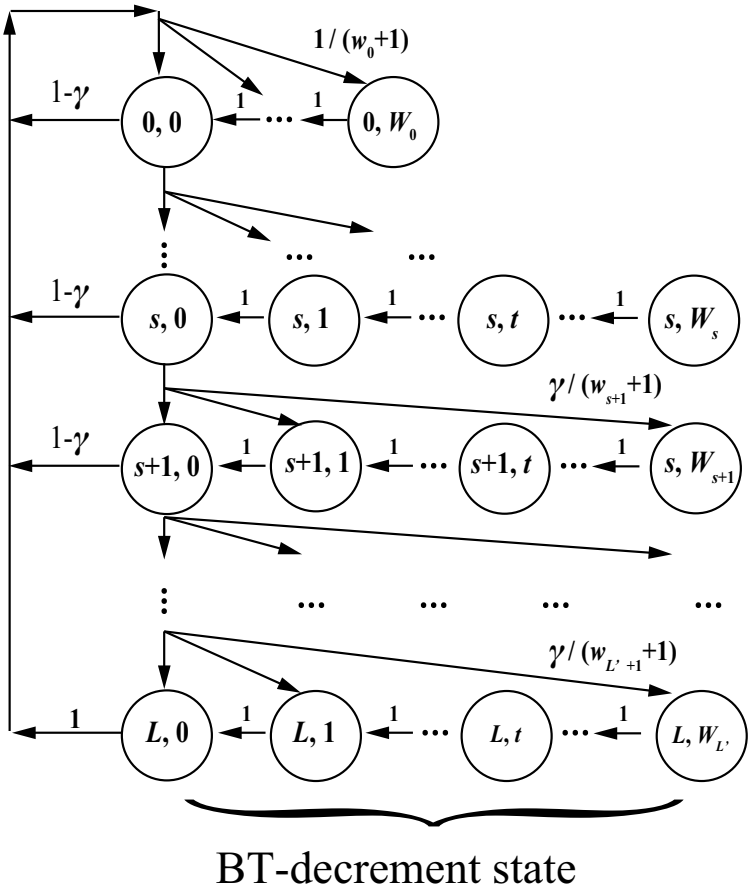

Figure 2.2: Bianchi's Markov-chain model for BT-decrement state.

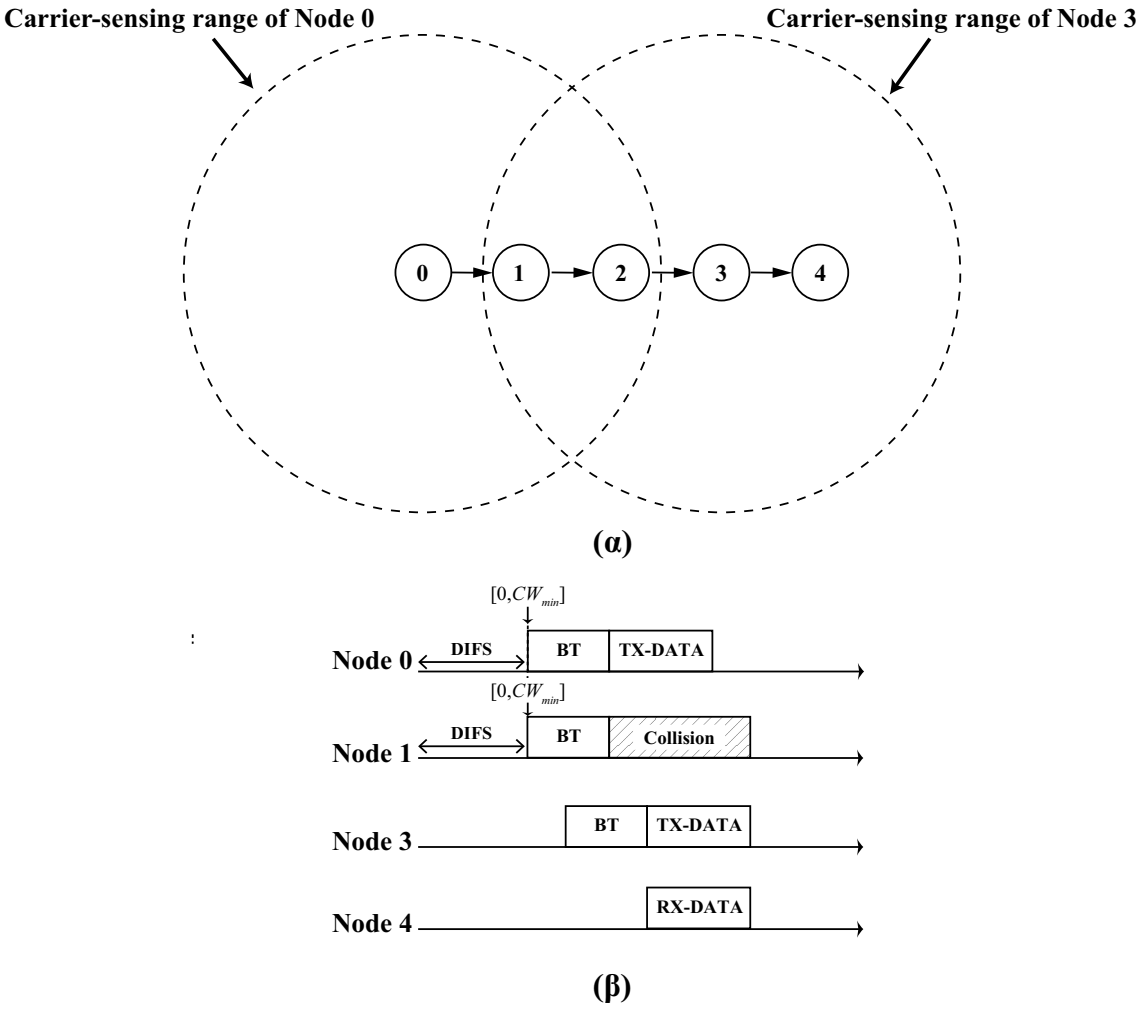

Figure 2.3: (α) String topology two-hop networks and (β) a timeline example of the channel access of the IEEE 802.11 DCF

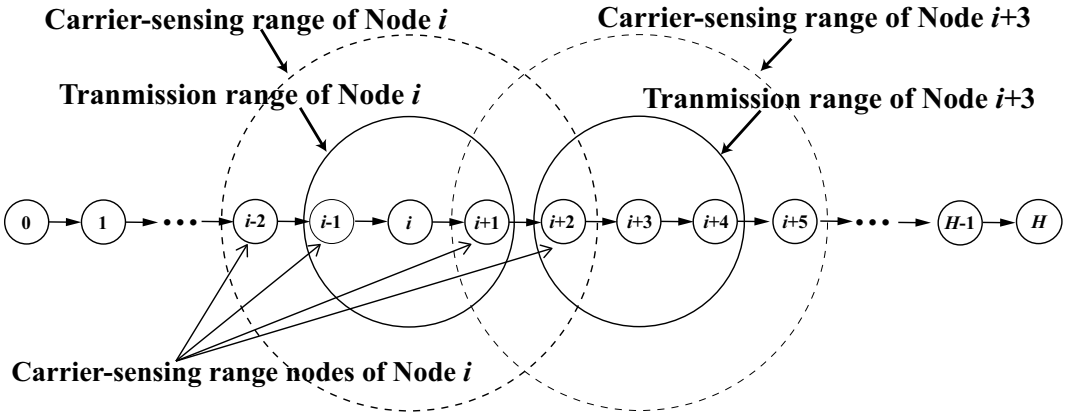

Figure 2.4: Network topology used for analysis.

Reference

[1] IEEE Computer Society LAN MAN Standards Committee, *Part 11: Wireless LAN medium access control (MAC) and physical layer (PHY) specifications*, IEEE Std 802.11-1999, Aug. 1999.

[2] G. Bianchi,"Performance analysis of the IEEE 802.11 distributed coordination function," *IEEE J. Sel. Areas Commun*, vol. 18, no. 3, pp. 535-547, Mar. 2000.

[3] H. Wu, Y. Peng, K. Long, S. Cheng, and J. Ma, "Performance of reliable transport protocol over IEEE 802.11 wireless LAN: analysis and enhancement," *Proc. IEEE INFOCOM*, vol. 2, pp. 599-607, 2002.

[4] D. Malone, K. Duffy and D. Leith,"Modeling the 802.11 distributed coordination function in non saturated heterogeneous conditions," *IEEE /ACM Trans. Netw.*, vol. 15, no. 1, pp. 159-172, Feb. 2007.

[5] K. Duffy, D. Malone and D. Leith,"Modeling the 802.11 distributed coordination function in non saturated conditions," *IEEE Comm. Letters*, vol. 9, no. 8, pp. 715-717, Aug. 2005.

[6] E. Felemban and E. Eric,"Single hop IEEE DCF analysis revisited: accurate modeling of channel access delay and throughput and unsaturated traffic cases," *IEEE Trans. Wireless Comm.*, vol. 10, no. 10, pp. 3256-3266, Oct. 2011.

[7] L. Dai and X. Sun,"A unified analysis of IEEE 802.11 DCF networks: stability, throughput, and delay," *IEEE Trans. Mobile Computing*, vol. 12, no. 8, pp. 1558-1572, Aug. 2013.

[8] Q.L. Zhao, D.H.K. Tsang, and T. Sakurai, "Modeling nonsaturated IEEE 802.11 DCF networks utilizing an arbitrary buffer size," *IEEE Trans. Mobile Computing*, vol. 10, no. 9, pp. 1248-1263, Nov. 2011.

[9] R.P. Liu, G.J. Sutton, and I.B. Collings, "A New Queueing Model for QoS Analysis of IEEE 802.11 DCF with Finite Buffer and Load," *IEEE Trans. Wireless Comm.*, vol. 9, no. 8, pp. 2664-2675, Aug. 2010.

[10] B. Jang and M. L. Sichitiu, "IEEE 802.11 saturation throughput analysis in the presence of hidden terminals", IEEE/ACM Trans. Networking, vol. 20, no. 2, pp. 557-570, April 2012.

[11] O. Ekici and A. Yongacoglu, "IEEE 802.11a throughput performance with hidden nodes", IEEE Communications, Letters, vol. 12, no 6, pp. 465-467, June 2008

[12] F. Y. Hung, I. Marsic, "Performance analysis of the IEEE 802.11 DCF in the presence of the hidden stations" Elsevier, Computer Networks, vol 56, no 15, pp. 2674-2687, Oct. 2010.

[13] P. C. Ng and S. C. Liew, "Throughput analysis of IEEE 802.11 multi-hop ad hoc networks," *IEEE/ACM Trans. Networking*, vol. 15, no. 2, pp. 309-322, Apr. 2007.

[14] M. Inaba, Y. Tsuchiya, H. Sekiya, S. Sakata, and K. Yagyu "Analysis and expression of maximum throughput analysis in wireless multi-hop networks for VoIP Application," *IEICE Trans. Communications.*, vol. E92-B, no. 11, pp. 3422–3431, Nov. 2009.

[15] Zhao H, Garcia-Palacios E, Wang S, Wei J, Ma D. "Evaluating the impact of network density, hidden nodes and capture effect for throughput guarantee in multi-hop wireless networks". *Ad Hoc Networks*, vol. 11, no. 1, pp. 54-69. Jan. 2013.

[16] H. Sekiya, Y. Tsuchiya, N. Komuro, and S. Sakata, "Maximum throughput for long-frame communication in one-way string wireless multi-hop networks ," *Wireless personal communications*, vol. 60, no. 1, pp. 29-41, Mar. 2011.

[17] Y. Gao, D. Chui, and J. C. S. Lui, "The fundamental role of hop distance in IEEE 802.11 multi-hop ad-hoc networks," *IEEE International Conference on Network Protocol*, Boston, Massachusetts, USA, Nov. 2005.

[18] Y. Gao, D. Chui, and J. C. S. Lui, "Determining the end-to-end throughput capacity in multi-hop networks: methodology applications," *ACM Special Interest Group on Performance Evaluation 2006*, pp. 39–50, Jun. 2006.

[19] T. D. Senthilkumar, A. Krishnan, P. Kumar. "New approach for throughput analysis of IEEE 802.11 in adhoc networks". *IEEE International Conference on Control Communication and Automation*, Kanpur, India, pp. 148-153, Dec. 2008.

[20] H. Zhao, S. Wang, Y. Xi, Wei J, "Modeling intra-flow contention problem in wireless multi-hop networks", *IEEE Communications Letters*, vol. 14, no. 1, pp. 18-20, Jan. 2010.

[21] A. Kumar, E. Altman, D. Miorandi, and M. Goyal,"New insights from a fixed point analysis of single cell IEEE 802.11 WLANs," *IEEE/ACM trans. Networking*, vol. 15, no. 3, pp. 538-601, Jun. 2007.

[22] K. Xu, M. Gerla, S. Bae, "How effective is the IEEE 802.11 RTS/CTS handshake in ad hoc networks?", *IEEE Global Telecommunication Conference 2002*, Taipei, Taiwan, vol. 1, pp. 17-21, Nov. 2002.

Chapter 3

Backoff-Stage Synchronization (BSS) in Multi-hop Networks

●● ABSTRACT ●●

In IEEE 802.11 WMHNs, from the design policy of DCF, it has been assumed that each node obtains transmission opportunities family and randomly. From the investigation in this chapter, however, the unexpected phenomenon occurrence in the multi-hop network, which collapses this assumption, is found. This special phenomenon is named as "Backoff-Stage Synchronization (BSS)". The occurrence mechanisms of BSS and the sufficient conditions for BSS occurrence are obtained. By using windows fairness index, the characteristic of BSS, which is coexistence of fair transmission in long time range and unfair transmission in short time range, is extracted. The impact of BSS on communication in IEEE 802.11 multi-hop network is discussed. By considering the characteristics of BSS, the detection method of BSS is proposed.

3.1 Backoff-Stage Synchronization (BSS) in IEEE 802.11 Multi-hop Networks

3.1.1 Unexpected Phenomenon in IEEE 802.11 Multi-hop Networks

In WMHNs, each node in the network decrements own BT individually. Therefore, it is assumed in conventional multi-hop network analyses [2]-[6] that each node obtains transmission opportunity fairly and randomly. In [6], analytical expression of maximum throughput for string-topology multi-hop networks with two-way flows has been obtained. Following the conventional analyses, it is also assumed that each node obtains the transmission opportunities fairly and randomly. Figure 3.1 shows versus number of hop in a string topology multi-hop network with two-way flows. It is seen from Fig. 3.1 that analytical predictions agree with simulation results well. However, only analytical prediction in three-hop network differs from simulation result. It is supposed that a special phenomenon, which is unexpected among network designers, occurs in string-topology three-hop network as shown in Figure 3.2.

The analysis from [6] is based on the assumptions as same as those in Section. 2.3.2. In Fig. 3.2, Nodes 0 and 3 are in the hidden-node relationship. It has been supposed that there is no mutuality among network nodes. This is because IEEE 802.11 DCF is designed for achieving fair and random transmission opportunities among network nodes.

Figure 3.3 shows timeline of transmission attempts for each node in the three-hop network. Table 3.1 gives the system parameters in this scenario. These are based on IEEE 802.11a [1]. It is seen from Fig. 3.3 that Node 1 and 2 obtain fair and random transmissions. In short-time range (a) and (c) in Fig. 3.3, however, consecutive transmission failures of Node 3 occurs. Namely, Node 3 has few transmission opportunities. In short-

time range (b) and (d) in Fig. 3.3, on the other hand, consecutive transmission failures of Node 0 occur. In this thesis, the consecutive transmission-success duration is named as WIN state. In addition, the consecutive transmission-failure duration is named as DEFEAT state. It is seen from Fig. 3.3 that WIN state and DEFEAT state appear alternatively. Namely, there is mutuality between Nodes 0 and 3. Following the IEEE 802.11 DCF design policy, it is supposed that there is no relationship between Nodes 0 and 3. The assumption that all the nodes obtain fair and random transmission opportunities is not satisfied in three-hop network.

3.1.2 The occurrence mechanism of BSS

The mechanism of this network-dynamics occurrence is explained by using the channel access examples of Nodes 0 and 3 in the three hop network as shown in Fig. 3.4. In this scenario, it is assumed that network offered load is heavy. Namely, all the nodes always have at least one frame in the transmission buffer. In this network topology, all the nodes sense the transmissions of Nodes 1 and 2. When Node 1 or 2 transmits a frame, both Nodes 0 and 3 do not decrease own BT. Namely, Nodes 1 and 2 do not make effect on the transmission-start-time difference between Nodes 0 and 3. Therefore, the channel access example of Nodes 1 and 2 is excluded from Fig. 3.4.

(a) in Fig. 3.4 is the situation that both Nodes 0 and 3 choose own initial value of BT from [0, CW_{min}]. Obviously, the transmission-start-time difference between Nodes 0 and 3 is smaller than CW_{min} even if Nodes 0 and 3 set any value of BT in this situation. h is defined as slot number for transmitting one frame, which is expressed as $h = (FRAME + SIFS + ACK)/\sigma$. In this situation, h is 20 slot following the explanation in [6]. In the network as shown in Fig 3.2, h for any FRAME length is larger than CW_{min}. Therefore, frame-transmission collision occurs in (b) because Node 0 starts a

frame transmission before Node 3 finishes a frame transmission. Following IEEE 802.11 DCF operations, both Nodes 0 and 3 double the CW value after the collision. When transmission-start-time difference between Nodes 0 and 3 is larger than h, Node 0 or 3 succeeds the frame transmission. The case that Node 0 succeeds the transmission (c) in Fig. 3.4 is considered. Due to transmission success, Node 0 resets the value of CW following the description in DCF. Because the BT of Node 0 is chosen from the range of [0,CW_{min}], Node 0 can transmit a frame with small holding time. On the other hand, Node 3 still decreases the BT in (c). In the situation, there is a high possibility that frame collision occurs between Nodes 0 and 3. In Fig. 3.4, it is assumed the case that the frame collision occurs in (d). Following the DCF, two nodes double the value of CW after the collision. Note that the Node-3 CW value is $4CW_{min}$ though Node-0 CW value is $2CW_{min}$. In the next transmission attempt, of course, Node 0 transmits a frame with high success probability because the holding time of Node 3 is much longer than that of Node 0. As a result, Node 0 always transmits a frame successfully with small holding time. Namely, Node 0 is in WIN state. On the other hand, Node 3 always fails the transmission. Therefore, Node 3 is in DEFEAT state. When Node 3 fails L-th frame transmission at (e) and the transmission frame is dropped, Node 3 can escape from DEFEAT state. Following the operation in DCF, Node 3 resets the value of CW for next frame transmission at (f). On the other hand, the value of CW with respect to Node 0 is $2CW_{min}$. In the next transmission attempts, Node 3 transmits a frame with high success probability. Therefore, the relationship between Nodes 0 and 3 reverses. Namely, Node 3 is in WIN state and Node 0 is in DEFEAT state. The network dynamics is repeated alternatively. In enough long-time range, Nodes 0 and 3 obtain fair transmission opportunities. In short-time range, however, the transmission opportunities of Nodes 0 and 3 become unfair. In this thesis, this phenomenon is named as "Backoff-Stage Synchronization (BSS)". This phenomenon is one of the coupling effects in IEEE 802.11 multi-hop

networks.

3.1.3 Sufficient Conditions for BSS Occurrence

For the explanation, it is assumed that BSS occurs between Nodes I and J. The receivers of the frame transmitted by Nodes I and J are Nodes i and j, respectively. Node I can not sense the frame transmission of Node J and vice versa. This means that Nodes I and J are in the hidden node relationship.

The case that Node I is in WIN state and Node J is DEFEAT state is considered. From above investigation in Section 3.1.1, for escaping from DEFEAT state, the Node J needs to succeed the frame transmission or drops the frame due to L-th frame-transmission failure. However, there is a low probability that Node J succeed the frame transmission. Node I always transmit a frame with small holding time because Node I is in WIN state. Most of Node-I holding time is decided from the range of [0,CW_{min}]. Because Node-I holding time for frame transmission is longer than h, Node I always transmits a frame before Node J finish the frame transmission. However, if h is smaller than CW_{min}, Node J can finish the frame transmission even Node J is in DEFEAT state. In this case that frame size is small, it is supposed that the consecutive transmission success does not occur and the fairness and randomness among network nodes are maintained. From above considerations, the one of the sufficient conditions for BSS occurrence is

$$h > CW_{min}. \tag{3.1}$$

There is a relationship between BSS occurrence and backoff operation of Nodes I and J. It is important factor that Nodes I and J always decrement own BT simultaneously. If Nodes I, which is in WIN state, has no frame in the buffer, Node J can transmit a frame successfully. Namely, one of the synchronization occurrence factors is that Nodes I and J always have at least one frame in the buffer. This means one of the sufficient

conditions is that network is in saturated condition.

If there are some nodes, which make effect on the transmission-star-time difference between Nodes I and J, the two node do not always decrement own BT simultaneously. If carrier-sensing range nodes of Node J is within the carrier-sensing range of Node I, both Nodes I and J always decrease own BT. Therefore, third condition for BSS occurrence is

$$\forall (\nu(I)) \in \nu(J), \tag{3.2}$$

where $\nu(I)$ is the set of carrier-sensing node number of Node I. In addition, it is necessary that Nodes-I frame collides with Node-J frame. Therefore, fourth condition for BSS occurrence is

$$i, j \in \nu(I) \cap \nu(J). \tag{3.3}$$

Now, four sufficient conditions for BSS occurrence are obtained. BSS occurs between Nodes I and J when these conditions are satisfied.

Here, the results in [6] are considered. As mentioned before, the analytical results in [6] agree with simulation ones except for three-hop network. When hop number is more than four, the two nodes, which are in the hidden node relationship, do not decrement the BT simultaneously. As the example, the case of five-hop network is considered. Figure 3.6 shows string topology five-hop network. In five-hop network, Nodes 0 and 3, 1 and 4, and, 2 and 5 are in the hidden node relationship. Because Nodes 4 and 5 can interrupt the BT-decrement of Node 3, Nodes 0 and 3 do not always decease the BT simultaneously. As hop number increases, these interruptions increase. Therefore, it is supposed that BSS disappears and network nodes obtain fair and random transmission opportunities. This is the cause that analytical results agree with simulation ones when the hop number is more than four. Namely, this result indicates that the cause of the difference in three-hop network is the effect of BSS occurrence.

3.1.4 BSS in Chain Topology Multi-hop Network with One-Way Flow: Another Example of BSS

In this subsection, another example of BSS is introduced. Figure 3.7 shows chain-topology 5 hop network with one-way flow. In Fig. 3.7, only Node 0 generates data frames of which destination is Node 4. The system parameter of this scenario is based on Tab. 3.1. Nodes 0 and 3 are in the hidden node relation ship. Nodes 0 and 3 sense the frame transmissions of Nodes 1, 2 and 4. Therefore, it is seen that the (3.2) and (3.3) are satisfied in Fig. 3.7. It is supposed that the BSS occurs when the network has heavy offered load and $h > CW_{min}$. Figure 3.8 shows the timeline of transmission attempts for each node in the chain-topology five-hop network topology. The simulation parameters are given in Tab. 3.1 and offered load is 1.32 Mbps. In this scenario, h is 20 slot, which is larger than CW_{min}. It is seen from Fig. 3.8 WIN and DEFEAT sates appear alternatively, which shows BSS occurrence. This results suggest that the BSS occurs even the simple network topology if the conditions are satisfied. The BSS causes the unfairness of transmission opportunities, large transmission delay and frame drop, which are serious problem for communication on IEEE 802.11. This results shows wireless multi-hop network should be designed carefully considering network dynamics.

3.2 Impact on Communication

3.2.1 Short-Time-Range Unfairness and Long-Time-Range Fairness

As mentioned in the previous section, the BSS causes unfairness of the transmission opportunities in the short time range. In long time range, however, fair transmissions

are kept because WIN and DEFEAT states appear alternatively. By using the window fairness index [8], this feature is confirmed.

A enough long sequence of transmission-success pattern of Nodes I and J is needed for calculating the index. As the first step, a sequence of which size is d length is extracted from the l-th elements of the enough long sequence as shown in as shown in Fig. 3.9. From the sequence of which size is d length, the rate of number of node-l transmission success to d elements $\zeta_{l,d}^{j}$ is obtained. In the example of Fig. 3.9, $\zeta_{I,4}^{1}$=0.25, $\zeta_{J,4}^{1}$=0.75, $\cdots$. In l-th window, it is always satisfied $\zeta_{I,4}^{l} + \zeta_{J,4}^{l} = 1$. The fairness index between Nodes-I and J transmission success at the l-th window is obtained as

$$\phi_{l}^{d} = \frac{(\zeta_{I,d}^{l} + \zeta_{J,d}^{l})^2}{2\left\{(\zeta_{I,d}^{l})^2 + (\zeta_{J,d}^{l})^2)\right\}}. \tag{3.4}$$

By calculating the sum of fairness index at all the window of which size is d, the index for evaluating fair transmission between Nodes I and J is obtained as

$$\Phi(d) = \frac{\sum_{j=1}^{N} \phi_{d}^{j}}{N}, \tag{3.5}$$

where N is the number of the elements included in long sequence. When Nodes I and J obtain fair transmission opportunities perfectly, the value of $\Phi(d)$ is equal to one. Conversely, when Nodes-i and J transmission is completely unfair, the value of $\Phi(d)$ is 0.5. By calculating each window size, fairness index for both short and long time range is obtained.

Figure 3.10 shows the window fairness index between the Nodes 0 and 3 transmissions versus the window size for fixed offered load in the string-topology three-hop network. The maximum throughput is 1.9 Mbps in this network. Therefore, it is supposed that the network has heavy offered load when offered load is higher than 1.9 Mbps. Fig. 3.10 shows that Nodes 0 and 3 obtain fair transmission successes in both short and long time range when network offered load is light. On the other hand, transmission successes between

Nodes 0 and 3 are unfair in short time range when offered load is higher than 1.9 Mbps. In addition, fair transmission success between Nodes 0 and 3 obtained in long time range when offered load is higher than 1.9 Mbps. It is confirmed that the fairness in long time range and the unfairness in short time range coexist, which is the one of the features of BSS. It is seen from the se results that $\Phi(d)$ is one of the index for evaluating whether BSS occurs or not.

By using window fairness index, the communication on IEEE 802.11 networks for various applications under the BSS occurrence is discussed. Figure 3.11 shows window fairness index versus the window size for fixed h in the three-hop network. In Fig. 3.11, $h = 20, 74$, and 84 are for voice, video, and background frame transmissions, respectively. The network offered load is adjusted for achieving the maximum throughput at any h. Fig. 3.11 shows that the fair transmission success in long time range and unfair transmission success in short time range coexists when h is 20. It is also seen from Fig. 3.11 that the value of $\Phi(d)$ for h=74 and 84 is higher than that for h=20. The transmission number decrease as the duration of one frame transmission is longer. Therefore, the transmission unfairness become weak when frame length is long. These results suggests that BSS regardless of data-frame type.

3.2.2 Network Dynamics with Request To Send / Clear To Send Handshake

There is a technology called as Request To Send/ Clear To Send (RTS/CTS) for mitigating the impact of hidden node problem. By using RTS/CTS handshake before data-frame transmission, hidden node collisions can be avoided. However, the duration for one frame-transmission success becomes longer because RTS/CTS handshakes are overheads. In this subsection, the network dynamics with and without RTS/CTS handshake is discussed.

Figure 3.12 shows maximum throughput versus number of hop in a string topology multi-hop network with and without RTS/CTS. In the communication with RTS/CTS, it is assumed that the transmission range is the same as carrier-sensing range. From the investigation in [7], it has been supposed that the network performance in this situation is similar to that in IEEE 802.11 DCF without RTS/CTS in which carrier-sensing range is twice as the transmission range. It is seen from Fig. 3.12 that this consideration is satisfied except for three hop network. When hop number is three, maximum throughput of IEEE 802.11 DCF without RTS/CTS is higher than that with RTS/CTS. As described in Section 3.1.1, BSS occurs in three-hop network with IEEE 802.11 DCF without RTS/CTS. On the other hand, BSS does not occur three hop network with IEEE 802.11 DCF with RTS/CTS because the duration for RTS-frame transmission is shorter than CW_{min}. This result suggests that the BSS occurrence enhances the network throughput. Under the BSS occurrence situation, a node can send a data frame consecutively with few overheads and small collision probability. In this sense, the BSS occurrence is similar to frame aggregation [9]. Note that the network dynamics makes the network performance enhanced.

In BSS occurrence, the network-throughput enhancing is positive effect for communication on IEEE 802.11. However, the frame drop and large transmission delay is negative factors. This relationship is trade off. From the viewpoint of transmission delay, the BSS should be avoided for real time applications such as VoIP and video streaming.

3.3 BSS Detection

As one of the features of BSS occurrence, WIN state and DEFEAT state always appear simultaneously as shown in Fig.3.3. Additionally, a node switches between the WIN and DEFEAT states alternatively. In this subsection, BSS detection method is proposed. Figure 3.13 shows the example of timelines of successful transmission, failed transmission

and their backoff-stage number for a certain node transmissions. In Fig. 3.13, the l-the duration of WIN state is obtained as

$$WD_l = \epsilon_{1,l} - \epsilon_{0,l}. \tag{3.6}$$

Additionally, the duration of DEFEAT state is obtained as

$$DD_l = \epsilon_{0,l+1} - \epsilon_{1,l}. \tag{3.7}$$

In this method, the definitions of ϵ_1 and ϵ_0 are important. When a node succeeds the frame transmissions, which are transmitted from the first, second and third backoff stage in the DEFEAT state, three times in a row, the node recognizes to transit to WIN state from DEFEAT state. When a node fails the transmission, which is transmitted from the fourth backoff state or later in the WIN state, the node recognizes to transit to DEFEAT state from WIN state. ϵ_0 is determined as the time when a node transit to WIN state from DEFEAT one. Similarly, ϵ_0 is determined as the time when a node transit to DEFEAT state from WIN one.

The index for the BSS detection with respect sequence time T_s is defined as a the ratio of the sum of WD_l and that of DD_l, namely

$$\Psi(T_s) = \frac{\sum_{l}^{T_s} DD_l}{\sum_{l}^{T_s} WD_l}. \tag{3.8}$$

When the BSS occurs, Ψ is equal to one.

Figure 3.14 shows an index for the BSS detection with respect to Node 0 versus the data sequence time T_s. It is seen from Fig. 3.14 that index for BSS detection approaches to one in three hop network with both 2.0 Mbps and 2.5 Mbps where BSS occurs. The BSS does not occur in the other cases. It is confirmed that proposed index can detect BSS occurrence.

3.4 Conclusion

This chapter has presented the investigation about the special phenomenon. This phenomenon is named as "Backoff-Stage Synchronization (BSS)". The BSS-occurrence mechanisms and the sufficient conditions for BSS occurrence have been obtained. By using windows fairness index, the characteristic of BSS, which is coexistence of fair transmission in long time range and unfair transmission in short time range, has been extracted. The impact of BSS on communication in IEEE 802.11 multi-hop network has been discussed. By considering the characteristics of BSS, the detection method of BSS has been proposed. Under the BSS occurrence, each node can not work following design policy of the protocol even each node operates following the description of the protocol. From the viewpoint of network science as well as communication, the BSS is interesting phenomenon.

Table 3.1: System Parameters

Data rate	18 Mbps
Control bit rate	12 Mbps
Transmission range	60 m
Carrier sensing range	115 m
Distance of each node	45 m
RTS-frame size	20 bytes (10 slot)
voice-frame size	200 bytes (20 slot)
video-frame size	1300 bytes (74 slot)
Background frame size	1500 bytes (84 slot)
ACK frame size	10 bytes
CW_{min}	15
CW_{max}	1023
SIFS	16 μsec
DIFS	34 μsec
σ	9 μsec
Retry limit limit (L)	7

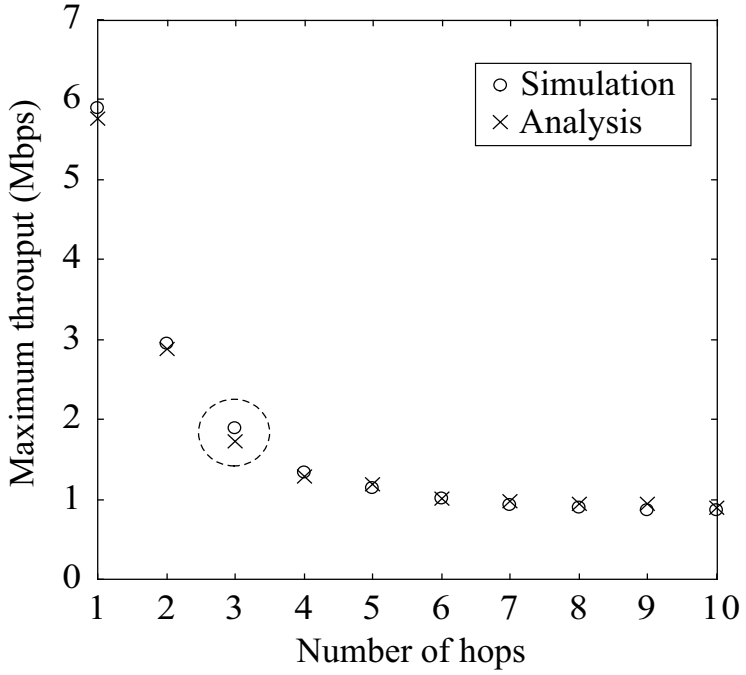

Figure 3.1: Maximum throughput versus number of hop in a string topology multi-hop network with two-way flows.

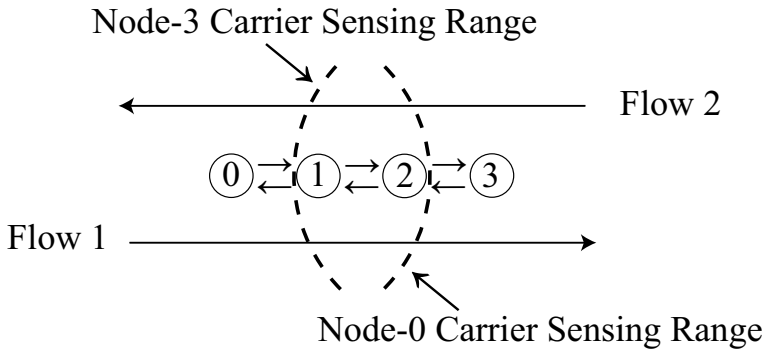

Figure 3.2: Three-hops network topology with two-way flows.

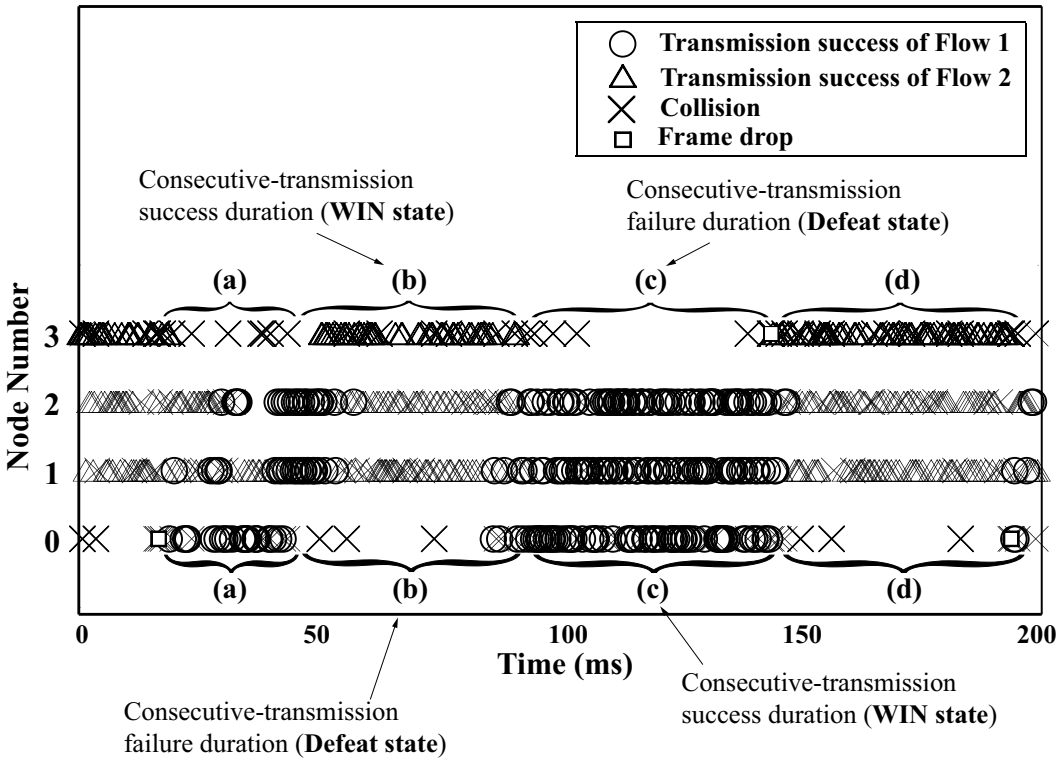

Figure 3.3: Timeline of transmission attempts for each node in the three-hop network.

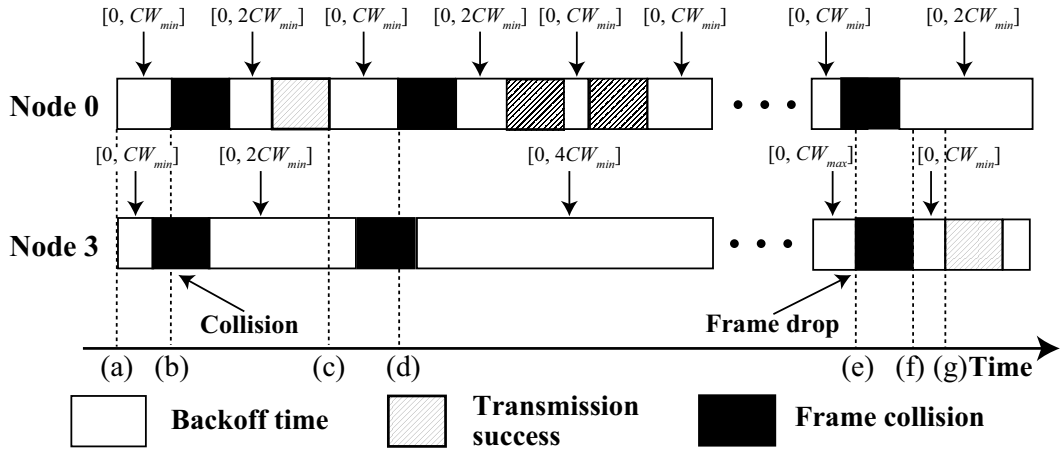

Figure 3.4: Channel-access example of Nodes 0 and 3.

Pattern 1

	Node 0	Node 3
Backoff stage	Small	Small
Collision probability	Low	Low

Pattern 2

	Node 0	Node 3
Backoff stage	Large	Small
Collision probability	High	Low

Pattern 3

	Node 0	Node 3
Backoff stage	Small	Large
Collision probability	Low	High

Figure 3.5: Relationship between backoff-stage number and collision probability.

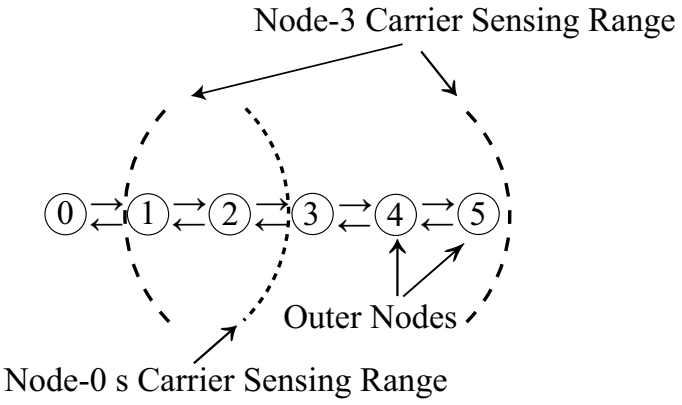

Figure 3.6: String-topology five-hops network with two-way flows.

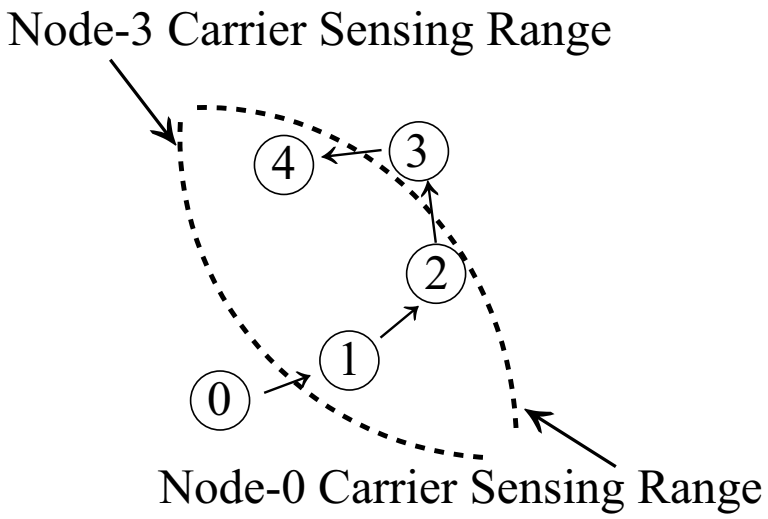

Figure 3.7: Chain-topology five-hop network with one-way flow

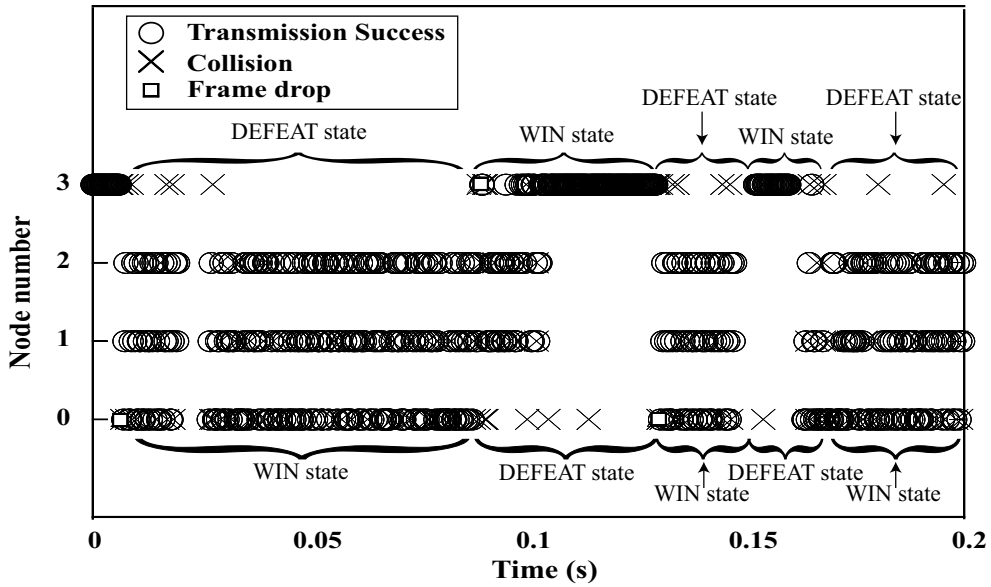

Figure 3.8: Timeline of transmission attempts for each node in the chain-topology five-hop network topology.

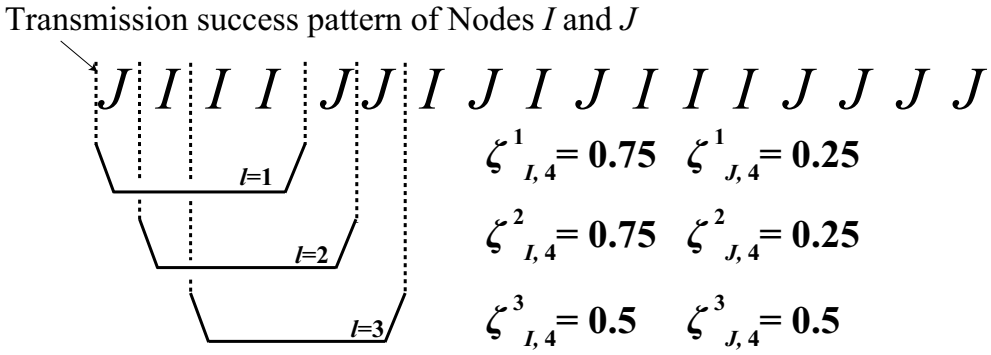

Figure 3.9: Window-fairness-index calculation for $d = 4$.

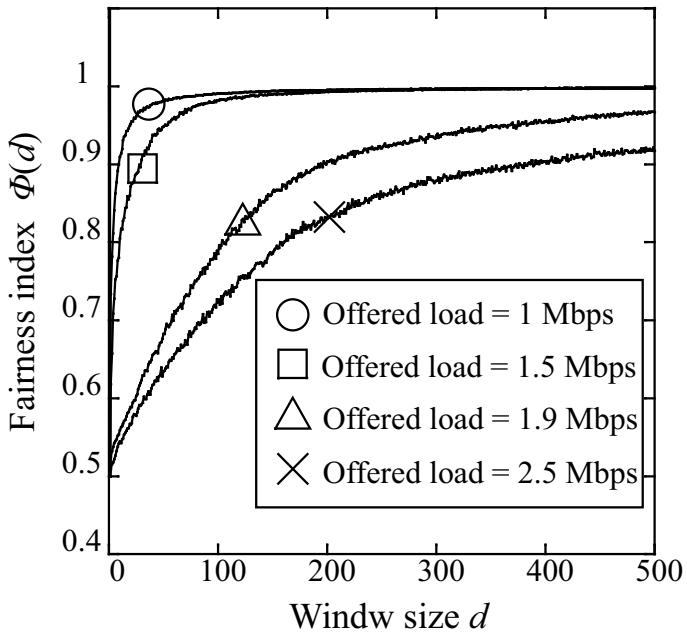

Figure 3.10: Window fairness index between the Nodes 0 and 3 transmissions versus the window size for fixed offered load in the three-hop network.

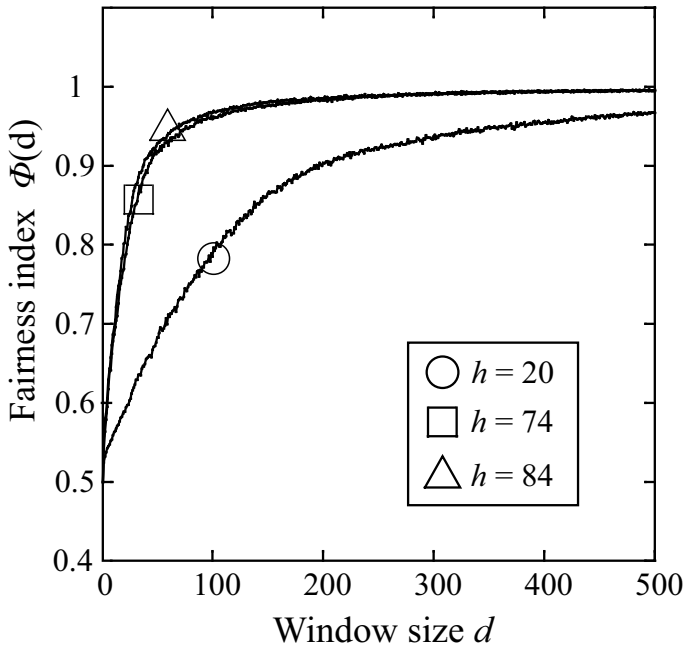

Figure 3.11: Window fairness index between the Nodes 0 and 3 versus window size for fixed h in the three-hop network.

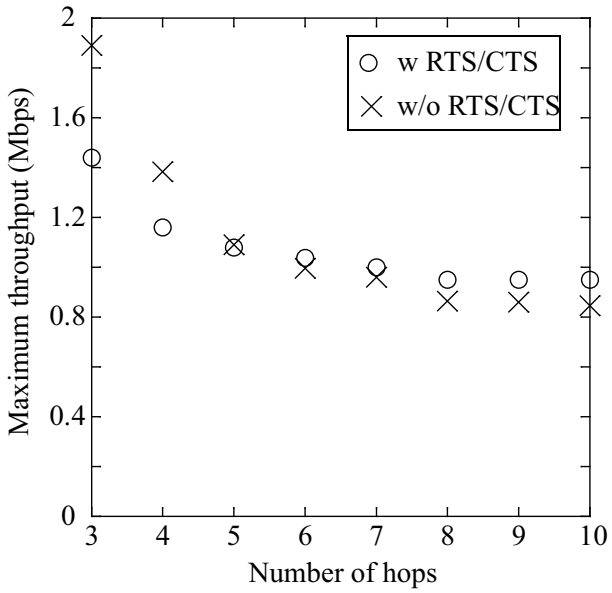

Figure 3.12: Maximum throughput versus number of hop in a string topology multi-hop network with and without RTS/CTS.

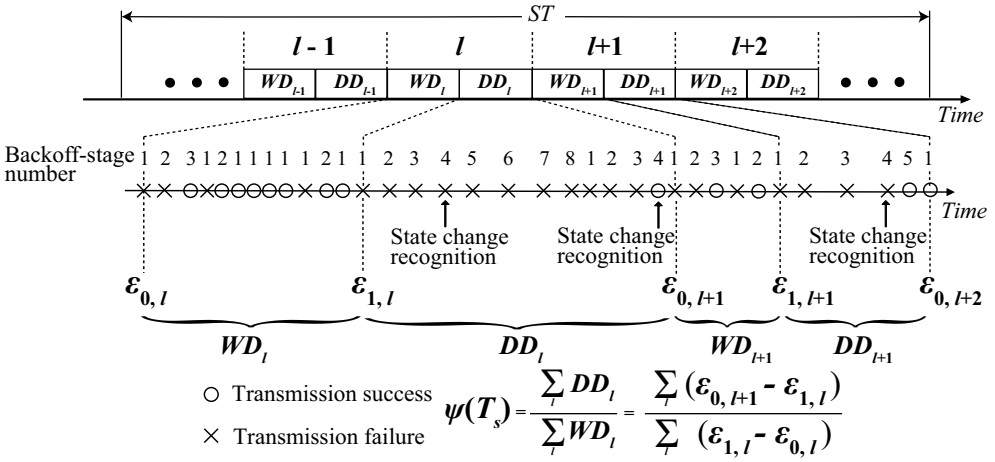

Figure 3.13: The example of timelines of successful transmission, failed transmission and their backoff-stage number.

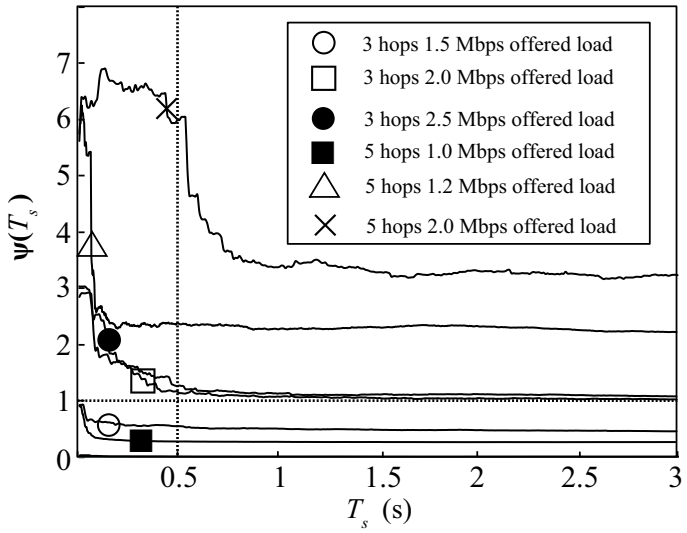

Figure 3.14: The fairness index for the BSS detection with respect to Node 0 versus the data sequence time T_s

[1] IEEE Computer Society LAN MAN Standards Committee, *Part 11: Wireless LAN medium access control (MAC) and physical layer (PHY) specifications*, IEEE Std 802.11-1999, Aug. 1999.

[2] P. C. Ng and S. C. Liew, "Throughput analysis of IEEE 802.11 multi-hop ad hoc networks," *IEEE/ACM Trans. Networking*, vol. 15, no. 2, pp. 309-322, Apr. 2007.

[3] H. Sekiya, Y. Tsuchiya, N. Komuro, and S. Sakata, "Maximum throughput for long-frame communication in one-way string wireless multi-hop networks ," *Wireless personal communications*, vol. 60, no. 1, pp. 29-41, Mar. 2011.

[4] Y. Gao, D. Chui, and J. C. S. Lui, "Determining the end-to-end throughput capacity in multi-hop networks: methodology applications," *ACM Special Interest Group on Performance Evaluation 2006*, pp. 39–50, Jun. 2006.

[5] M. Inaba, Y. Tsuchiya, H. Sekiya, S. Sakata, and K. Yagyu "Analysis and expression of maximum throughput analysis in wireless multi-hop networks for VoIP Application," *IEICE Trans. Communications.*, vol. E92-B, no. 11, pp. 3422–3431, Nov. 2009.

[6] Y. Tsuchiya, M. Inaba, M. Matsumoto, H. Sekiya, S. Sakata and K. Yagyu, "Analysis of maximum UDP throughput of short-hop string networks for VoIP applications," in *Proc. IEEE WPMC*, Sendai, Japan, Sept. 2009.

[7] K. Xu, M. Gerla, S. Bae, "How effective is the IEEE 802.11 RTS/CTS handshake in ad hoc networks?",*IEEE Global Telecommunication Conference 2002*, Taipei, Taiwan, vol. 1, pp. 17-21, Nov. 2002.

[8] C. E. Koksal, H. Kassab, and H. Balakrishnam "An analysis of short-term fairness in wireless media access protocol" *Proc. 2000 ACM SIGMETRICS* , vol. 28. no. 1, pp 118-119, June 2000.

[9] Y. Kim, S. Choi, K. Jang, and H. Hwang "Throughput enhancement of IEEE 802.11 WLAN via frame aggregation," *Proc. IEEE Vehicular Technology Conference*, vol. 4, pp. 3030-3034, Sept. 2004.

Chapter 4

Analytical Expressions for IEEE 802.11 Multi-hop Network with Backoff-Stage Synchronization

●● ABSTRACT ●●

Backoff-Stage Synchronization (BSS), which is special network dynamics in the multi-hop network, causes a serious problem on communication. In the network with the coupling effect, each node can not work along with the design policy of IEEE 802.11 DCF even though they do based on the description of the protocol. This chapter presents analytical expressions for IEEE 802.11 multi-hop network with BSS. For taking the features of the coupling effect into account the analytical expressions, the modified Bianchi's Markov-chain models, which express the operation with respect to each network node, are proposed. Obtained analytical expressions are verified by the comparison with simulation and experimental results.

4.1 Maximum Throughput Analysis taking into account BSS

The string-topology three-hop network with two-way flows as shown in Fig. 3.2 is the analysis subject in this chapter. The analysis in this chapter is based on the following assumptions, which follow the assumptions in [1]-[8].

1. Each node has a single radio transceiver and all the network nodes use the same radio channel.

2. Nodes 0 and 3 generate the fixed sized UDP data of which payload size is P.

3. Channel conditions of all the links are ideal. Namely, transmission failures occur only due to frame collisions.

4. The network is in saturated condition. Therefore, all the nodes have at least one frame in the buffer.

The following explanation, the network link from Node i to Node $i \pm 1$ is expressed as $(i, i \pm 1)$.

4.1.1 Derivation of Maximum Throughput

In this chapter, we use the airtime expressions. The transmission airtime for $(i, i \pm 1)$ is expressed by

$$x_{(i,i\pm1)} = \lim_{Time\to\infty} \frac{S_{(i,i\pm1)}}{Time}, \tag{4.1}$$

where $S_{(i,i\pm1)}$ is the sum of the durations of the DATA transmission, ACK transmission, DIFS and SIFS for $(i, i \pm 1)$. $S_{(i,i\pm1)}$ includes both the successful- and the failure-transmission durations with respect to $(i, i \pm 1)$. Because Node i has two links, the

transmission airtime of Node i is expressed as

$$X_i = x_{(i,i+1)} + x_{(i,i-1)}, \tag{4.2}$$

where $x_{(0,-1)} = x_{(3,4)} = 0$.

Following (2.15), carrier-sensing airtime of Node i is

$$Y_i = \begin{cases} X_1 + X_2, & \text{for } i = 0 \text{ and } 3 \\ X_0 + X_2 + X_3 - \dfrac{X_0 X_3}{1 - X_1 - X_2}, & \text{for } i = 1 \\ X_0 + X_1 + X_3 - \dfrac{X_0 X_3}{1 - X_1 - X_2}, & \text{for } i = 2 \end{cases}. \tag{4.3}$$

The channel-idle airtime is obtained as (2.16).

For deriving the maximum throughput of network, the transmission airtimes with respect to each link need to be fixed. In the maximum throughput situation, throughputs of all the links are same as maximum throughput. Because no frame drops occur in Nodes 1 and 2, throughputs of all links should be the same. Therefore, the flow constraint is obtained as

$$\begin{aligned} e_{(0,1)} &= e_{(1,2)} = e_{(2,3)}, \\ e_{(3,2)} &= e_{(2,1)} = e_{(1,0)}, \end{aligned} \tag{4.4}$$

where $e_{(i,i\pm1)}$ is throughput for $(i, i \pm 1)$, which is expressed as

$$e_{(i,i\pm1)} = x_{(i,i\pm1)}(1 - \gamma_{(i,i\pm1)})\frac{P}{T}. \tag{4.5}$$

In (4.5), $\gamma_{(i,i\pm1)}$ is the collision probability of $(i, i \pm 1)$. From the assumption investigated in Section 3.1.1, the end-to-end throughput of Flow 1 is same as that of Flow 2. Therefore, we have

$$\begin{aligned} e_{(1,2)} &= e_{(1,0)} \\ e_{(2,1)} &= e_{(2,1)} \end{aligned}. \tag{4.6}$$

When Node m is the link which limits the network capacity, link capacity equation is obtained as (2.22). From (4.5), (4.4), (4.6) and (2.22), we have six algebraic equations which are

$$\begin{cases} X_m = (1 - X_m - Y_m)\tau'_m \dfrac{T}{\sigma}, \\ x_{(0,1)}(1 - \gamma_{(0,1)}) = x_{(1,2)}(1 - \gamma_{(1,2)}), \\ x_{(0,1)}(1 - \gamma_{(0,1)}) = x_{(2,3)}(1 - \gamma_{(2,3)}), \\ x_{(0,1)}(1 - \gamma_{(0,1)}) = x_{(3,2)}(1 - \gamma_{(3,2)}), \\ x_{(0,1)}(1 - \gamma_{(0,1)}) = x_{(2,1)}(1 - \gamma_{(2,1)}), \\ x_{(0,1)}(1 - \gamma_{(0,1)}) = x_{(0,1)}(1 - \gamma_{(0,1)}). \end{cases} \tag{4.7}$$

When we have the expressions of $\gamma_{(i,j)}$ and τ'_i, these equations can be fixed. When we consider $m = 0, 1, 2$ and 3 in (4.7), we obtain four maximum network throughputs. The minimum value of them should be the maximum throughput in the network. In the following section, derivations of $\gamma_{(i,j)}$ and τ_i are investigated by tanking into account the features of the BSS in string-topology three-hop network.

4.1.2 Frame-collision probability and transmission probability: The analytical expression of BSS in three-hop network

Obviously, Nodes 1 and 2 have two links though Nodes 0 and 3 have one link. For deriving the transmission and collision probabilities with respect to each link, therefore, it is necessary to consider Nodes 1 and 2, and Nodes 0 and 3, separately. New Markov-chain models for Nodes 1 and 2 and Nodes 0 and 3 are proposed. In the case of Nodes 1 and 2, we a Markov-chain model taking into account two-way flows are proposed. In the case of Nodes 0 and 3, additionally, we Markov-chain models taking into account the BSS are proposed. Note that four features of the BSS are considered for deriving the collision and transmission probabilities with respect to Nodes 0 and 3.

4.1.2.1 Nodes 1 and 2

Nodes 1 and 2 have two links. For expressing two different links, Bianchi's Markov-chain model is modified. Figure 4.1 shows a Markov-chain model, which corresponds to two-way flows. In Fig. 4.1, two Bianchi's Markov-chain models are coupled by the flow-usage probabilities $\upsilon_{(i,i\pm1)}$. The left-hand side and the right-hand side of Fig. 4.1 express the BT decrements of $(i, i-1)$ and $(i, i+1)$, respectively. The flow-usage probability of $(i, i\pm1)$ is defined as the probability that the destination node of transmission frame at the top of Node-i buffer is Node $i\pm1$. We assume the flow-usage probability of $(i, i\pm1)$ is equal to the rate of throughput for $(i, i\pm1)$ to sum of the throughputs of $(i, i+1)$ and $(i, i-1)$, namely

$$\upsilon_{(i,i\pm1)} = \frac{e_{(i,i\pm1)}}{e_{(i,i+1)} + e_{(i,i-1)}}, \quad \text{for } i = 1 \text{ and } 2. \tag{4.8}$$

In Fig. 4.1, transition probabilities are

$$\begin{aligned}
&P\{[s,t-1,f]|[s,t,f]\} = 1,\\
&P\{[0,t,1]|[s,0,f]\} = \frac{\upsilon_{(i,i+1)}(1-\gamma_{(i,i\pm1)})}{w_0+1},\\
&P\{[0,t,2]|[s,0,f]\} = \frac{\upsilon_{(i,i-1)}(1-\gamma_{(i,i\pm1)})}{w_0+1},\\
&P\{[0,t,1]|[L,0,f]\} = \frac{\upsilon_{(i,i+1)}}{w_0+1},\\
&P\{[0,t,2]|[L,0,f]\} = \frac{\upsilon_{(i,i-1)}}{w_0+1},\\
&P\{[s,t,1]|[s-1,0,1]\} = \frac{\gamma_{(i,i+1)}}{w_i+1},\\
&P\{[s,t,2]|[s-1,0,2]\} = \frac{\gamma_{(i,i-1)}}{w_i+1}.
\end{aligned} \tag{4.9}$$

Let the stationary distribution of the Markov-chain model in Fig. 4.1 be $a[s,t,f]$. Because sum of the stationary distribution of Markov-chain model is equal to one, we have

$$\begin{aligned}
\sum_{s=0}^{L}\sum_{t=0}^{W_s}\sum_{f=1}^{2} a[s,t,f] &= \sum_{s=0}^{L}\left(\gamma^s_{(i,i+1)}a[0,0,1] + \gamma^s_{(i,i-1)}a[0,0,2]\right)\left(\frac{W_s+2}{2}\right)\\
&= 1
\end{aligned} \tag{4.10}$$

From (4.9),

$$\begin{aligned} a[0,0,1] &= \upsilon_{(i,i+1)}\left[(1-\gamma_{(i,i+1)})\sum_{s=0}^{L-1} a[s,0,1]+a[L,0,1]\right] \\ &\quad +\upsilon_{(i,i-1)}\left[(1-\gamma_{(i,i-1)})\sum_{s=0}^{L-1} a[s,0,2]_{+}a[L,0,2]\right] \\ &= \upsilon_{(i,i+1)}a[0,0,1]+\upsilon_{(i,i+1)}a[0,0,2], \end{aligned} \tag{4.11}$$

from which

$$\frac{a[0,0,1]}{a[0,0,2]}=\frac{\upsilon_{(i,i+1)}}{1-\upsilon_{(i,i+1)}}=\frac{\upsilon_{(i,i+1)}}{\upsilon_{(i,i-1)}}. \tag{4.12}$$

From (4.6), we have $\upsilon_{(i,i\pm1)}=\frac{1}{2}$. Therefore, from (4.10) and (4.12), we have

$$\begin{aligned} a[0,0,1] &= \frac{1}{\sum_{s=0}^{L}(w_s+2)\gamma^s_{(i,i+1)}} \\ a[0,0,2] &= \frac{1}{\sum_{s=0}^{L}(w_s+2)\gamma^s_{(i,i-1)}} \end{aligned}. \tag{4.13}$$

The transmission probability of Node i is expressed as

$$\begin{aligned} \tau_i &= \sum_{s=0}^{L}\sum_{f=1}^{2} a[s,0,f] \\ &= \frac{\sum_{s=0}^{L}(\gamma^s_{(i,i+1)}+\gamma^s_{(i,i-1)})}{\sum_{s=0}^{L}(\frac{w_s+2}{2})(\gamma^s_{(i,i+1)}+\gamma^s_{(i,i-1)})}. \end{aligned} \tag{4.14}$$

It is seen from Fig. 3.2 that the frames transmitted by Nodes 1 and 2 collides with the node in the carrier-sensing range. Therefore, collision probabilities of links $(i, i\pm1)$ are

$$\gamma_{(i,i+1)}=\begin{cases} 1-(1-\tau_0)(1-\tau_2)(1-\tau_3), & \text{for } i=1 \\ 1-(1-\tau_1)(1-\tau_3), & \text{for } i=2 \end{cases} \tag{4.15}$$

and

$$\gamma_{(i,i-1)}=\begin{cases} 1-(1-\tau_0)(1-\tau_1)(1-\tau_3), & \text{for } i=2 \\ 1-(1-\tau_2)(1-\tau_0), & \text{for } i=1 \end{cases} \tag{4.16}$$

4.1.2.2 Nodes 0 and 3

For obtaining the analytical expressions for Nodes 0 and 3, the hidden-node collision and BSS should be considered. We focus on four features of the BSS: (1) the collision probability for the low backoff stage is much lower than that for high backoff stage, (2) Node 3 is always in low backoff stage when Node 0 is in high backoff stage and vice versa, (3) a node in WIN state and a node in DEFEAT state always appear simultaneously.

Figure 4.2 shows the Markov-chain model for Nodes 0 and 3. For expressing the feature (1), the Markov-chain model is divided into two parts, namely the front part and the rear part [10]. In Fig. 4.2, backoff stages from 0 to B is the front part and the backoff stages from $B+1$ to L is the rear part. From the feature of the BSS, the boundary between front part and rear part is depends on the duration of the frame transmission and the value of CWmin. Let F be the minimum backoff stage which satisfies $w_F \geq h$, where h. If the backoff stages of Nodes 0 and 3 are smaller than l, both frame transmissions are collided. Namely, which node is in WIN state or DEFEAT state is not decided in this situation. Therefore, backoff stages from 0 to $F-1$ should belong the front part. The boundary exists at least F to L. Therefore, we define the boundary of the backoff-stage number between front and rear parts is $B = F + \lceil \frac{L-F}{2} \rceil$.

In Fig. 4.2, γ_{FP_i} and γ_{RP_i} is collision probability of front part and that of rear part of Node i, respectively. In Markov-Chain model as shown in Fig. 4.2, transition probabilities

are

$$\begin{aligned}
&P\{[s,t]|[s,t-1]\} = 1, && 0 \le s \le L \\
&P\{[0,t]|[s,0]\} = (1-\gamma_{FP_i})/(w_0+1), && 0 \le s \le B \\
&P\{[0,t]|[s,0]\} = (1-\gamma_{RP_i})/(w_0+1), && B+1 \le s \le L \\
&P\{[s,t]|[s-1,0]\} = \gamma_{FP_i}/(w_s+1), && 1 \le s \le B \\
&P\{[s,t]|[s-1,0]\} = \gamma_{RP_i}/(w_s+1), && B+1 \le s \le L \\
&P\{[0,t]|[L,0]\} = 1/(w_0+1).
\end{aligned} \tag{4.17}$$

Let the stationary distribution of the Markov-chain model in Fig. 4.1 be $b[s,t]_i$. The sum of the stationary distribution is equal to one, namely

$$\sum_{s=0}^{L}\sum_{t=0}^{w_s} b[s,t]_i = b[0,0]_i \left[\sum_{s=0}^{B}\gamma_{FP_i}^{s}(\frac{w_s+2}{2}) + \gamma_{FP_i}^{B}\sum_{s=B+1}^{L}\gamma_{RP_i}^{s-B}(\frac{w_s+2}{2})\right] = 1 \tag{4.18}$$

From (4.18), we have

$$b[0,0]_i = \frac{1}{\sum_{s=0}^{B}\gamma_{FP_i}^{s}(\frac{w_s+2}{2}) + \gamma_{FP_i}^{B}\sum_{s=B+1}^{L}\gamma_{RP_i}^{s-B}(\frac{w_s+2}{2})}. \tag{4.19}$$

Therefore, front and rear-part transmission probability of Node i is

$$\begin{aligned}
\tau_{FP_i} &= \sum_{s=0}^{B} b[s,0]_i = \sum_{s=0}^{B}\gamma_{FP_i}^{s} b[0,0]_i \\
&= \frac{\sum_{i=0}^{B}\gamma_{FP_i}^{s}}{\sum_{s=0}^{B}\gamma_{FP_i}^{s}(\frac{w_s+2}{2}) + \gamma_{FP_i}^{B}\sum_{s=B+1}^{L}\gamma_{RP_i}^{s-B}(\frac{w_s+2}{2})},
\end{aligned} \tag{4.20}$$

and

$$\begin{aligned}
\tau_{RP_i} &= \sum_{i=B+1}^{L} b[s,0]_i = \gamma_{FP_i}^{B}\sum_{s=B+1}^{L}\gamma_{RP_i}^{s-B} b[0,0]_i \\
&= \frac{\gamma_{FP_i}^{F}\sum_{s=B+1}^{L}\gamma_{FP_i}^{s}}{\sum_{s=0}^{B}\gamma_{FP_i}^{s}(\frac{w_s+2}{2}) + \sum_{s=B+1}^{L}\gamma_{FP_i}^{B}\gamma_{RP_i}^{s-B}(\frac{w_s+2}{2})},
\end{aligned} \tag{4.21}$$

respectively.

The transmission probabilities of Nodes 0 and 3 are expressed as

$$\tau_i = \tau_{FP_i} + \tau_{RP_i}. \tag{4.22}$$

The collision probability of $(0,1)$ and $(3,2)$ are expressed as average of $\gamma_{f_{(i,j)}}$ and $\gamma_{r_{(i,j)}}$, namely

$$\begin{aligned} \gamma_{(0,1)} &= \frac{\tau_{FP_0}}{\tau_0}\gamma_{FP_0} + \frac{\tau_{RP_0}}{\tau_0}\gamma_{RP_0} \\ \gamma_{(3,2)} &= \frac{\tau_{FP_3}}{\tau_3}\gamma_{FP_3} + \frac{\tau_{RP_3}}{\tau_3}\gamma_{RP_3} \end{aligned}. \tag{4.23}$$

The analytical expressions of γ_{FP_i} and γ_{RP_i} are obtained by considering the BSS feature (2), (3) and (4). From Table 4.1, Node 0 is WIN state or DEFEAT state when Node 3 is in front part, and vice versa. Conversely, Node 0 is DEFEAT state when node 3 is in rear part, and vice versa. Here, another Markov-chain model for Nodes 0 and 3 as shown in Fig. 4.3, which expresses WIN and DEFEAT states of Nodes 0 and 3, is proposed.

(a) in Fig. 4.3 indicates the operation of a Node i in WIN state and (b) in Fig. 4.3 indicates that in DEFEAT state. The collision probabilities with respect to two states is defined as γ_{WS_i} for the WIN state and γ_{DS_i} for the DEFEAT one. This is because the collision probability of the WIN state is much lower than the DEFEAT state, that is obviously seen from Fig. 3.5. In Fig. 4.3, transition probabilities are

$$\begin{aligned} &P\{[s,t-1]_{WS_i}|[s,t]_{WS_i}\} = 1 \\ &P\{[s,t]_{WS_i}|[s-1,0]_{WS_i}\} = \gamma_{WS_i}/(w_s+1), \quad 1 \le s \le B \\ &P\{[0,t]_{WS_i}|[s,0]_{WS_i}\} = (1-\gamma_{WS_i})/(w_0+1), \quad 0 \le s \le B \\ &P\{[0,t]_{WS_i}|[B,0]_{WS_i}\} = 1/(w_0+1). \end{aligned} \tag{4.24}$$

and

$$\begin{aligned}
&P\{[s,t-1]_{DS_i}|[s,t]_{DS_i}\} = 1 \\
&P\{[s,t]_{DS_i}|[s-1,0]_{DS_i}\} = \gamma_{DS_i}/(w_s+1), \qquad 1 \le s \le L \\
&P\{[0,t]_{DS_i}|[s,0]_{DS_i})\} = (1-\gamma_{DS_i})/(w_0+1), \quad 0 \le s \le L-1 \\
&P\{[0,t]_{DS_i}|[L,0]_{DS_i}\} = 1/(w_0+1).
\end{aligned} \tag{4.25}$$

The stationary distributions of the Markov-chain model of WIN state and that of DEFEAT state are defined as $c[s,t]_{WS_i}$ and $c[s,t]_{DS_i}$, respectively. Because the sum of the stationary distribution of the Markov-chain is equal to one, we have

$$\begin{aligned}
\sum_{s=0}^{B}\sum_{t=0}^{w_i} c[s,t]_{WS_i} &= c[0,0]_{WS_i}\sum_{s=0}^{B}\gamma_{w_i}^{s}(\frac{w_s+2}{2}) = 1 \\
\sum_{s=0}^{L}\sum_{t=0}^{w_i} c[s,t]_{DS_i} &= c[0,0]_{DS_i}\sum_{s=0}^{L}\gamma_{w_i}^{s}(\frac{w_s+2}{2}) = 1
\end{aligned} \tag{4.26}$$

From (4.26),

$$\begin{aligned}
c[0,0]_{WS_i} &= \frac{1}{\sum_{s=0}^{B}\frac{w_s+2}{2}\gamma_{WS_i}^{s}} \\
c[0,0]_{DS_i} &= \frac{1}{\sum_{s=0}^{L}\frac{w_s+2}{2}\gamma_{DS_i}^{s}}
\end{aligned}. \tag{4.27}$$

Transmission probability of Node i in WIN state and that in DEFEAT state is expressed as

$$\begin{aligned}
\tau_{WS_i} &= \sum_{s=0}^{B} c(s,0)_{WS_i} = \frac{\sum_{s=0}^{B}\gamma_{WS_i}^{s}}{\sum_{i=0}^{B}\gamma_{WS_i}^{s}(\frac{w_s+2}{2})} \\
\tau_{DS_i} &= \sum_{s=0}^{L} c(s,0)_{DS_i} = \frac{\sum_{s=0}^{L}\gamma_{DS_i}^{s}}{\sum_{i=0}^{L}\gamma_{DS_i}^{s}(\frac{w_s+2}{2})}
\end{aligned}, \tag{4.28}$$

respectively.

The mean duration that Node i is in WIN state and that in DEFEAT state is expressed as

$$\begin{aligned}\Theta_{WS_i} &= (1-\tau_{WS_i})\,\sigma + \tau_{WS_i}\left[(1-\gamma_{WS_i})T + \gamma_{WS_{(i,j)}}T_c\right] \\ \Theta_{DS_i} &= (1-\tau_{DS_i})\,\sigma + \tau_{DS_i}\left[(1-\gamma_{DS_i})T + \gamma_{DS_i}T_c\right]\end{aligned}, \tag{4.29}$$

where $T_c = DIFS + FRAME$. When Node 0 or 3 is in the front part, the node belongs to between the two states. Because WIN state and DEFEAT state appear alternatively, the probability that Node i belongs to WIN state is expressed as the ratio of Θ_{WS_i} to the sum of Θ_{WS_i} and Θ_{DS_i}, namely

$$\Omega_i = \frac{\Theta_{WS_i}}{\Theta_{WS_i} + \Theta_{DS_i}}. \tag{4.30}$$

The collision probability of front part with respect to Node i is obtained as

$$\gamma_{FP_i} = \Omega_i\gamma_{WS_i} + (1-\Omega_i)\gamma_{DS_i} \tag{4.31}$$

Because the DEFEAT state is composed of rear parts, the collision probability of rear part with respect to Node i is obtained as

$$\gamma_{RP_i} = \gamma_{DS_i}. \tag{4.32}$$

From the backoff-stage-synchronization features of (2) and (3), WIN-state node and DEFEAT-state node appear simultaneously. The transmission frame of Node 0, which is in WIN-state, is collided by Node 3, which is in DEFEAT state, vice versa. Additionally, the transmission frames of Nodes 0 and 3 collide with those of Nodes 1 and 2. A frame transmitted by Node 0 collides with that from Node 3 when BT of Node 3 is smaller than h at the frame-transmission instance of Node 0, vice versa. The probability that BT of Node i, which is in WIN state, is smaller than h is defined as g_{WS_i}. Additionally, the probability that BT of Node$i$, which is in DEFEAT state, is smaller than h is defined as

g_{DS_i}. Therefore, γ_{WS_i} and γ_{DS_i} are expressed as

$$\begin{aligned}
\gamma_{WS_0} &= 1-(1-\tau_1)(1-\tau_2)+g_{DS_3},\\
\gamma_{WS_3} &= 1-(1-\tau_1)(1-\tau_2)+g_{DS_0},\\
\gamma_{DS_0} &= 1-(1-\tau_1)(1-\tau_2)+g_{WS_3},\\
\gamma_{DS_3} &= 1-(1-\tau_1)(1-\tau_2)+g_{WS_0}
\end{aligned} \tag{4.33}$$

where

$$\begin{aligned}
g_{DS_i} &= 1-\frac{\sum_{s=F}^{L}\sum_{t=h}^{w_s} c[s,t]_{DS_i}}{\Theta_{DS_i}}\\
&= 1-\frac{c[0,0]_{DS_i}}{\Theta_{DS_i}}\sum_{s=F}^{L}\left\{\gamma_{DS_i}^{s}\left[\frac{w_s+2}{2}-h+\frac{h(h+1)}{2w_s}\right]\right\}\\
&= 1-\frac{\sum_{s=F}^{L}\left\{\gamma_{DS_i}^{s}\left[\frac{w_s+2}{2}-h+\frac{h(h+1)}{2w_s}\right]\right\}}{\left\{(1-\tau_{DS_i})\,\sigma+\tau_{DS_i}\left[(1-\gamma_{DS_i})T+\gamma_{DS_i}T_c\right]\right\}\times\sum_{i=0}^{L}\gamma_{DS_i}^{s}(\frac{w_s+2}{2})}
\end{aligned} \tag{4.34}$$

and

$$\begin{aligned}
g_{WS_i} &= 1-\frac{\sum_{s=F}^{B}\sum_{t=h}^{w_s} c[s,t]_{WS_i}}{\Theta_{WS_i}}\\
&= 1-\frac{c[0,0]_{WS_i}}{\Theta_{WS_i}}\sum_{s=F}^{B}\left\{\gamma_{WS_i}^{s}\left[\frac{w_s+2}{2}-h+\frac{h(h+1)}{2w_s}\right]\right\}\\
&= 1-\frac{\sum_{s=l}^{B}\left\{\gamma_{WS_i}^{s}\left[\frac{w_s+2}{2}-h+\frac{h(h+1)}{2w_s}\right]\right\}}{\left\{(1-\tau_{WS_i})\,\sigma+\tau_{WS_i}\left[(1-\gamma_{WS_i})T+\gamma_{WS_i}T_c\right]\right\}\times\sum_{i=0}^{B}\gamma_{WS_i}^{s}(\frac{w_s+2}{2})}
\end{aligned} \tag{4.35}$$

4.2 Simulation and Experiment Verifications

In this section, the simulation and experiment are carried out to validate the analysis by network simulator ns-3 [15]. Table 4.2 gives system parameters. The network topology used for the simulation and the experiment is the same as shown in Fig. 3.2. The throughput is calculated from the number of the data frames received Nodes 0 and 3. the data from 10 sec to 30 sec in each simulation are used for avoiding the measurements in the transient state. The throughput is obtained as average of five measurements. The Mesh Access Points (MAPs) [17] shown in Figure 4.4 are used for experiments. Table 4.3 gives the specifications of the WLAN node from [6]. The preliminary experiments as same as [6] for investigating the transmission range and the carrier-sensing range of the MAPs are conducted. As a result, the radius of the transmission range is 60m and the radius of the carrier-sensing range is 115m. Figure 4.5 shows the string topology three-hop network for the experiment. Figure 4.6 shows the experiment environment. The routing table of each MAP is fixed and the distance between each MAP is 45m. The PC 1 generates the UDP traffic streams with fixed packet size by using Multi-GENerator (MGEN) [16]. The PCs 1 and 2 are connected with MAPs 1 and 4 with wired line, respectively. The MAPs 1 and 2, 2 and 3, 3 and 4 are connected with wireless. The measurements are conducted for 30 seconds. The throughput of experiment is obtained as average of five measurements.

Figure 4.7 shows maximum throughput as a function of data-payload size. It is seen from Fig. 4.7 that the maximum throughput from the analytical expressions agree with that from simulations, and experiment quantitatively, that shows the validity of the analytical expressions in this paper. Additionally, we plot analytical result without considering the BSS. It is seen from these plots that the BSS enhances the throughput. This is because BSS has the similar effect as the frame aggregation [13]. It shows occurrence of the coupling effect analytically.

4.3 Conclusion

This chapter has presented analytical expressions for IEEE 802.11 multi-hop networks with BSS. For taking the features of the BSS into account the analytical expressions, the modified Bianchi's Markov-chain models, which express the operation with respect to each network node, have been proposed. Obtained analytical expressions have been verified by the comparison with simulation and experimental results. By comparing the analytical result without the coupling effect, the occurrence of the coupling effect has been shown analytically.

Table 4.1: Relationship between backoff stage and state of nodes

Node 0		Node 3
Backoff stage	State	State
front part	WIN state	DEFEAT state
	DEFEAT state	WIN state
rear part	DEFEAT state	WIN state

Table 4.2: System Parameters

Data rate	18 Mbps
Control bit rate	12 Mbps
ACK frame size	10 bytes
Distance of each node	45m
Transmission range	60m
Carrier-sensing range	115m
ACK	32 μsec
SIFS time ($SIFS$)	16 μsec
DIFS time ($DIFS$)	34 μsec
Buffer size	100 frames
σ	9 μsec
CW_{min}	15
CW_{Max}	1023
L	7

Table 4.3: Specifications of WLAN node

Protocol	IEEE 802.11a
Wireless LAN driver	Atheros reference driver
Wireless LAN card	Atheros AR5213A
	miniPCI card
Transmission range for 18 Mbps	60m
Carrier-sensing range	115m

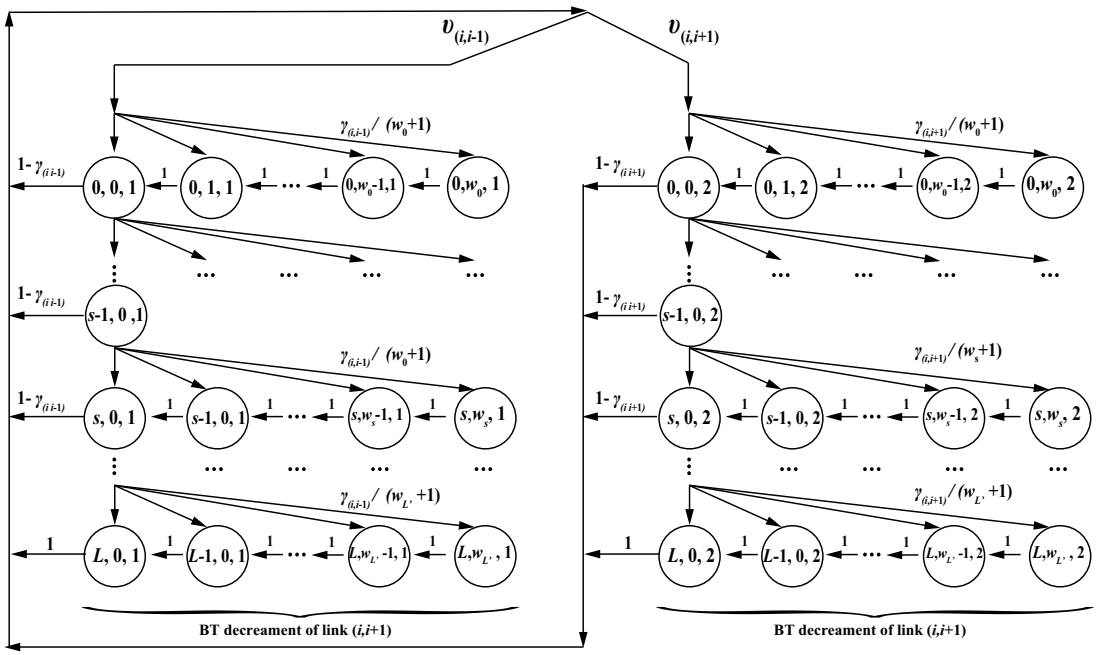

Figure 4.1: Markov chain model considering two-way flows.

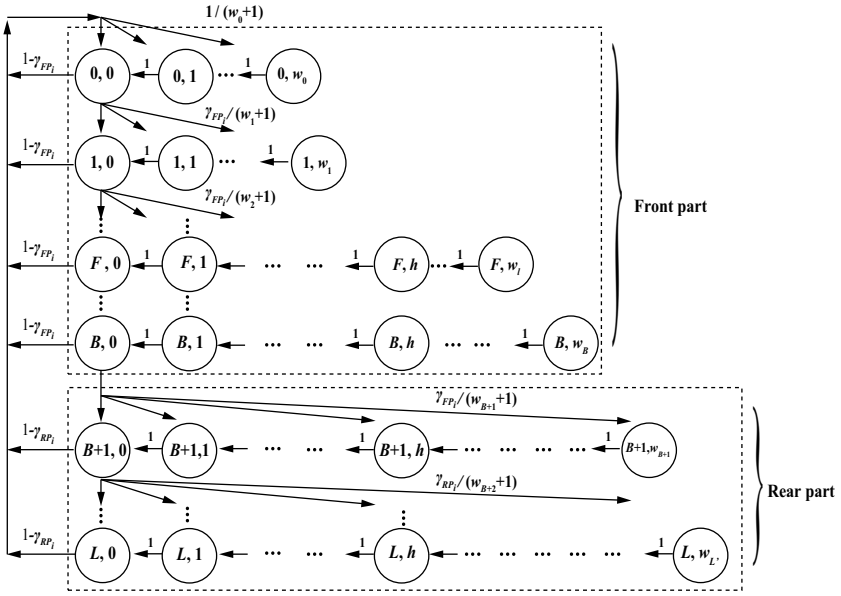

Figure 4.2: Markov-chain model for Nodes 0 and 3 with front part and rear part.

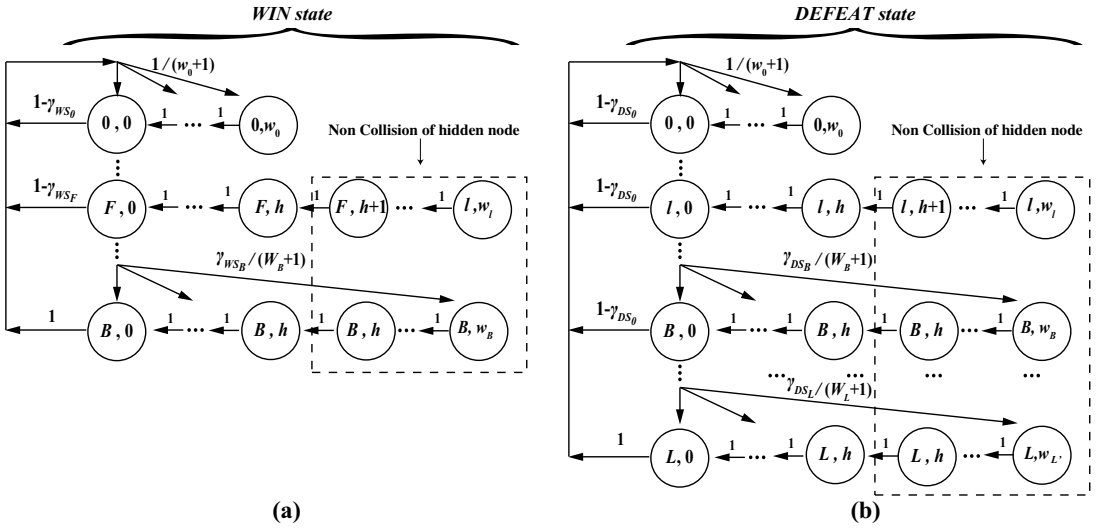

Figure 4.3: Markov-chain model of Node 0 and 3 expressing (a) WIN state and (b) DEFEAT state.

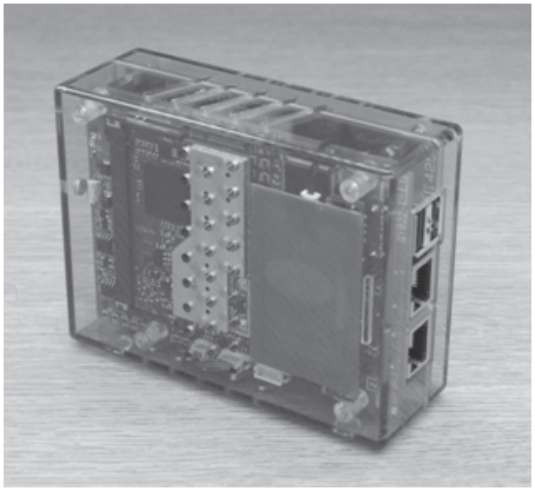

Figure 4.4: Mesh access point (MAP) for experiment.

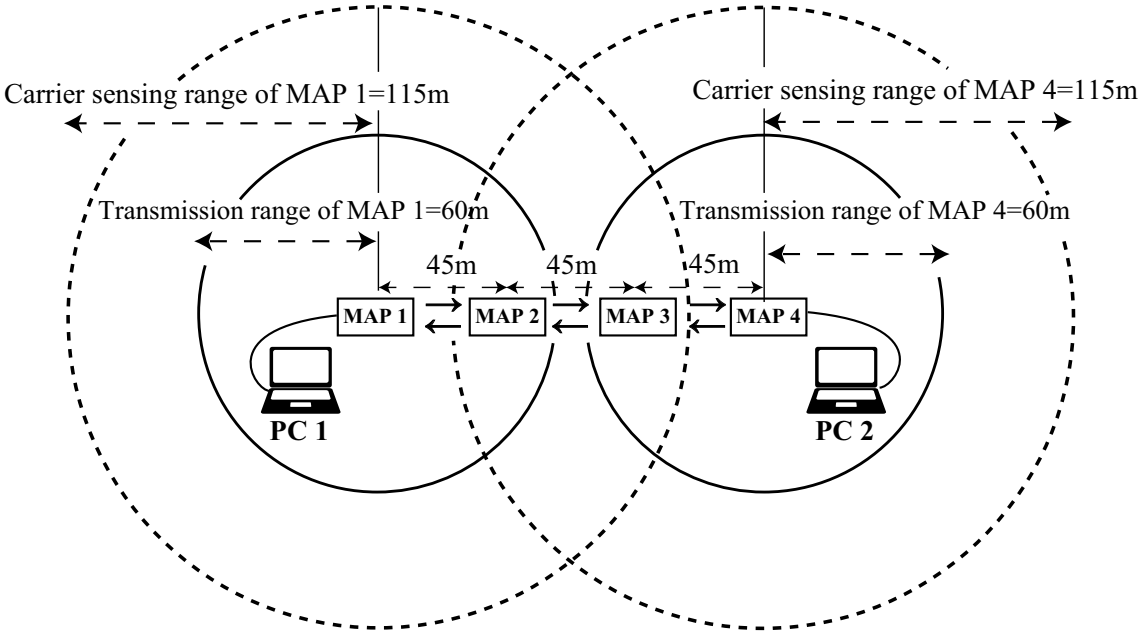

Figure 4.5: String-topology three-hop network for experiment.

Figure 4.6: Experiment environment.

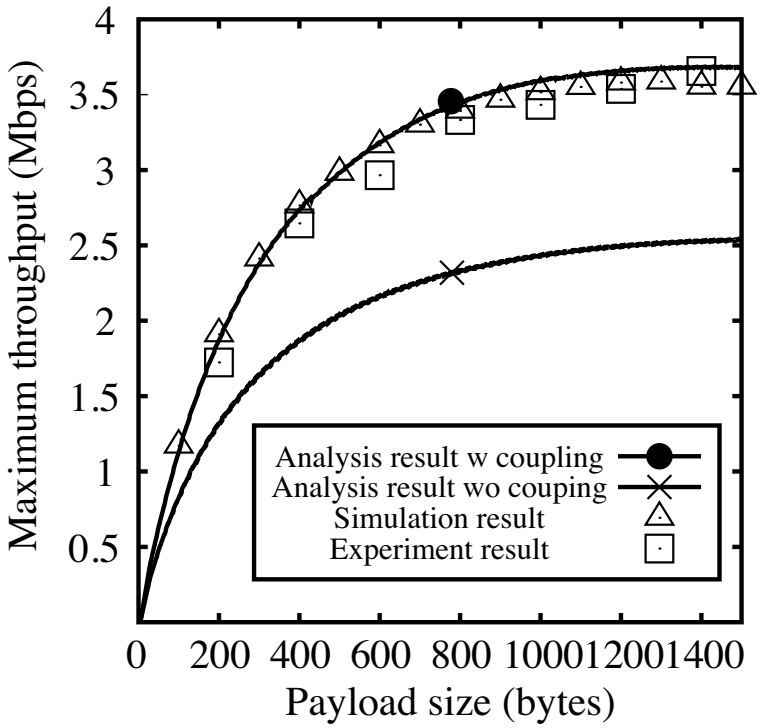

Figure 4.7: Maximum throughput as a function of payload size.

[1] P. C. Ng and S. C. Liew, "Throughput analysis of IEEE 802.11 multi-hop ad hoc networks," *IEEE/ACM Transactions Networking*, vol. 15, no. 2, pp. 309–322, Apr. 2007.

[2] P. C. Ng and S. C. Liew, "Offered load control in IEEE 802.11 multi-hop ad-hoc networks," *IEEE International Conference on Mobile Ad-hoc and Sensor Systems(MASS)*, pp. 80-89, Oct. 2004

[3] Y. Gao, D. Chui, and J. C. S. Lui, "Determining the end-to-end throughput capacity in multi-hop networks: methodology applications," *Proc. the SIGMETRICS/Performance 2006*, pp. 39–50, June. 2006.

[4] H. Zhao, S. Wang, Y. Xi, et al., "Modeling intra-flow contention problem in wireless multi-hop networks, " *IEEE Communications Letters* 14 (1) (2010) 18-20.

[5] J. Yoo and J. Kim, "Maximum end-to-end throughput of chain-topology wireless multi-hop networks," in *Proc. IEEE WCNC*, Hong Kong, China, Mar. 2007, pp. 4279-4283.

[6] M. Inaba, Y. Tsuchiya, H. Sekiya, S. Sakata, and K. Yagyu "Analysis and expression of maximum throughput analysis in wireless multi-hop networks for VoIP Application," *IEICE Trans. on Communications.*, vol. E92-B, no. 11, pp. 3422–3431, Nov. 2009

[7] G. Bianchi,"Performance analysis of the IEEE 802.11 distributed coordination function,"*IEEE J. Sel. Areas Commun*, vol. 18, no. 3, pp. 535-547, Mar. 2000.

[8] Y. Tsuchiya, M. Inaba, M. Matsumoto, H. Sekiya, S. Sakata and K. Yagyu, "Analysis of Maximum UDP Throughput of Short-hop String Networks for VoIP Applications," *Proc. WPMC*, Sept. 2009.

[9] A. Kumar, E. Altman, D. Miorandi, and M. Goyal, "New insights from a fixed-point analysis of single cell IEEE 802.11 WLANs," *IEEE/ACM Trans. Netw.,* vol. 15, pp. 588-601, June 2007.

[10] T. Kim and J. T. Lim, "Throughput analysis considering coupling effect in IEEE 802.11 networks with hidden stations" *IEEE Communication Letters*, vol. 13, no. 3, pp. 175–177, Mar. 2009.

[11] E. Felemban and E. Ekici, "Single Hop IEEE 802.11 DCF Analysis Revisited: Accurate Modeling of Channel Access Delay and Throughput for Saturated and Unsaturated Traffic Cases," *IEEE Trans. Wireless Commun.*, vol. 10, no. 10, pp. 3256-3266, Oct. 2011.

[12] IEEE Computer Society LAN MAN Standards Committee, itPart 11: Wireless LAN medium access control (MAC) and physical layer (PHY) specifications, IEEE Std 802.11 - 1999, Aug. 1999.

[13] K. Sanada, H. Sekiya, N. Komuro and S. Sakata, "Backoff-stage synchronization in three-hop string-topology wireless networks with hidden nodes," *NOLTA, IEICE*, vol. 3, no. 2, pp. 200-214, Apr. 2012.

[14] K. Xu, M. Gerla, S. Bae, "How Effective is the IEEE 802.11 RTS/CTS Handshake in Ad Hoc Networks?", *IEEE, GLOBECOM' 02*, vol. 1, pp. 17–21, Nov. 2002.

[15] The network simulater - ns-3, http://www.nsnam.org

[16] Multi-Generator- MGEN, http://www.nrl.navy.mil/itd/ncs/products/mgen

[17] Koji Omae, "Mobile Ubiquitous Communication Platform Based on Harmonized Cellular and Mesh Networks," IEEE *Consumer Communications and Networking Conference 2005*, Demos, Jan. 2005.

Chapter 5

End-to-End Delay Analysis for IEEE 802.11 String-Topology Multi-hop Networks

●● ABSTRACT ●●

This chapter presents analytical expressions for end-to-end delay for IEEE 802.11 string-topology multi-hop networks. For obtaining those expressions with high accuracy, frame-collision and carrier-sensing probabilities with respect to each node under the non-saturated condition are obtained. A new parameter, which is called as frame-existence probability, is defined for expressing the operation in non-saturated condition. These expressions are associated as a network flow. The end-to-end delay of a string-topology multi-hop network can be derived as the sum of the transmission delays in the network flow. The validity of the analytical expressions are shown by comparing with simulation results.

5.1 End-to-End throughput and Delay Analysis

This chapter presents end-to-end throughput and delay for the IEEE 802.11 string-topology multi-hop networks. The most important contribution of the proposed analysis is that the non-saturated network dynamics model is constructed by using airtimes. In the proposed analytical expressions, all the MAC-layer properties such as frame-collision probability and frame-existence probability are expressed as functions of transmission airtime and offered load. By using the MAC-layer model, the problem of end-to-end delay derivation is narrowed to the transmission-airtime determinations with respect to each node. For obtaining the transmission airtime, the MAC-layer properties of individual nodes are associated to network flow, which is regarded as Network-layer characteristics. By using the associations, the transmission airtimes of network nodes are fixed uniquely and the end-to-end throughput and delay of the string-topology network can be obtained. From the analysis in this paper, we can obtain transmission delays, throughputs, collision probabilities, and frame-existence probabilities as functions of offered load with respect to each node, which provide the end-to-end delay and the end-to-end throughput.

In this chapter, H-hop string-topology multi-hop network as shown in Fig. 2.4 is considered. The analysis in this thesis is based on the following assumptions, which follow the assumptions in [1]-[20].

1. Each node has a single radio transceiver and all the network nodes use the same radio channel.

2. Only the source node (Node 0) generates fixed sized UDP data frames following Poisson distribution. The destination of the frames is Node H.

3. Channel conditions of all the links are ideal. Namely, transmission failures occur only due to frame collisions.

4. Frame collisions between DATA and ACK frames and those among the ACK-frames transmissions can be ignored because ACK-frame length is shorter than DATA-frame length.

5. Node i can transmit DATA and ACK frame only to Nodes $i \pm 1$. Additionally, Nodes $i \pm 1$ and $i \pm 2$ can sense Node-i transmissions. Namely, Nodes i and $i + 3$ are in the hidden node relationships [22].

6. Each node has an infinite buffer for storing frames.

5.1.1 MAC-Layer Operations of Individual Node

5.1.1.1 Airtime

In this analysis, we use the airtime expressions. The transmission airtime of Node i X_i, carrier-sense airtime of Node i Y_i and channel-idle airtime of Node Z_i is obtained as (2.14), (2.15) and (2.16), respectively. It is possible for a node to decrease BT when the channel of the node is in the channel-idle state. In spite of channel-idle state, the node does not work when the node has empty buffer. This is a difference between the saturated and non-saturated conditions.

5.1.1.2 Collision Probability

In string-topology networks, two types of frame collisions with hidden nodes and carrier-sensing range nodes occur. Because these two collisions are disjoint events, the frame-collision probability of Node i is expressed as

$$\gamma_i = \gamma_{H_i} + \gamma_{C_i}, \tag{5.1}$$

where γ_{H_i} is hidden node collision probability of Node i and γ_{C_i} is carrier-sensing nodes collision probability of Node i. γ_{H_i} is obtained as (2.20).

The carrier-sensing range node collisions occur only when the BTs of multiple nodes in the carrier-sensing range are zero simultaneously. In single-hop network such as WLAN, all the nodes decrease the BT simultaneously because they can sense the transmission of the other nodes. In multi-hop networks, however, each node does not decrease the BT simultaneously because of the hidden nodes [3]. For obtaining the expression of γ_{C_i}, therefore, it is necessary to consider that node decreases the BT with respect to carrier-sensing range node of Node i. In the string-topology network as shown in Fig. 2.4, additionally, frame transmissions of Node i does not collide with frames transmitted by Node $i-2$ although Node $i-2$ is in carrier-sensing range of Node i. This is because Node $i-2$ is the outside of the carrier-sensing range of Node $i+1$, which is the receiver of the frames transmitted by Node i. Each node decreases own BT independently. Additionally, each node has different carrier-sense property. Therefore, it is supposed that the frame transmissions of all the nodes are independent events [3], [17]-[20]. From above, the carrier-sensing range node collision probability is obtained as

$$\gamma_{C_i} = 1 - \prod_{\substack{j=i-1 \\ j \neq i}}^{i+2} (1 - \tau_j). \tag{5.2}$$

where τ_i is frame-transmission probability of Node i, which is expressed as the probability that BT of Node i is zero.

5.1.1.3 Frame-Transmission Probability and Frame-Existence Probability

The frame-existence probability is considered for expressing the non-saturated condition in this analysis. The frame-existence probability q_i is defined as the probability that Node i has at least one frame when it is in the channel-idle state. The BT decrement is carried out only when a node, which is in the channel-idle state, has frames. Therefore, an airtime that Node i decreases the BT in whole time can be expressed as

$$W_i = q_i Z_i. \tag{5.3}$$

Because U_i is the average slot number of BT-decrement for one-frame transmission success, the average spending time of BT decrement for one frame transmission success is expressed as $U_i\sigma$, where σ is system slot time. Therefore, an airtime that Node i decreases the BT in whole time is also expressed as

$$W_i = \lambda_i U_i \sigma. \tag{5.4}$$

where λ_i is frame-reception rate of Node i. By equating right-hand side of (5.3) and (5.4), frame-existence probability is obtained as

$$q_i = \frac{\lambda_i U_i \sigma}{Z_i} = \frac{\lambda_i(w_0 + w_1\gamma_i + w_2\gamma_i^2 + \cdots + w_L\gamma_i^L)\sigma}{1 - X_i - \sum\limits_{\substack{j=i-2 \\ j\neq i}}^{i+2} X_j + \sum\limits_{j=i-2}^{i-1}\left(\frac{X_j X_{j+3}}{1 - X_{j+1} - X_{j+2}}\right) + \frac{X_{i-2}X_{i+2}}{1 - X_i}}. \tag{5.5}$$

By using frame-existence probability, transmission probability of Node i in both non-saturated and saturated conditions is

$$\tau_i = W_i G_i = q_i Z_i G_i = \lambda_i(1 + \gamma_i + \gamma_i^2 + \cdots + \gamma_i^L)\sigma. \tag{5.6}$$

In the string-topology network as shown in Fig 2.4, it is regarded that the frame-reception rate of Node i is the same as throughput of Node $i-1$. The reception rate for Node 0 is network offered load O, namely $E_{-1} = O$. From (2.17), the frame-reception rate of Node i is expressed as

$$\lambda_i = \frac{E_{i-1}}{P} = \frac{X_{i-1}(1 - \gamma_{i-1})}{T}. \tag{5.7}$$

5.1.2 Flow Constraint in Multi-hop Networks

The transmission airtimes of network nodes are fixed by taking into account Network-layer properties. Because each airtime depends on the states of neighbor nodes, transmission airtimes of network nodes are associated with Network-layer properties.

When the retransmission counter reaches the retransmission limit L, the frame is dropped following the DCF policy. Therefore, the throughput of each node should satisfy

$$E_i = E_{i-1}(1 - \gamma_i^{L+1}). \tag{5.8}$$

Because $E_{-1} = O$, the relationship in (5.8) expresses the network-layer property with respect to network offered load O.

By eliminating E_i and P from (2.17), (5.7), and (5.8), we have

$$\begin{aligned} X_i &= \frac{\lambda_i T(1 - \gamma_i^{L+1})}{1 - \gamma_i} \\ &= \lambda_i T(1 + \gamma_i + \gamma_i^2 + \cdots + \gamma_i^L) = \lambda_i T R_i. \end{aligned} \tag{5.9}$$

From (5.1), (2.20), (5.2), (5.6), and (5.9), frame-collision probability can be expressed as a function of transmission airtime, namely

$$\gamma_i = 1 - \prod_{\substack{j=i-1 \\ j \neq i}}^{i+2} (1 - \frac{X_j \sigma}{T}) + \frac{a(X_{i+3} + X_i)}{1 - X_{i+1} - X_{i+2}}. \tag{5.10}$$

From (5.7), (5.9), and (5.10), $3H$ algebraic equations are obtained. These equations contain $3H$ unknown parameters, which are X_i, γ_i, and λ_i, for $i = 0, 1, 2, \cdots, H-1$. It is possible to fix the $3H$ unknown parameters when the system parameters and the offered load are given. In this chapter, Newton's method is applied for obtaining the $3H$ unknown parameters. The end-to-end throughput of the network for given O is E_{H-1}.

5.1.3 Comparison with Maximum Throughput Analysis

The frame-existence probabilities increase as the network offered load increases. The increase in the frame-existence probability depends on the network node. This is because the effects of carrier sensing and frame-retransmission number depend on the neighbor node environments. Therefore, a buffer of a certain node becomes full firstly as the offered

load increases. The node is called "bottleneck node". The offered load for which the frame-existence probability of the bottleneck node becomes one is the boundary offered load between the non-saturated and saturated conditions. Generally, the maximum throughput can be obtained for the boundary offered load.

When Node B is the bottleneck node of the flow, q_B should be one. From (5.9), we have

$$X_B = (1 - X_B - Y_B)\frac{R_B}{U_B}\frac{T}{\sigma} = (1 - X_B - Y_B)G_B\frac{T}{\sigma}, \tag{5.11}$$

which is the same as link capacity equation in (2.22). This result means that the analytical expressions presented in this analysis includes all the results of maximum throughput analyses completely, which is one of the evidence of the validity of the proposed expressions.

5.1.4 End-to-End Delay

In the string-topology multi-hop networks as shown in Fig. 2.4, the end-to-end delay is defined as the duration from the instant when a frame is generated at the source node to the one when the frame is received at the destination node, which is the sum of the single-hop transmission delay from Node 0 to Node $H-1$. Each single-hop transmission delay consists of two parts, which are the MAC access delay and the queueing delay.

The MAC access delay is defined as the time interval between the instant when a frame reaches the top of the transmission-node buffer and the one when the frame is transmitted successfully to the next node. Namely, it contains the transmission, BT-freezing, and BT-decrement durations for one-frame transmission success. Note that the frame-existence probability q_i is defined in the channel idle state. It is assumed that the frame existence probability in the carrier-sensing state is the same as that in whole time. The frame-

existence probability in whole time with respect to Node i is expressed as

$$Q_i = X_i + q_i Z_i + Q_i Y_i. \tag{5.12}$$

From (5.12), we obtain

$$Q_i = \frac{X_i + q_i Z_i}{1 - Y_i} = \frac{X_i + q_i Z_i}{X_i + Z_i}. \tag{5.13}$$

Because the ratio of the sum of the BT-freezing and BT-decrement durations to transmission duration is $\frac{Q_i Y_i + q_i Z_i}{X_i}$, the MAC access delay of Node i is expressed as

$$D_{M_i} = TR_i \left(1 + \frac{Q_i Y_i + q_i Z_i}{X_i}\right) = \frac{TR_i(X_i + q_i Z_i)}{X_i(X_i + Z_i)}. \tag{5.14}$$

The queueing delay is the durations from the instant when a frame arrive at Node i to the one when the frame reaches to the top of the buffer. For obtaining the queueing delay, we use M/M/1 buffer-queueing model as shown in Figure 5.1. From the memoryless property of Poisson distribution, buffer queueing is modeled by the birth-and-death process [23]. In Fig. 5.1, μ_i is frame-service rate, which is expressed as

$$\mu_i = \frac{1}{D_{M_i}} = \frac{X_i(X_i + Z_i)}{TR_i(X_i + q_i Z_i)}. \tag{5.15}$$

From (5.9) and (5.15), the utilization rate of Node i is expressed as

$$\rho_i = \frac{\lambda_i}{\mu_i} = \frac{\lambda_i TR_i(X_i + q_i Z_i)}{X_i(X_i + Z_i)} = \frac{X_i + q_i Z_i}{X_i + Z_i}. \tag{5.16}$$

From the buffer-queueing model in Fig. 5.1, the steady-state probability that the Node i has k frame is expressed as

$$\pi_{i,k} = \frac{\lambda_i}{\mu_i}\pi_{i,k-1} = \left(\frac{\lambda_i}{\mu_i}\right)^k \pi_{i,0} = Q_i^k \pi_{i,0}. \tag{5.17}$$

The sum of all the buffer-state probability should be one, we have

$$\sum_{k=0}^{\infty} \pi_{i,k} = \frac{\pi_{i,0}}{1 - Q_i} = 1. \tag{5.18}$$

From (5.17) and (5.18), therefore, we have

$$\pi_{i,k} = Q_i^k - Q_i^{k+1}. \tag{5.19}$$

By using the buffer-state probability, queueing delay of Node i is expressed as

$$\begin{aligned} D_{Q_i} &= \sum_{k=1}^{\infty} \left[\frac{D_{M_i}}{2} + (k-1)D_{M_i} \right] \pi_{i,k} \\ &= D_{M_i} \sum_{k=1}^{\infty} \left[\frac{1}{2} + (k-1) \right] (Q_i^k - Q_i^{k+1}) \\ &= \frac{D_{M_i} Q_i (1+Q_i)}{2(1-Q_i)}. \end{aligned} \tag{5.20}$$

In (5.20), $\frac{D_{M_i}}{2}$ expresses the average time for transmitting the frame in top of the buffer of Node i, and $(k-1)D_{M_i}$ expresses the time from when a frame arrives at Node i, which has k frames in the buffer, to when the frame reaches to top of the buffer. Each single-hop transmission delay consists of D_{M_i} and D_{Q_i}, therefore, transmission delay of Node i is obtained as

$$\begin{aligned} D_i &= D_{M_i} + D_{Q_i} = \frac{D_{M_i}(2 - Q_i + Q_i^2)}{2(1-Q_i)} \\ &= \frac{TR_i Q_i (2 - Q_i + Q_i^2)}{2X_i(1-Q_i)}. \end{aligned} \tag{5.21}$$

Because the end-to-end delay is the sum of the single-hop transmission delay from Node 0 to Node H, the end-to-end delay of string-topology network is

$$D = \sum_{i=0}^{H-1} D_i = \sum_{i=0}^{H-1} \frac{TR_i Q_i (2 - Q_i + Q_i^2)}{2X_i(1-Q_i)}. \tag{5.22}$$

It is seen from (2.23), (5.5), (5.10), and (5.13) that the end-to-end delay is a function of transmission airtime. Therefore, we can obtain the end-to-end throughput and end-to-end delay by deriving the fixed airtime from (5.9).

5.2 Simulation Verification

In this section, the validities of the obtained analytical expressions in this chapter are discussed by comparing with simulation results. Table 5.1 gives the system parameters for evaluations. These parameters are based on the IEEE 802.11a [24]. The network topologies used for the simulations are the string-topology H-hop networks as shown in Fig. 2.4. An original simulator, which was implemented by author, was used in this paper because it is necessary to obtain the detailed data from simulations. The credibility of the simulator is confirmed by quantitative agreements of throughputs compared with the results from ns-3 simulator [25].

Figure 5.2 shows maximum end-to-end throughputs versus number of hops. In Fig. 5.2, analytical results from [6] are also plotted. Fig. 5.2 shows that the maximum throughputs obtained from the analytical expressions in this paper agree with those from [6]. It can be stated from this result that the proposed analytical expressions include the maximum analytical expressions in [6] completely, which is one of the validities of our analytical expressions. Namely, the installation of the frame-existence probability does not affect the maximum throughput derivations and the proposed analytical expressions provide all the results obtained from [6]. In [6], it is necessary to find a bottleneck node by brute-force computations. In the proposed analytical expressions, a bottleneck node can be comprehended by checking the frame-existence probability of each node.

Figure 5.3 shows frame-existence probabilities in nine-hop network versus the offered load at fixed node number. Fig. 5.2 and Fig. 5.3 show that the maximum throughput of nine-hop network is obtained when the frame-existence probability of Node 2 reaches one at $O = 0.65$ Mbps. It is seen from Fig. 5.3 that Node 2 is the bottleneck node of nine-hop. The bottleneck node of the network can be detected because the frame-existence probabilities with respect to each node are expressed individually.

Figure 5.4 shows the collision probabilities of nine-hop network versus offered load for fixed node number. Fig. 5.4 shows that the collision probabilities from analytical expressions agree with those from simulation results qualitatively. However, there are some differences of the collision probabilities at light offered loads. This analysis assumes that only Node 0 generates data frames, which are relayed along the network flow. When Nodes i and $i+3$ transmit frames simultaneously, only the frame transmission from Node i to Node $i+1$ is in failure due to the hidden-node collision. For example, we consider how to appear the situation that Nodes 3 and 6 have frames simultaneously when the offered load is light. It can be considered naturally that this situation appears via the situations that Nodes 0 and 3, Nodes 1 and 4, and Nodes 2 and 5 have frames simultaneously. However, when the frame collisions occur in above three situations, there is low possibility that Nodes 3 and 6 have frames simultaneously. Namely, the situation appearance probability that Node i and $i+3$ have a frame simultaneously are decreases as i increases in actual network dynamics in low offered load, in particular. Therefore, the frame-collision probability also decreases as the increase in the node number. In the analytical model, however, it is assumed that arrival interval of the frame at each node follows Poisson distribution independently and the amount of frame arrivals depends on the throughput of the previous node, which means that the situation-appearance probabilities are uniform at light offered loads. Therefore, the collision probabilities at nodes, which have a hidden node, are identical in the analytical model at light offered loads.

On the other hand, it can be confirmed from Fig. 5.4 that the analytical results agree with the simulation results in the saturated condition. Nodes $i+1$ or $i+2$ has a frame when Nodes i and $i+3$ have frame in saturated condition. Namely the network dynamics satisfies our assumptions in the saturated condition. Therefore, the difference between analytical expressions and simulation results disappear. Additionally, this result shows the validity of the assumption "the probability that a frame transmitted by Node i is

collided with a frame from Node $i+3$ due to the Node $i+3$ transmission start" is the approximately equal to "the probability that Node i transmits a DATA frame when the BT of Node $i+3$ is zero" [1]-[8].

Fig. 5.4 shows that collision probabilities of Nodes 0 and 3 are much higher than those of Node 6 as shown in Fig. 5.4. This is because Nodes 0 and 3 have a hidden node. It is confirmed from Fig. 5.4 that the hidden node and carrier-sensing range node collisions, can be expressed. The presented analytical expressions are valid for cases when there are not only nodes with hidden node but also nodes without hidden node in the network flow.

Figure 5.5 shows transmission delays in nine-hop network versus offered load for fixed node number. It is confirmed from Fig. 5.4 and Fig. 5.5 that the analytical expressions reflect high correlated relationship between the frame-collision probability and transmission delay. It can be obviously understood that the transmission delay increases as the frame-collision probability increases. The frame-existence probability in (5.13) contains the effect of frame-transmission collisions as shown in (5.5). By expressing the transmission delay as a function of the frame-existence probability as given in (5.21), the effect of frame-collision probability can be reflected on the transmission delay can be expressed. It is confirmed from Fig. 5.5 that the transmission delay with respect to each node can be predicted with high accuracy at any offered load.

Figure 5.6 shows end-to-end delays versus offered load for fixed hop numbers. It is seen from Fig. 5.6 that end-to-end delays obtained from analytical expressions show the quantitative agreements with those obtained from simulations regardless of the hop number and offered load.

In the analytical model, the queueing delay of each node is derived by M/M/1 queueing model. The distribution of MAC access delay in the one-hop network with one transmitter and one receiver follows uniform distribution because no collision occurs. Therefore, it can be considered naturally that the variance of MAC access delay in one-hop network

based on M/M/1 queueing model is higher than that in simulations. This is the reason why end-to-end delay from the analytical expressions for one-hop network is larger than that from simulation at one-hop network.

Figure 5.7 shows end-to-end delays versus offered load for one-hop network. One-hop network topology is identical to one-station WLAN topology. Therefore, the end-to-end delay for one station case from the WLAN analysis in [9] are also plotted in Fig. 5.7. Fig. 5.7 shows that analytical results from the proposed model agree with those from [9] well. Additionally, analytical results from the proposed model show good agreements with simulation ones, which is one of the evidences of the validities of the network-delay expressions in (5.21).

Figure 5.8 shows end-to-end delays of the nine-hop network versus offered load. In Fig. 5.8, analytical results from the proposed analytical expressions and from the model in [20] are plotted. It is seen from Fig. 5.8 that analytical results in [20] have differences from simulation results. This is because the MAC layer properties of network nodes are considered in average. Namely it is assumed that all the properties are identical for all the network nodes in the conventional analysis approach. Therefore, the asymmetric properties with respect to each network node cannot be expressed in [20]. Fig. 5.8 shows that analytical results from the proposed expressions agree with simulation result well. This is because the MAC-layer properties with respect to each node can be expressed individually in the presented analysis. This paper presents an approach in which analytical expressions of individual node are associated as network flow by using the flow constraint. It is confirmed from Fig. 5.8 that the proposed analysis approach is effective for expressing the analysis of multi-hop network property.

5.3 Conclusion

This chapter has presented analytical expressions for end-to-end delay for IEEE 802.11 string-topology multi-hop networks. For obtaining those expressions with high accuracy, frame-collision and carrier-sensing probabilities with respect to each node under the non-saturated condition have been obtained. A new parameter, which is called as frame-existence probability, has been defined for expressing the operation in non-saturated condition. These expressions have been associated as a network flow. The end-to-end delay of a string-topology multi-hop network can be derived as the sum of the transmission delays in the network flow. The validity of the analytical expressions have been shown by comparing with simulation results.

Table 5.1: System Parameters

Frame payload(P)	100 bytes
Data rate	18 Mbps
ACK bit rate	12 Mbps
$DATA$	84 μsec
ACK	32 μsec
$SIFS$	16 μsec
$DIFS$	34 μsec
slot time(σ)	9 μsec
CW_{min}	15
CW_{Max}	1023
Retransmission limit(L)	7

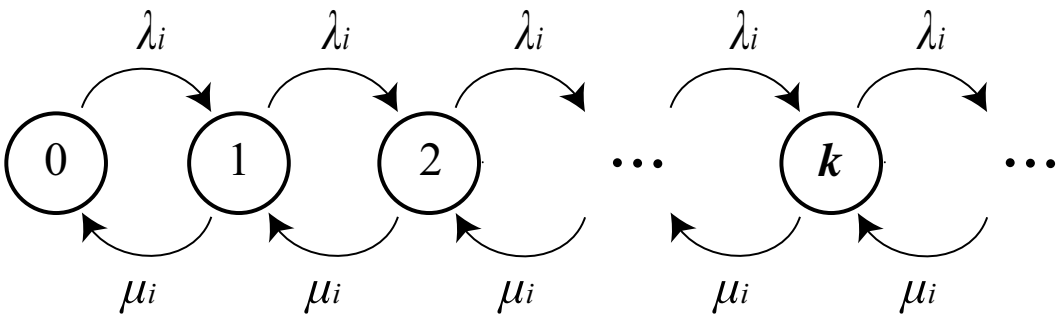

Figure 5.1: Buffer-queueing model of Node i.

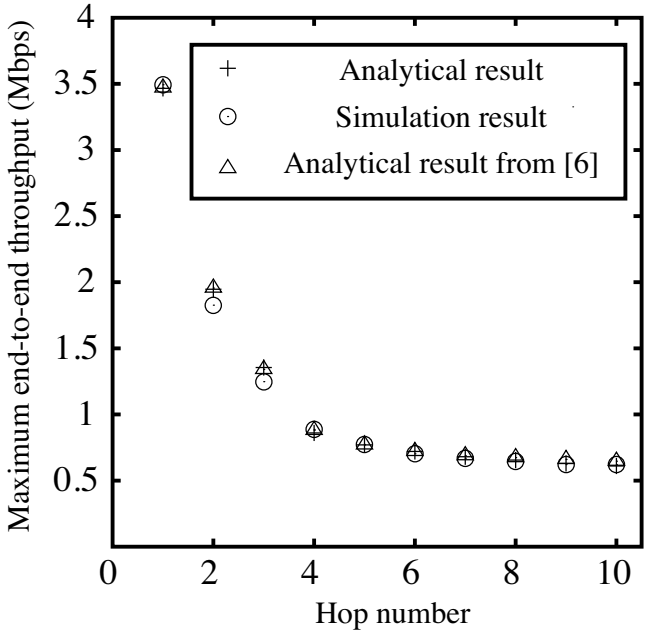

Figure 5.2: Maximum throughput versus number of hops.

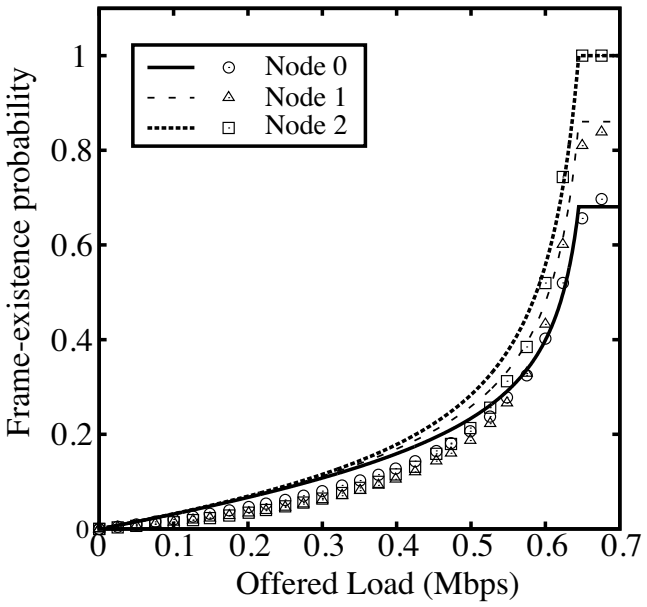

Figure 5.3: Frame-existence probabilities of analytical (lines) and simulation (plots) results versus the offered load for fixed node numbers in nine-hop network.

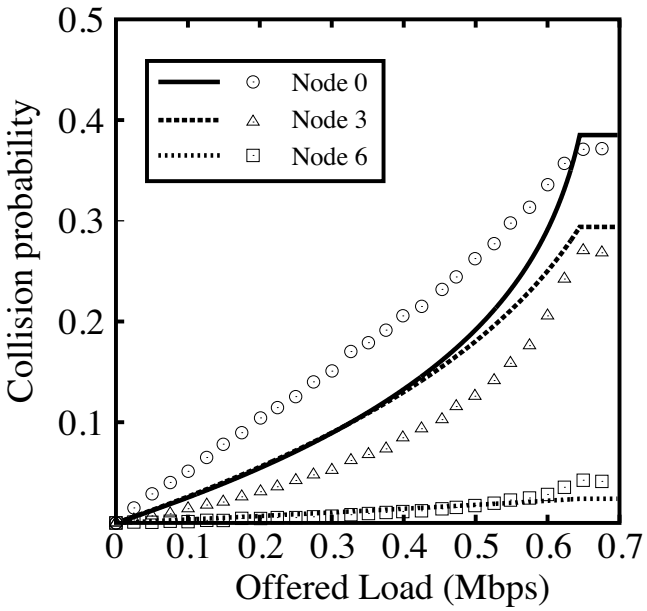

Figure 5.4: Collision probabilities of analytical (lines) and simulation (plots) results versus offered load for fixed node numbers in nine-hop network.

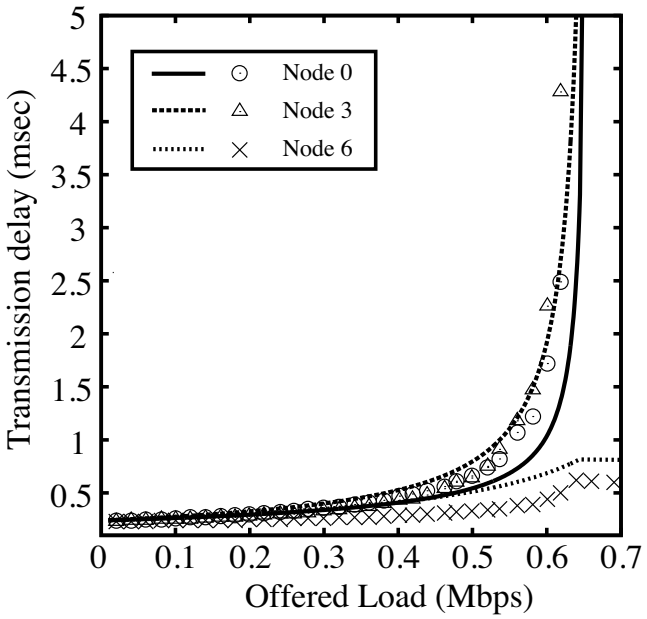

Figure 5.5: Transmission delays of analytical results (lines) and simulation ones (plots) versus offered load for fixed node numbers in nine-hop network.

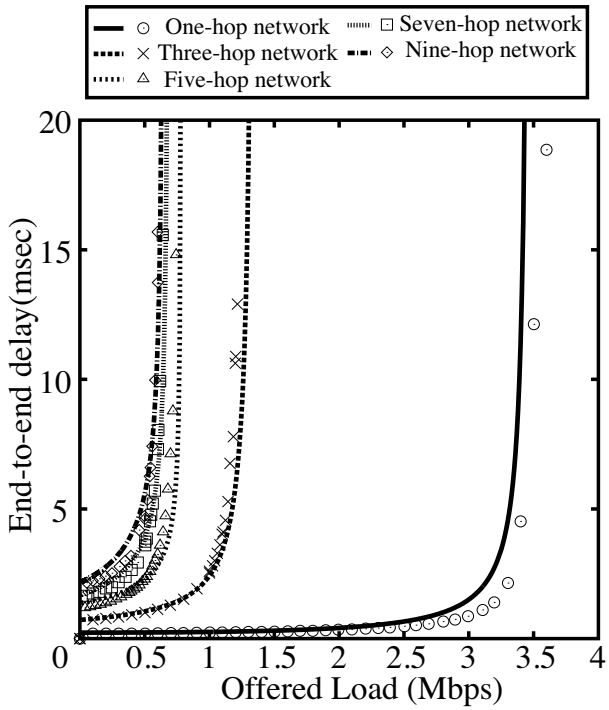

Figure 5.6: End-to-end delays of analytical results (lines) and simulation ones (plots) versus offered load for fixed hop numbers.

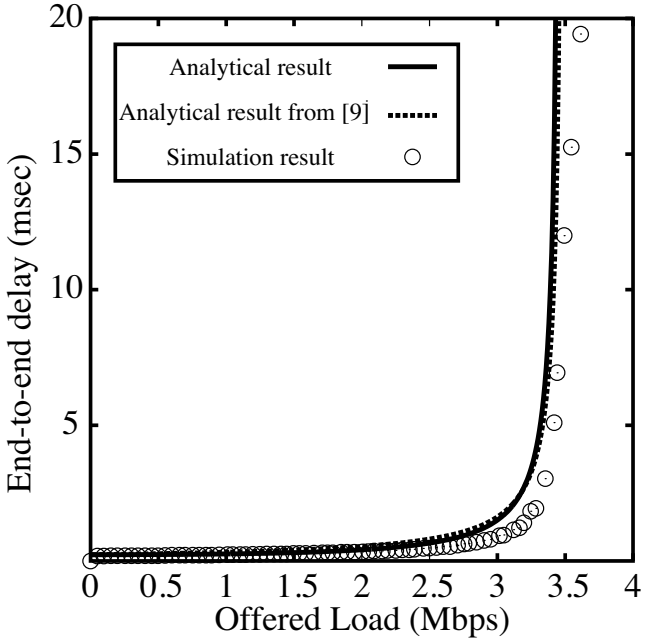

Figure 5.7: End-to-end delays of analytical results (lines) and simulation ones (plots) versus offered load for one-hop network.

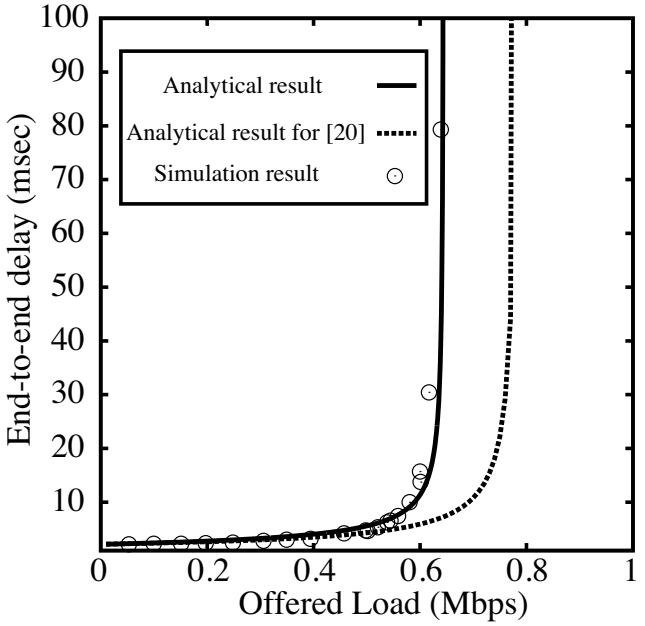

Figure 5.8: End-to-end delay of nine-hop network versus offered load.

Reference

[1] P. C. Ng and S. C. Liew, "Throughput analysis of IEEE 802.11 multi-hop ad hoc networks," *IEEE/ACM Trans. Networking*, vol. 15, no. 2, pp. 309-322, Apr. 2007.

[2] M. Inaba, Y. Tsuchiya, H. Sekiya, S. Sakata, and K. Yagyu "Analysis and expression of maximum throughput analysis in wireless multi-hop networks for VoIP Application," *IEICE Trans. Communications.*, vol. E92-B, no. 11, pp. 3422–3431, Nov. 2009.

[3] H. Zhao, E. Garcia-Palacios, S. Wang, J. Wei, D. Ma, "Evaluating the impact of network density, hidden nodes and capture effect for throughput guarantee in multi-hop wireless networks". *Ad Hoc Networks*, vol. 11, no. 1, pp. 54-69. Jan. 2013.

[4] H. Sekiya, Y. Tsuchiya, N. Komuro, and S. Sakata, "Maximum throughput for long-frame communication in one-way string wireless multi-hop networks," *Wireless personal communications*, vol. 60, no. 1, pp. 29-41, Mar. 2011.

[5] Y. Gao, D. Chui, and J. C. S. Lui, "The fundamental role of hop distance in IEEE 802.11 multi-hop ad-hoc networks," *IEEE International Conference on Network Protocol*, Boston, Massachusetts, USA, Nov. 2005.

[6] Y. Gao, D. Chui, and J. C. S. Lui, "Determining the end-to-end throughput capacity in multi-hop networks: methodology applications," *ACM Special Interest Group on Performance Evaluation 2006*, pp. 39-50, Jun. 2006.

[7] T. D. Senthilkumar, A. Krishnan, P. Kumar. "New approach for throughput analysis of IEEE 802.11 in adhoc networks". *IEEE International Conference on Control Communication and Automation*, Kanpur, India, pp. 148-153, Dec. 2008.

[8] H. Zhao, S. Wang, Y. Xi, Wei J, "Modeling intra-flow contention problem in wireless multi-hop networks", *IEEE Communications Letters* , vol. 14, no. 1, pp. 18-20, Jan. 2010.

[9] Q.L. Zhao, D.H.K. Tsang, and T. Sakurai, "Modeling nonsaturated IEEE 802.11 DCF networks utilizing an arbitrary buffer size," *IEEE Trans. Mobile Computing*, vol. 10, no. 9, pp. 1248-1263, Nov. 2011.

[10] A. Banchs, P. Serrano, and A. Azcorra, "End-to-end delay analysis and admission control in 802.11 DCF WLANs" *Elsevier Computer Commubications* , vol. 29, no. 7, pp. 842-854, Apr. 2006.

[11] G. R. Gupta and N. B. Shroff, "Delay analysis for multi-hop wireless networks," *IEEE INFOCOM*, Rio de Janeiro, Brazil, pp. 412-421, Apr. 2009.

[12] Y. Chen, Y. Tang, and I Darwazeh. "A Cross-layer analytical model of end-to-end delay performance for wireless multi-hop environments. *IEEE Global Telecommunication Conference 2010*, Miami, Florida, USA, pp. 1-6, Dec. 2010.

[13] X. Min and H. Martin, "Towards an end-to-end delay analysis of wireless multihop networks," *Ad Hoc Networks*, vol. 7, no. 5, pp. 849-861, Jul. 2009.

[14] A. Abdullah, F. Gebali, and L.Cai, "Modeling the throughput and delay in wireless multihop ad-hoc networks," *IEEE Global Telecommunication Conference*, Honolulu, Hawaii, USA, pp. 1-6, Nov. 2009.

[15] Khalaf, R. and Rubin, I. "Throughput and delay analysis single hop and multi hop IEEE 802.11 networks" *The Third International Conference on Broadband Communications* , Networks, and Systems, San Jose, California, USA, pp. 1-9, Oct. 2006.

[16] N. Bisnik and A. Abouzeid, "Queuing network models for delay analysis of multihop wireless ad hoc networks," *Ad Hoc Networking* , vol. 7, no.1, pp. 79-97, Jan. 2009.

[17] R. Khalaf, I. Rubin, J. Hsu, "Throughput and delay analysis of multihop IEEE 802.11 networks with capture", *IEEE International Conference on Communications*, pp. 3787-3792, Jun. 2007.

[18] H. Li, Y. Cheng, C. Zhou, and W. Zhuang. "Minimizing end-to-end delay: a novel routing metric for multi-radio wireless mesh networks" *IEEE International Conference on Communications* , Glasgow, Scotland, pp. 46-54, Apr. 2009.

[19] W. Jiao, M. Sheng, and K. S. Lui and Y. Shi "End-to-end delay distribution analysis for stochastic admission control in multi-hop wireless networks," *IEEE Trans. Wireless Communications*, vol. 13, no. 3, pp. 1308-1320, Mar. 2014.

[20] Ghadimi. E, Khonsari. A, Diyanat. A, Frarmani. M, Yazdani. N, "An analytical model of delay in multi-hop wireless ad hoc networks", *Wireless Networks* , vol. 17, no. 7, pp. 1679-1697, Oct. 2011.

[21] A. Kumar, E. Altman, D. Miorandi, and M. Goyal,"New insights from a fixed point analysis of single cell IEEE 802.11 WLANs," *IEEE/ACM trans. Networking*, vol. 15, no. 3, pp. 538-601, Jun. 2007.

[22] K. Xu, M. Gerla, S. Bae, "How effective is the IEEE 802.11 RTS/CTS handshake in ad hoc networks?",*IEEE Global Telecommunication Conference 2002*, Taipei, Taiwan, vol. 1, pp. 17-21, Nov. 2002.

[23] H. Kobayashi, B. L. Mark, System modeling and analysis: foundations of system performance evaluation, Upper Saddle River, NJ: Pearson Education, Inc., 2009.

[24] IEEE Computer Society LAN MAN Standards Committee, *Part 11: Wireless LAN medium access control (MAC) and physical layer (PHY) specifications*, IEEE Std 802.11-1999, Aug. 1999.

[25] The network simulater - ns3, http://www.nsnam.org

Chapter 6

Analytical Expressions of End-to-End Throughput for IEEE 802.11 Multi-hop Networks

●● ABSTRACT ●●

This chapter presents analytical expressions for IEEE 802.11 string-topology multi-hop networks. The analytical expressions obtained in this paper give end-to-end throughput at any hop number, any frame length, and any offered load by taking into account relationship between BT decrement and transmission time and Markov-chain model for two-way flow. The analytical expressions are verified by comparisons with simulation results.

6.1 Analytical expressions of end-to-end throughput for IEEE 802.11 multi-hop networks

This chapter presents analytical expressions for IEEE 802.11 string-topology multi-hop networks. For achieving that, the proposed analysis procedure includes two proposals, which are: (i) a relationship between the backoff timer and frame length can be expressed by merging the Bianchi's Markov-chain model [17] and airtime expression [1]-[9], (ii) the Bianchi's Markov-chain models are modified for expressing the transmission process of two-way flows with asymmetric offered-load individually. In the proposed model, the problem of end-to-end throughput and delay derivation is narrowed to the transmission-airtime determinations with respect to each link. For obtaining the transmission airtime, the MAC-layer properties of individual nodes are associated to network flow, which is regarded as Network-layer characteristics. By using the associations, the transmission airtimes of network links are fixed uniquely and the end-to-end throughput and delay of the string-topology network can be obtained.

Figure. 6.1 shows the network topology considered in this chapter. In this chapter, H-hop string topology with two-way flow, which is named Flow 1 and Flow 2, is considered. The source and destination nodes of Flow 1 is Nodes 0 and H, respectively. At Flow 2, Nodes H and 0 are the source and destination nodes, respectively. The network link from Node i to Node $i \pm 1$ is expressed as $(i, i \pm 1)$. The analysis in this paper is based on the following assumptions [1]-[7], [15]-[28]

1. Each node has a single radio transceiver and all the network nodes use the same radio channel.

2. Only the source nodes (Nodes 0 and H) generate fixed sized UDP data frames, payload size of which is P bytes, following Poisson distribution. The destinations

of the frames generated by Nodes 0 is Nodes H, and vice versa.

3. Channel conditions of all the links are ideal. Namely, transmission failures occur only due to frame collisions.

4. Frame collisions between DATA and ACK frames and those among the ACK-frames transmissions can be ignored because ACK-frame length is shorter than DATA-frame length. [1]-[7]

5. Node i can transmit DATA and ACK frame only to Nodes $i \pm 1$. Additionally, Nodes $i \pm 1$ and $i \pm 2$ can sense Node-i transmissions. Namely, Nodes i and $i \pm 3$ are in the hidden node relationships [28]

6.1.1 Airtime and Throughput

In this chapter, we use the airtime expressions. The transmission airtime for $(i, i \pm 1)$ is obtained as (4.1). Because Node i has two links, the transmission airtime of Node i is expressed as

$$X_i = x_{(i,i+1)} + x_{(i,i-1)}, \tag{6.1}$$

where $x_{(0,-1)} = x_{(H,H+1)} = 0$.

By using the airtime expressions, the throughput for $(i, i \pm 1)$ is expressed as (4.5)

The carrier-sense airtime of Node i Y_i and the channel-idle airtime of Node Z_i is obtained as (2.15) and (2.16), respectively.

6.1.2 Transmission Probability and Collision Probability: Markov Chain Model for Two-way Flows

6.1.2.1 Transmission Probability

Figure 6.2 shows the Markov-chain model for BT-decrement and transmission states model of Node i. In Fig. 6.2, $h = DATA/\sigma$ and F is the minimum backoff stage which satisfies $h \leq w_s$.

The Markov-chain model is defined in the DATA-frame transmission and channel idle state, which includes BT-decrement state. The durations of ACK transmission, SIFS and DIFS are not included in the Markov-chain model. In the previous analyses, the BT-decrement state and the DATA frame-transmission one are considered separately as shown in Fig 2.2. Therefore, the relationship between two states are ignored, which is a reason why the previous analyses are valid for long-frame communications [7]. By including the transmission state in Bianchi's Markov-chain model as shown in Fig. 6.2, the relationship between the BT-decrement time and frame length can be expressed explicitly. Additionally, the BT-decrement and frame transmission for Flow 1 and Flow 2 of Node i are modeled separately and they are coupled by flow-usage probabilities. It is assumed that the flow usage probability for $(i, i \pm 1)$ is the rate of the frame-reception rate of $(i, i \pm 1)$ and the frame-reception rate of Node i. Therefore, the flow-usage probability for $(i, i \pm 1)$ is expressed as

$$\upsilon_{(i,i\pm1)} = \frac{\lambda_{(i,i\pm1)}}{\Lambda_i} = \frac{\lambda_{(i,i\pm1)}}{\lambda_{(i,i-1)} + \lambda_{(i,i+1)}}. \tag{6.2}$$

In (6.2), Λ_i is frame-reception rate of Node i and $\lambda_{(i,i\pm1)}$ is frame-reception rate for $(i, i\pm1)$, which is expressed as

$$\lambda_{(i,i\pm1)} = \frac{e_{(i,i\pm1)}}{P} = \frac{x_{(i,i\pm1)}(1 - \gamma_{(i,i\pm1)})}{T}. \tag{6.3}$$

From above modeling, it is possible to express the transmission process of two-way flows

with asymmetric offered-load. In Fig. 6.2, the transition probabilities among the states are

$$\begin{aligned}
&P\{[s,t-1,f]|[s,t,f]\} = 1 \\
&P\{[s,t,1]|[s-1,-h,1]\} = \frac{\gamma_{(i,i+1)}}{w_s+1}, && 0 \le t \le w_s \\
&P\{[0,t,1]|[s,-h,f]\} = \frac{\upsilon_{(i,i+1)}(1-\gamma_{(i,i+1)})}{w_0+1} && 0 \le t \le w_0 \\
&P\{[0,t,1]|[L,-h,f)\} = \frac{\upsilon_{(i,i+1)}}{w_0+1} && 0 \le t \le w_0 \\
&P\{[s,t,2]|[s-1,-h,2]\} = \frac{\gamma_{(i,i-1)}}{w_s+1}, && 0 \le t \le w_s \\
&P\{[0,t,2]|[s,-h,f]\} = \frac{\upsilon_{(i,i-1)}(1-\gamma_{(i,i-1)})}{w_0+1} && 0 \le t \le w_0 \\
&P\{[0,t,2]|[L,-h,f)\} = \frac{\upsilon_{(i,i-1)}}{w_0+1} && 0 \le t \le w_0
\end{aligned} \tag{6.4}$$

Let $b[s,t,f]_i$ be the stationary distribution of the Markov-chain model. In this Markov-chain model, the sum of the stationary distributions of the Markov-chain model is equal to one, namely

$$\begin{aligned}
\sum_{s=0}^{L}\sum_{t=-h}^{w_s}\sum_{f=1}^{2} b[s,t,f]_i &= \sum_{s=0}^{L}\left(b[s,0,1]_i + b[s,0,2]_i\right)\left(h+\frac{w_s+2}{2}\right) \\
&= \sum_{s=0}^{L}\left(\gamma^s_{(i,i+1)}b[0,0,1]_i + \gamma^s_{(i,i-1)}b[0,0,2]_i\right)\left(h+\frac{w_s+2}{2}\right) \\
&= 1.
\end{aligned} \tag{6.5}$$

From (6.4), we obtain

$$\begin{aligned}
b[0,0,1]_i &= \upsilon_{(i,i+1)}(1-\gamma_{(i,i+1)})\sum_{s=0}^{L-1} b[s,-h,1]_i + \upsilon_{(i,i+1)}b[L,0,1] \\
&\quad +\upsilon_{(i,i+1)}(1-\gamma_{(i,i-1)})\sum_{s=0}^{L-1} b[s,-h,2]_i + \upsilon_{(i,i+1)}b[L,0,2] \\
&= \upsilon_{(i,i+1)}b[0,0,1]_i + \upsilon_{(i,i+1)}b[0,0,2]_i,
\end{aligned} \tag{6.6}$$

from which

$$\frac{b[0,0,1]_i}{b[0,0,2]_i} = \frac{\upsilon_{(i,i+1)}}{1-\upsilon_{(i,i+1)}} = \frac{\upsilon_{(i,i+1)}}{\upsilon_{(i,i-1)}}. \tag{6.7}$$

By submitting (6.7) into (6.5), we obtain

$$\begin{aligned} b[0,0,1]_i &= \frac{\upsilon_{(i,i+1)}}{\sum_{s=0}^{L}\left(\upsilon_{(i,i+1)}\gamma^s_{(i,i+1)} + \upsilon_{(i,i-1)}\gamma^s_{(i,i-1)}\right)\left(h + \frac{w_s+2}{2}\right)} \\ b[0,0,2]_i &= \frac{\upsilon_{(i,i-1)}}{\sum_{s=0}^{L}\left(\upsilon_{(i,i+1)}\gamma^s_{(i,i+1)} + \upsilon_{(i,i-1)}\gamma^s_{(i,i-1)}\right)\left(h + \frac{w_s+2}{2}\right)} \end{aligned}. \tag{6.8}$$

Transmission probability of Node i in saturated condition is obtained as

$$\begin{aligned} \tau'_i &= \frac{\sum_{s=0}^{L} b[s,0,1]_i + \sum_{s=0}^{L} b[s,0,2]_i}{\sum_{s=0}^{L}\sum_{t=0}^{W_s} b[s,t,1]_i + \sum_{s=0}^{L}\sum_{t=0}^{W_s} b[s,t,2]_i} \\ &= \frac{b[0,0,1]_i \sum_{s=0}^{L}\gamma^s_{(i,i+1)} + b[0,0,2]_i \sum_{s=0}^{L}\gamma^s_{(i,i-1)}}{b[0,0,1]_i \sum_{s=0}^{L}\frac{\gamma^s_{(i,i+1)}(W_s+2)}{2} + b[0,0,2]_i \sum_{s=0}^{L}\frac{\gamma^s_{(i,i-1)}(w_s+2)}{2}} \\ &= \frac{\upsilon_{(i,i+1)} \sum_{s=0}^{L}\gamma^s_{(i,i+1)} + \upsilon_{(i,i-1)} \sum_{s=0}^{L}\gamma^s_{(i,i-1)}}{\upsilon_{(i,i+1)} \sum_{s=0}^{L}\frac{\gamma^s_{(i,i+1)}(w_s+2)}{2} + \upsilon_{(i,i-1)} \sum_{s=0}^{L}\frac{\gamma^s_{(i,i-1)}(w_s+2)}{2}}. \end{aligned} \tag{6.9}$$

The operation in non-saturation condition is not considered in the proposed Markov-chain model. Transmission probability in both non-saturated and saturated condition is contained for the product of transmission probability in saturated condition and frame-existence probability [10], [16]. By using frame existence probability of Node i Q_i, the transmission probability of Node i is expressed as

$$\tau_i = q_i \tau'_i. \tag{6.10}$$

From the explanation in Section. 5.1.1.3, the frame-existence probability of Node i is

obtained as

$$q_i = \frac{\left(\upsilon_{(i,i+1)} u_{(i,i+1)} + \upsilon_{(i,i-1)} u_{(i,i-1)}\right) \Lambda_i (1 - V_i)\sigma}{Z_i}, \tag{6.11}$$

where V_i is the buffer-blocking probability of Node i. The expression of V_i is described in Section 6.1.4. $u_{(i,i\pm1)}$ is the average slot number of BT-decrement for one-frame transmission success for $(i, i \pm 1)$, which is expressed as

$$u_{(i,i\pm1)} = \sum_{s=0}^{L} \frac{\gamma_{(i,i\pm1)}^{s}(w_s + 2)}{2}. \tag{6.12}$$

By substituing (6.11) and (6.12) into (6.10), q_i is eliminated, namely

$$\tau_i = \frac{\Lambda_i(1 - V_i)\sigma \left(\upsilon_{(i,i+1)} \sum_{s=0}^{L} \gamma_{(i,i+1)}^{s} + \upsilon_{(i,i-1)} \sum_{s=0}^{L} \gamma_{(i,i+1)}^{s} \right)}{Z_i} \tag{6.13}$$

6.1.2.2 Collision Probability

In string-topology networks, two types of frame collisions with carrier-sensing range nodes and hidden nodes occur. Because these two collisions are disjoint events, the frame-collision probability of $(i, i \pm 1)$ is expressed as

$$\gamma_{(i,i\pm1)} = \gamma_{C_{(i,i\pm1)}} + \gamma_{H_{(i,i\pm1)}}, \tag{6.14}$$

where $\gamma_{H_{(i,i\pm1)}}$ is hidden node collision probability of $(i, i \pm 1)$ and $\gamma_{C_{(i,i\pm1)}}$ is carrier-sensing nodes collision probability of $(i, i \pm 1)$.

The carrier-sensing range node collisions occur only when the BTs of multiple nodes in the carrier-sensing range are zero simultaneously. From the explanation of [6], [10], [17]-[25], the carrier-sensing range node collision probability is obtained as

$$\begin{aligned} \gamma_{C_{(i,i+1)}} &= 1 - \prod_{\substack{j=i-1 \\ j\neq i}}^{i+2} (1 - \tau_j) \\ \gamma_{C_{(i,i-1)}} &= 1 - \prod_{\substack{j=i-2 \\ j\neq i}}^{i+1} (1 - \tau_j) \end{aligned}. \tag{6.15}$$

A hidden node collision occurs when Node i starts to transmit a frame for Node $i \pm 1$ during the Node $i \pm 3$ transmitting a DATA-frame. When Node $i \pm 3$ is in data-transmission state at the instant that the BT of Node i is zero, hidden node collision occurs. Therefore, the collision probability of this type of hidden-node collision is expressed as

$$\gamma^{(1)}_{H_{(i,i\pm1)}} = \frac{(aX_{i\pm3} + q_{i\pm3}Z_{i\pm3}) \left(\sum_{s=0}^{L} \sum_{t=-h}^{-1} \sum_{f=1}^{2} b[s,t,f]_{i\pm3} \right)}{1 - X_{i\pm1} - X_{i\pm2}}. \tag{6.16}$$

Additionally, a hidden-node collision also occurs when Node $i \pm 3$ starts to transmit a frame during the Node-i transmission for Node $i \pm 1$. Namely, when "BT of Node $i \pm 3$ is smaller than h" and "Nodes $i \pm 4$ and $i \pm 5$, which are the carrier-sensing range nodes of Node $i \pm 3$, are not in transmission state" at the instant that the BT of Node i is zero, the collision occurs. Therefore, this type of hidden-node collision probability is expressed as

$$\begin{aligned} \gamma^{(2)}_{H_{(i,i\pm1)}} = & \left[(aX_{i\pm3} + q_{i\pm3}Z_{i\pm3}) \left(\sum_{s=0}^{F-1} \sum_{t=0}^{W_s} \sum_{f=1}^{2} b[s,t,f]_{i\pm3} + \sum_{s=F}^{L} \sum_{t=1}^{h} \sum_{f=1}^{2} b[s,t,f]_{i\pm3} \right) \right] \\ & \times \frac{1 - (X_{i\pm4} + X_{i\pm5})}{1 - X_{i\pm1} - X_{i\pm2}}. \end{aligned} \tag{6.17}$$

Because the two types of hidden node collisions are disjoint events, the hidden node collision-probability is

$$\gamma_{H_{(i,i\pm1)}} = \gamma^{(1)}_{H_{(i,i\pm1)}} + \gamma^{(2)}_{H_{(i,i\pm1)}}. \tag{6.18}$$

6.1.3 Flow Constraint in Multi-hop Networks

The transmission airtimes of network nodes are fixed by taking into account Network-layer properties. Because each airtime depends on the states of neighbor nodes, transmission airtimes of network nodes are associated with Network-layer properties.

When the retransmission counter reaches the retransmission limit L, the frame is dropped following the DCF policy. Additionally, the frame is dropped when the buffer of

receiver is full. Therefore, the throughput of each node should satisfy

$$e_{(i,i\pm1)} = e_{(i\mp1,i)}(1-\gamma_{(i\mp1,i)}^{L+1})(1-V_i). \tag{6.19}$$

The relationship in (6.19), which is called as the flow-constraint condition, expresses the network-layer property. By eliminating E_i and P from (4.5), (6.3), and (6.19), we have

$$\begin{aligned} x_{(i,i\pm1)} &= \frac{\lambda_{(i,i\pm1)}(1-V_i)T(1-\gamma_{(i,i\pm1)}^{L+1})}{1-\gamma_{(i,i\pm1)}} \\ &= \lambda_{(i,i\pm1)}(1-V_i)T(1+\gamma_{(i,i\pm1)}+\gamma_{(i,i\pm1)}^2+\cdots+\gamma_{(i,i\pm1)}^L) \\ &= \lambda_{(i,i\pm1)}(1-V_i)Tr_{(i,i\pm1)}, \end{aligned} \tag{6.20}$$

where $r_{(i,i\pm1)}$ is the average number of transmission attempts for $(i, i\pm1)$. From (6.1) (6.2) and (6.20), we have

$$X_i = \Lambda_i(1-V_i)T(\upsilon_{(i,i+1)}r_{(i,i+1)}+\upsilon_{(i,i+1)}r_{(i,i+1)}), \tag{6.21}$$

From (2.16), (6.13) and (6.20), transmission probability can be expressed as a function of transmission airtime, namely

$$\begin{aligned} \tau_i &= \frac{X_i\sigma}{Z_iT} \\ &= \frac{\left(x_{(i,i+1)}+x_{(i,i-1)}\right)\sigma}{T}\Bigg/\Bigg[1-\sum_{\substack{j=i-2\\ j\neq i}}^{i+2}\left(x_{(j,j+1)}+x_{(j,j-1)}\right) \\ &\quad -\sum_{j=i-2}^{i-1}\left(\frac{(x_{(j,j+1)}+x_{j,j-1})(x_{(j+3,j+4)}+x_{j+3,j+2})}{1-x_{(j+1,j+2)}-x_{(j+1,j)}-x_{(j+2,j+3)}-x_{(j+2,j+1)}}\right) \\ &\quad -\frac{(x_{(i-2,i-1)}+x_{i-2,i-3})(x_{(i+2,i+3)}+x_{i+2,i+1})}{1-x_{(i,i+1)}-x_{(i,i-1)}}\Bigg]. \end{aligned} \tag{6.22}$$

From (6.2), (6.11), (6.12), (6.20) and (6.21), we have

$$\begin{aligned} aX_i + q_i Z_i &= \Lambda_i(1-V_i)\sigma\left[\upsilon_{(i,i+1)}\left(u_{(i,i+1)} + hr_{(i,i+1)}\right) + \upsilon_{(i,i-1)}\left(u_{(i,i-1)} + hr_{(i,i-1)}\right)\right] \\ &= \Lambda_i(1-V_i)\sigma \times \left[\upsilon_{(i,i+1)}\left(\sum_{s=0}^{L}\frac{\gamma^s_{(i,i\pm1)}(w_s+2)}{2} + h\sum_{s=0}^{L}\gamma^s_{(i,i+1)}\right)\right. \\ &\quad \left. + \upsilon_{(i,i-1)}\left(\sum_{s=0}^{L}\frac{\gamma^s_{(i,i-1)}(w_s+2)}{2} + h\sum_{s=0}^{L}\gamma^s_{(i,i-1)}\right)\right] \\ &= \Lambda_i(1-V_i)\sigma \times \left[\sum_{s=0}^{L}\left(\gamma^s_{(i,i+1)}\upsilon_{(i,i+1)} + \gamma^s_{(i,i-1)}\upsilon_{(i,i-1)}\right) \times \left(\frac{w_s+2}{2} + h\right)\right] \\ &= \frac{\Lambda_i(1-V_i)\sigma}{b[0,0,1] + b[0,0,2]}. \end{aligned} \tag{6.23}$$

By submitting (6.20) and (6.23) into (6.16) and (6.17), $\gamma^{(1)}_{(i,i\pm1)}$ and $\gamma^{(2)}_{(i,i\pm1)}$ can be expressed as a function of transmission airtime and collision probability, namely

$$\begin{aligned} \gamma^{(1)}_{H_{(i,i\pm1)}} &= \Lambda_{i\pm3}(1-V_{i\pm3})\sigma\left[\upsilon_{(i\pm3,i\pm4)}\sum_{s=0}^{L}\sum_{t=-1}^{-h}\gamma^s_{(i\pm3,i\pm4)}\right. \\ &\quad \left. + \upsilon_{(i\pm3,i\pm2)}\sum_{s=0}^{L}\sum_{t=-1}^{-h}\gamma^s_{(i\pm3,i\pm2)}\right] \times \frac{1}{1-X_{i\pm1}-X_{i\pm2}}. \\ &= \frac{aX_{i\pm3}}{1-X_{i\pm1}-X_{i\pm2}} \end{aligned} \tag{6.24}$$

and

$$\begin{aligned} \gamma^{(2)}_{H_{(i,i\pm1)}} &= \left\{\sum_{s=0}^{F-1}(\lambda_{(i\pm3,i\pm4)}\gamma^s_{(i\pm3,i\pm4)} + \lambda_{(i\pm3,i\pm2)}\gamma^s_{(i\pm3,i\pm2)})(\frac{w_s}{2})\right. \\ &\quad + \sum_{s=F}^{L}\left[(\lambda_{(i\pm3,i\pm4)}\gamma^s_{(i\pm3,i\pm4)} + \lambda_{(i\pm3,i\pm2)}\gamma^s_{(i\pm3,i\pm2)})\right. \\ &\quad \left.\left.\left(h+1-\frac{h^2+h}{2w_s+2}\right)\right]\right\}\frac{(1-V_{i\pm3})(1-X_{i\pm4}-X_{i\pm5})}{1-X_{i\pm1}-X_{i\pm2}} \end{aligned} \tag{6.25}$$

From (6.1), (6.13), (6.14), (6.15), (6.24) and (6.25), collision probability of $(i, i\pm1)$ is

rewritten as

$$
\begin{aligned}
\gamma_{(i,i+1)} = 1 - & \prod_{\substack{j=i-1 \\ j\neq i}}^{i+2} (1-\tau_j) \\
& + \frac{a(x_{(i+3,i+4)} + x_{(i+3,i+2)})}{1 - x_{(i+1,i+2)} - x_{(i+1,i)} - x_{(i+2,i+3)} - x_{(i+2,i+1)}} \\
& + \left\{ \sum_{s=0}^{F-1} (\lambda_{(i+3,i+4)} \gamma^s_{(i+3,i+4)} + \lambda_{(i+3,i+2)} \gamma^s_{(i+3,i+2)}) (\frac{w_s+2}{2}) \right. \\
& + \sum_{s=F}^{L} \left[(\lambda_{(i+3,i+4)} \gamma^s_{(i+3,i+4)} + \lambda_{(i+3,i+2)} \gamma^s_{(i+3,i+2)}) \right. \\
& \left. \left. \times \left(h + 1 - \frac{h^2+h)}{2w_s+2} \right) \right] \right\} \times (1 - V_{i+3}) \\
& \times \frac{1 - x_{(i+4,i+5)} - x_{(i+4,i+3)} - x_{(i+5,i+6)} - x_{(i+5,i+4)}}{1 - x_{(i+1,i+2)} - x_{(i+1,i)} - x_{(i+2,i+3)} - x_{(i+2,i+1)}} \\
\gamma_{(i,i-1)} = 1 - & \prod_{\substack{j=i-2 \\ j\neq i}}^{i+1} (1-\tau_j) \\
& + \frac{a(x_{(i-3,i-4)} + x_{(i-3,i-2)})}{1 - x_{(i-1,i-2)} - x_{(i-1,i)} - x_{(i-2,i-3)} - x_{(i-2,i-1)}} \\
& + \left\{ \sum_{s=0}^{F-1} (\lambda_{(i+3,i+4)} \gamma^s_{(i+3,i+4)} + \lambda_{(i+3,i+2)} \gamma^s_{(i-3,i-2)}) (\frac{w_s+2}{2}) \right. \\
& + \sum_{s=F}^{L} \left[(\lambda_{(i-3,i-4)} \gamma^s_{(i-3,i-4)} + \lambda_{(i-3,i-2)} \gamma^s_{(i-3,i-2)}) \right. \\
& \left. \left. \times \left(h + 1 - \frac{h^2+h)}{2w_s+2} \right) \right] \right\} \times (1 - V_{i-3}) \\
& \times \frac{1 - x_{(i-4,i-5)} - x_{(i-4,i-3)} - x_{(i-5,i-6)} - x_{(i-5,i-4)}}{1 - x_{(i-1,i-2)} - x_{(i-1,i)} - x_{(i-2,i-3)} - x_{(i-2,i-1)}}
\end{aligned}
\quad . \tag{6.26}
$$

6.1.4 Buffer-Blocking Probability

Figure 6.3 shows the buffer queuing model of Node i, where K is the buffer size and μ_i is frame-service rate of Node i. The frame-service time is defined as the average time interval between the instant when a frame reaches the top of the transmission-node buffer and the one when the frame is transmitted successfully to the next node. Namely, it contains the transmission, BT-freezing, and BT-decrement durations for one-frame transmission success. Note that the frame-existence probability q_i is defined in the channel idle state.

It is assumed that the frame existence probability in the carrier-sensing state is the same as that in whole time [10]. The frame-existence probability in whole time with respect to Node i is expressed as The frame-existence probability in whole time with respect to Node i is expressed as

$$Q_i = X_i + q_i Z_i + Q_i Y_i. \tag{6.27}$$

where Q_i is frame existence probability of Node i. From (6.27), we obtain

$$Q_i = \frac{X_i + q_i Z_i}{1 - Y_i} = \frac{X_i + q_i Z_i}{X_i + Z_i}. \tag{6.28}$$

Because the ratio of the sum of the BT-freezing and BT-decrement durations to transmission duration is $\frac{Q_i Y_i + q_i Z_i}{X_i}$, the frame-service time of Node i is expressed as

$$\begin{aligned} D_{M_i} &= T(\upsilon_{(i,i+1)} r_{(i,i+1)} + \upsilon_{(i,i+1)} r_{(i,i+1)}) \left(1 + \frac{Q_i Y_i + q_i Z_i}{X_i}\right) \\ &= \frac{X_i + q_i Z_i}{\Lambda_i (1 - V_i)(X_i + Z_i)}. \\ &= \frac{\lambda_{(i,i+1)}(Tr_{(i,i+1)} + \sigma u_{(i,i+1)}) + \lambda_{(i,i-1)}(Tr_{(i,i-1)} + \sigma u_{(i,i-1)})}{\Lambda_i (X_i + Z_i)} \\ &= \frac{\upsilon_{(i,i+1)}(Tr_{(i,i+1)} + \sigma u_{(i,i+1)}) + \upsilon_{(i,i-1)}(Tr_{(i,i-1)} + \sigma u_{(i,i-1)})}{X_i + Z_i}. \end{aligned} \tag{6.29}$$

Therefore, the frame-service rate of Node i is expressed as

$$\begin{aligned} \mu_i &= \frac{1}{D_{M_i}} \\ &= \frac{X_i + Z_i}{\upsilon_{(i,i+1)}(Tr_{(i,i+1)} + \sigma u_{(i,i+1)}) + \upsilon_{(i,i-1)}(Tr_{(i,i-1)} + \sigma u_{(i,i-1)})}. \end{aligned} \tag{6.30}$$

From (6.21) and (6.30), utilization rate of Node i is obtained as

$$\begin{aligned}\rho_i &= \frac{\Lambda_i}{\mu_i} \\ &= \frac{\lambda_{(i,i+1)}(Tr_{(i,i+1)} + \sigma u_{(i,i+1)}) + \lambda_{(i,i-1)}(Tr_{(i,i-1)} + \sigma u_{(i,i-1)})}{X_i + Z_i}. \\ &= \frac{X_i + q_i Z_i}{(X_i + Z_i)(1 - V_i)}. \\ &= \frac{Q_i}{1 - V_i}. \end{aligned} \tag{6.31}$$

From the buffer-queueing model in Fig. 6.3, the steady state probability that the Node i has k frame is expressed as

$$\pi_{i,k} = \frac{\Lambda_i}{\mu_i}\pi_{i,k-1} = \left(\frac{\Lambda_i}{\mu_i}\right)^k \pi_{i,0} = \rho_i^k \pi_{i,0}. \tag{6.32}$$

The sum of all the buffer-state probability should be one, we have

$$\sum_{k=0}^{K} \pi_{i,k} = \frac{(1 - \rho_i^{K+1})\pi_{i,0}}{1 - \rho_i} = 1. \tag{6.33}$$

From (6.32) and (6.33), therefore, we have

$$\pi_{i,k} = \frac{\rho_i^k - \rho_i^{k+1}}{1 - \rho_i^{K+1}}. \tag{6.34}$$

Because the buffer-blocking probability is the same as the steady state probability that the Node i has K frame, namely

$$\begin{aligned} V_i &= \pi_{i,K} \\ &= \frac{\rho_i^K - \rho_i^{K+1}}{1 - \rho_i^{K+1}} \\ &= \frac{\left(\frac{Q_i}{1 - V_i}\right)^K - \left(\frac{Q_i}{1 - V_i}\right)^{K+1}}{1 - \left(\frac{Q_i}{1 - V_i}\right)^{K+1}}. \end{aligned} \tag{6.35}$$

From (2.16), (6.12), (6.20) and (6.31), we obtain

$$\begin{aligned}
\rho_i &= \frac{Q_i}{1-V_i} \\
&= \Big[x_{(i,i+1)} + x_{(i,i-1)} \\
&\quad + \lambda_{(i,i+1)} \sum_{s=0}^{L} \frac{(w_s+2)\gamma^s_{(i,i+1)}}{2} + \lambda_{(i,i-1)} \sum_{s=0}^{L} \frac{(w_s+2)\gamma^s_{(i,i-1)}}{2} \Big] \\
&\quad / \Bigg[1 - \sum_{\substack{j=i-2 \\ j\neq i}}^{i+2} (x_{(j,j+1)} + x_{j,j-1}) \\
&\quad - \sum_{j=i-2}^{i-1} \left(\frac{(x_{(j,j+1)} + x_{j,j-1})(x_{(j+3,j+4)} + x_{j+3,j+2})}{1 - x_{(j+1,j+2)} - x_{(j+1,j)} - x_{(j+2,j+3)} - x_{(j+2,j+1)}} \right) \\
&\quad - \frac{(x_{(i-2,i-1)} + x_{i-2,i-3})(x_{(i+2,i+3)} + x_{i+2,i+1})}{1 - x_{(i,i+1)} - x_{(i,i-1)}} \Bigg]. \qquad (6.36)
\end{aligned}$$

From above expression, buffer blocking probability is a function of transmission airtime and collision probability and frame-reception rate.

From (6.3), (6.20), (6.26) and (6.35), $7H$ algebraic equations are obtained. These equations contain $8H$ unknown parameters, which are $x_{(i,i\pm1)}$, $\gamma_{(i,i\pm1)}$, $\lambda_{(i,i\pm1)}$, and V_i, for $i = 0, 1, 2, \ldots, H$. It is possible to fix the $7H$ unknown parameters and the offered loads are given. In this paper, Newton's method is applied for obtaining the $7H$ unknown parameters.

6.2 Simulation Verification

In this section, the analytical expressions proposed in this chapter are verified by comparing with simulation results. Table 6.1 gives system parameters based on the IEEE 802.11a standards [29]. The network topologies used for the simulations are the string-topology H-hop networks as shown in Fig. 6.1. An original simulator, which was implemented by authors, was used in this paper because it is necessary to obtain the detailed

data from simulations. The credibility of the simulator is confirmed by quantitative agreements of simulator is compared with the results from ns-3 simulator [30].

6.2.1 One-way flow

Figure 6.4 shows end-to-end throughputs of six-hop network with one-way flow versus offered load of Flow 1 for $O_2 = 0$ Mbps and $P = 200$ bytes. Fig. 6.4 shows that quantitative agreements with simulation ones. At $O_1 = 1.15$ Mbps, the maximum throughput is obtained. The end-to-end throughput is saturated at $O_1 = 1.6$ Mbps. It is confirmed analytical expression presented in this paper can express the network behavior both in non-saturated condition and saturated one.

Figure 6.5 shows maximum throughputs of eight-hop network versus payload size. Fig. 6.5 shows that all the results from proposed analysis, analysis in [1], and simulations show quantitative agreements in short-frame length. The throughput obtained from [1] has difference from the simulation result as the payload size increases. The proposed analysis gives accurate maximum throughput prediction regardless of the payload size. This result shows that the importance to consider the relationship between the BT decrement time and frame-transmission one for achieving the accurate predictions.

6.2.2 Two-way flow

Figure 6.6 shows end-to-end throughput in five-hop network as a function of O_1 for O_2 = 0.8 Mbps, $P = 200$ bytes. At $O_1 = 0$, the network flow is only Flow 2, namely one-way flow. For $0 < O_1 < 0.3$ Mbps, throughput of Flow 2 keeps 0.8 Mbps and that of Flow 1 increases in proportion to O_1. This means that network is in non-saturation state. The maximum network throughput can be obtained at $O_1 = 0.3$ Mbps, in which the frame existence probability of Node 4 is one. Namely, Node 4 is the bottleneck node in this

scenario. In the range of 0.3 Mbps $\leq O_1 \leq$ 1.5 Mbps, throughput of Flow 2 decreases in spite of $O_2 = 0.8$ Mbps. This result denotes that buffer over flow occurs at the bottleneck node. At $O_1 = O_2 = 0.8$ Mbps, throughput of Flow 1 is the same as that of Flow 2 because of symmetric offered load. For $O_1 > 1.5$ Mbps, both throughputs of Flow 1 and Flow 2 are constant regardless of O_1.

It is confirmed from Fig. 6.6 that the analytical predictions agree with the simulation results quantitatively. This means that the analytical equations presented in this paper can express all the situations described above. Namely, analytical expressions are valid for asymmetric offered loads including the one-way flow case, non-saturation conditions, and saturation ones.

Table 6.1: System Parameters

Data rate	18 Mbps
ACK bit rate	12 Mbps
ACK	32 μsec
SIFS time ($SIFS$)	16 μsec
DIFS time ($DIFS$)	34 μsec
Buffer size (K)	100 frames
slot time(σ)	9 μsec
CW_{min}	15
CW_{Max}	1023
Retransmission limit(L)	7

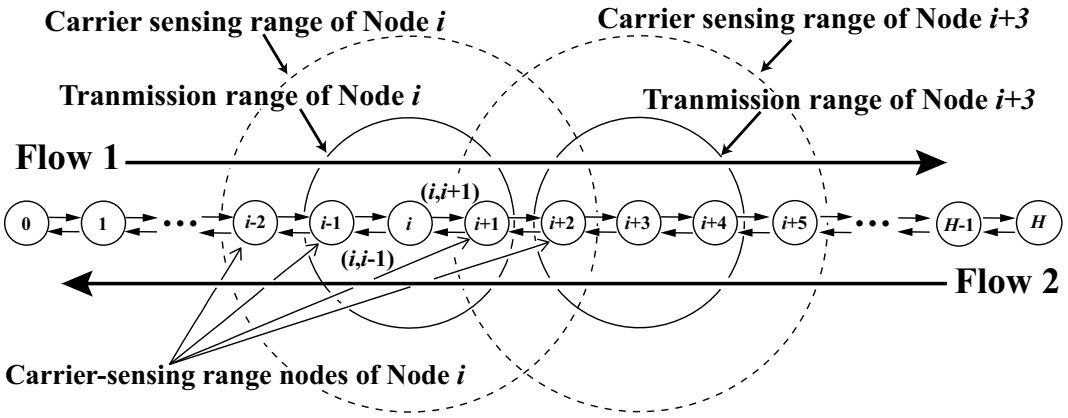

Figure 6.1: H-hop string-topology network with two-way flow.

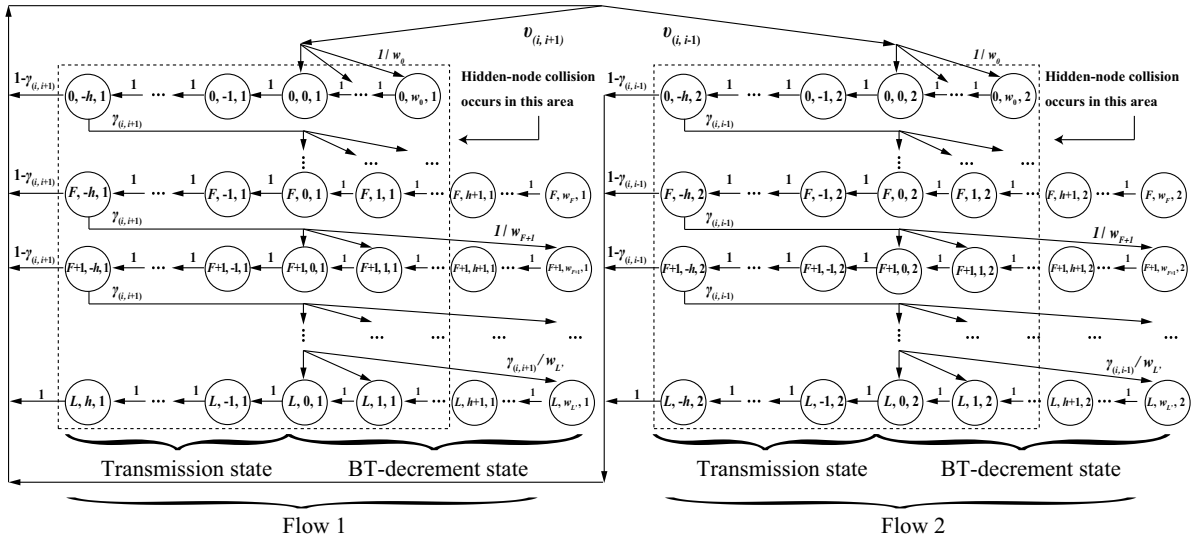

Figure 6.2: Markov-chain model for BT-decrement and transmission state model of Node i.

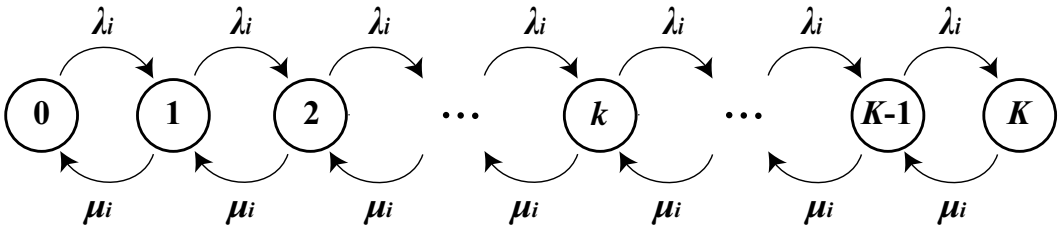

Figure 6.3: Buffer-queueing model of Node i.

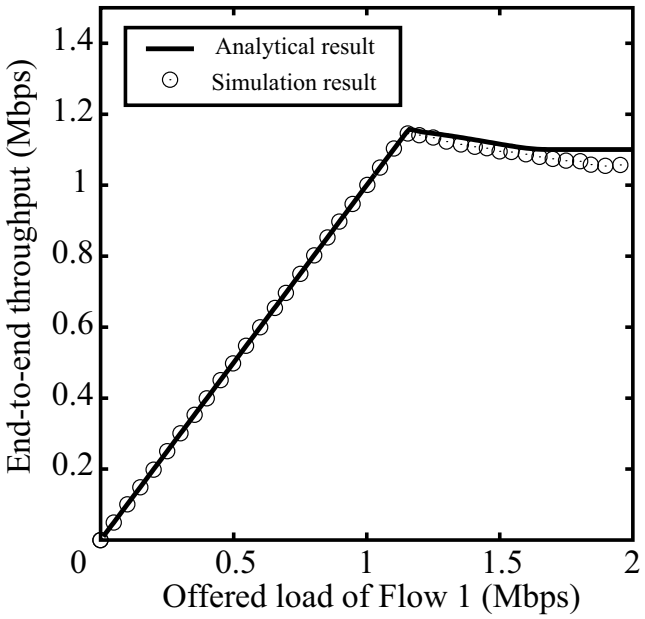

Figure 6.4: End-to-end throughputs of six-hop network with one-way flow versus offered load of Flow 1 for $O_2 = 0$ Mbps and $P = 200$ bytes.

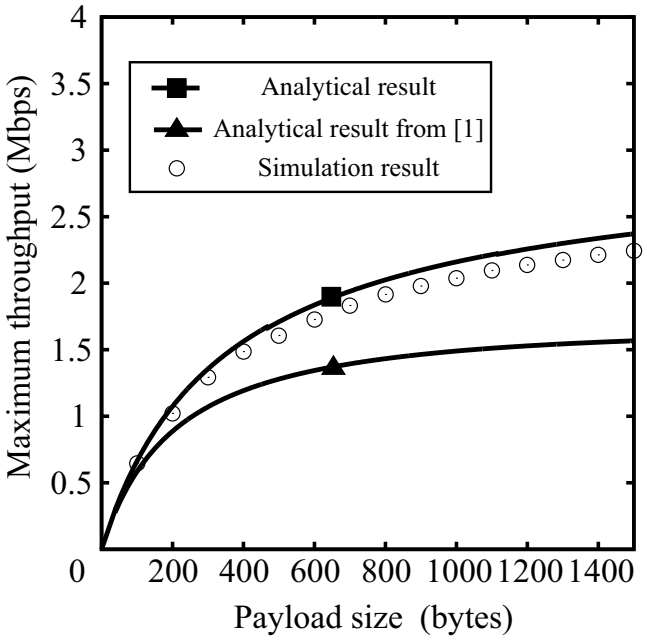

Figure 6.5: Maximum throughputs with one-way flow versus payload size for eight hop network.

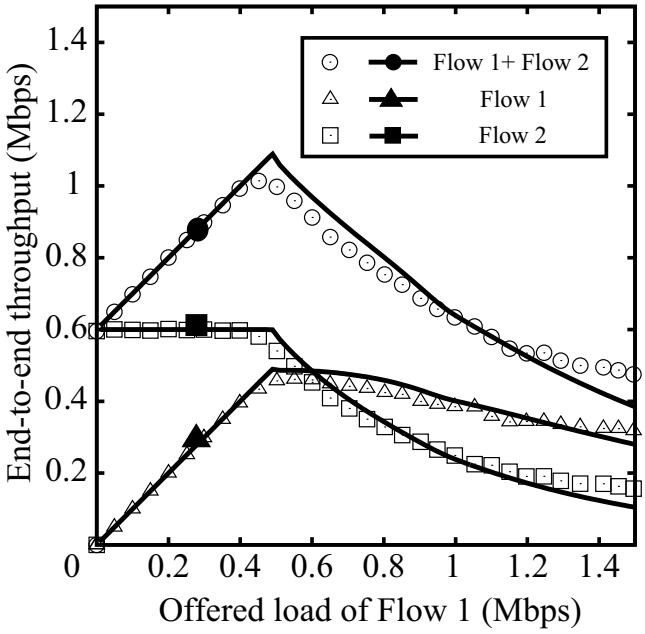

Figure 6.6: End-to-end throughputs of six-hop network with two-way flow as a function of offered load of Flow 1 for $O_2 = 0.8$ Mbps and $P = 200$ bytes.

[1] P. C. Ng and S. C. Liew, "Throughput analysis of IEEE 802.11 multi-hop ad hoc networks," *IEEE/ACM Transactions Networking*, vol. 15, no. 2, pp. 309-322, Apr. 2007.

[2] Y. Gao, D. Chui, and J. C. S. Lui, "The fundamental role of hop distance in IEEE 802.11 multi-hop ad-hoc networks," *IEEE International Conference on Network Protocol* , Boston, Massachusetts, USA, Nov. 2005.

[3] Y. Gao, D. Chui, and J. C. S. Lui, "Determining the end-to-end throughput capacity in multi-hop networks: methodology applications," in *Proc. SIGMETRICS/Performance* , New York, NY, USA, Jun. 2006, pp. 39–50.

[4] T. D. Senthilkumar, A. Krishnan, P. Kumar. "New approach for throughput analysis of IEEE 802.11 in adhoc networks".*IEEE International Conference on Control Communication and Automation*, Kanpur, India, pp. 148-153, Dec. 2008.

[5] H. Zhao, S. Wang, Y. Xi, Wei J, "Modeling intra-flow contention problem in wireless multi-hop networks", *IEEE Communications Letters* , vol. 14, no. 1, pp. 18-20, Jan. 2010.

[6] Zhao H, Garcia-Palacios E, Wang S, Wei J, Ma D. "Evaluating the impact of network density, hidden nodes and capture effect for throughput guarantee in multi-hop wireless networks". *Ad Hoc Networks,* vol. 11, no. 1, pp. 54-69. Jan. 2013.

[7] H. Sekiya, Y. Tsuchiya, N. Komuro, and S. Sakata, "Maximum throughput for long-frame communication in one-way string wireless multi-hop networks," *Wireless Personal Communications*, vol. 60, no. 1, pp. 29-41, Mar. 2011.

[8] M. Inaba, Y. Tsuchiya, H. Sekiya, S. Sakata, and K. Yagyu "Analysis and expression of maximum throughput analysis in wireless multi-hop networks for VoIP application," *IEICE Trans. on Communications.*, vol. E92-B, no. 11, pp. 3422–3431, Nov. 2009

[9] Y. Tsuchiya, M. Inaba, M. Matsumoto, H. Sekiya, S. Sakata and K. Yagyu, "Analysis of maximum UDP throughput of short-hop string networks for VoIP applications," in *Proc. IEEE WPMC*, Sendai, Japan, Sept. 2009.

[10] K. Sanada, N. Komuro and H. Sekiya. "End-to-end delay analysis for IEEE 802.11 string-topology multi-hop networks" . *IEICE Trans. on Communication,* vol. , no. , pp. . . 2015. (to be published)

[11] B. Bellalta, E. Belyaev, M. Jonsson, and A. Vinel, "Performance evaluation of IEEE 802.11p-enabled vehicular video surveillance system", *IEEE Communications Letters.*, vol. 18, no. 4, pp. 708-711, Apr. 2014.

[12] Lianghua Wu, Yuzhuo Fu, and Liang DongLianghua, "End-to-end throughput optimization in multi-hop wireless ad hoc networks", *the 15th Asia-Pacific Conference on Communication (APCC 2009)-010*, Shanghai, China, pp. 40-43, Oct. 2009.

[13] Wararkar, P, Dorle, S.S. "Vehicular adhoc networks handovers with metaheuristic algorithms", *Electronic Systems, Signal Processing and Computing Technologies (ICESC)*, 2014 International Conference on, pp. 160-165, Jan. 2014.

[14] G. Karagiannis, O. Altintas, E. Ekici, G. Hejenk, B. Jarupan, K. Line and T. Weil, "Vehicular networking: a survey and tutorial on requirements, architectures, challenges, standards and solutions",*IEEE trans.*, vol. 13, no. 4, pp. 584-615, Jul. 2011.

[15] A. Kumar, E. Altman, D. Miorandi, and M. Goyal,"New insights from a fixed point analysis of single cell IEEE 802.11 WLANs," *IEEE/ACM trans. Networking* , vol. 15, no. 3, pp. 538-601, Jun. 2007.

[16] Q.L. Zhao, D.H.K. Tsang, and T. Sakurai, "Modeling nonsaturated IEEE 802.11 DCF networks utilizing an arbitrary buffer size," *IEEE Trans. Mobile Computing*, vol. 10, no. 9, pp. 1248-1263, Nov. 2011.

[17] G. Bianchi,"Performance analysis of the IEEE 802.11 distributed coordination function," *IEEE J. Sel. Areas Commun*, vol. 18, no. 3, pp. 535-547, Mar. 2000.

[18] B. Jang and M. L. Sichitiu, "IEEE 802.11 saturation throughput analysis in the presence of hidden terminals", *IEEE/ACM Trans. Networking*, vol. 20, no. 2, pp. 557-570, April 2012.

[19] O. Ekici and A. Yongacoglu, "IEEE 802.11a throughput performance with hidden nodes", *IEEE Communications Letters*, vol. 12, no 6, pp. 465-467, June 2008

[20] F. Y. Hung, I. Marsic, "Performance analysis of the IEEE 802.11 DCF in the presence of the hidden stations" *Elsevier, Computer Networks*, vol 56, no 15, pp. 2674-2687, Oct. 2010.

[21] Y. Jae-Yong, and K. JongWon, "Maximum end-to-end throughput of chain-topology wireless multi-hop networks," in *Proc. IEEE WCNC*, Hong Kong, Mar. 2007, pp. 4279-4283.

[22] B. Shrestha, E. Hossain and S. Camorlings, "Hidden node collision mitigated CSMA/CA-based multihop wireless sensor networks," *Proc. IEEE ICC*, Budapest. Hungary, June. 2013, pp. 1570-1575.

[23] S. Parvin and T. Fujii, "A novel routing scheme with high sensitive sensing for multi hop wireless mesh network" *IEEE INCOS*, Thessaloniki. Macedonia, Nov. 2010, pp. 398-403

[24] F. Liu, Chuang Lin, Hao Wen, and Peter Ungsunan. "Throughput analysis of wireless multi-hop chain networks". in *Proc. IEEE/ACIS International Conference on Computer and Information Science*, Shanghai, China, Jun. 2009, pp. 834-839.

[25] E. Ghadimi, A. Khonsari, A. Diyanat, M. Farmani, and N. Yazdani, "An analytical model of delay in multi-hop wireless ad hoc networks". *Wireless Networks*, vol. 17, no. 7, pp. 1679-1697, Oct. 2011.

[26] F. Alizadeh-Shabdiz and S. Subramaniam, "Analytical models for single-Hop and multi-hop ad hoc networks", *Mobile Networks and Applications* vol. 11, no. 1, pp. 75-90, Feb. 2006.

[27] W. Jiao, M. Sheng, K. Lui, Y. Shi, "End-to-end delay distribution analysis for stochastic admission control in multi-hop wireless networks" *IEEE Trans. Wireless Communications*, vol. 13, pp. 1308-1320, Feb. 2014.

[28] K. Xu, M. Gerla, S. Bae, "How Effective is the IEEE 802.11 RTS/CTS handshake in ad hoc networks?", *IEEE, GLOBECOM*, Taipei, Taiwan, Nov. 2002, pp. 17–21, .

[29] IEEE Computer Society LAN MAN Standards Committee, *Part 11: Wireless LAN medium access control (MAC) and physical layer (PHY) specifications*, IEEE Std 802.11 - 1999, Aug. 1999.

[30] The network simulater - ns3, http://www.nsnam.org

Chapter 7

Overall Conclusion and Future Problems

7.1 Overall Conclusion

This thesis presents performance analysis for IEEE 802.11 string-topology multi-hop networks.

Chapter 2 has introduced analysis for IEEE 802.11 networks. The operation about IEEE 802.11 DCF is explained. As an analysis model for single-hop network, Bianchi's Markov-chain model is introduced. In addition, Hidden node problem in the multi-hop network is explained. As analytical procedure for multi-hop networks, airtime expression is introduced.

In Chapter 3, the occurrence of a special phenomenon in WMHNs is pointed out. This mutuality has been named as "backoff-stage synchronization". The mechanisms and the sufficient conditions for backoff-stage synchronizaion occurrence have been obtained from detail investigation. By using windows fairness index, the characteristic of this phenomenon, which is coexistence of fair transmission in long time range and unfair transmission in short time range, has been extracted. The impact of this phenomenon on communication in IEEE 802.11 multi-hop network has been discussed. By considering

the characteristics, the detection method of this phenomenon has been proposed.

In Chapter 4, analytical expressions for IEEE 802.11 multi-hop network with backoff-stage synchronization have been presented. For taking the features of the backoff-stage synchronization into account the analytical expressions, the modified Bianchi's Markov-chain models, which express the operation with respect to each network node, have been proposed. Obtained analytical expressions have been verified by the comparison with simulation and experimental results. By comparing the analytical result without the coupling effect, the occurrence of the coupling effect has been shown analytically.

In Chapter 5, analytical expression for end-to-end delay for IEEE 802.11 string-topology multi-hop networks has been presented. For obtaining those expressions with high accuracy, frame-collision and carrier-sensing probabilities with respect to each node under the non-saturated condition have been obtained. A new parameter, which is called as frame-existence probability, has been defined for expressing the operation in non-saturated condition. These expressions are associated as a network flow. The end-to-end delay of a string-topology multi-hop network can be derived as the sum of the transmission delays in the network flow. The validity of the analytical expressions have been shown by comparing with simulation results.

In Chapter 6, analytical expressions for IEEE 802.11 string-topology multi-hop networks have been presented. The analytical expressions are the enhanced version of the third proposed analytical model. The analytical expressions give throughput and end-to-end delay at any hop number, any frame length, and any offered load. For achieving that, the proposed analysis procedure includes two proposals for two problems, which are (i) analytical expressions in WMHNs until now are not valid for long frame communication such as video streaming, and (ii) there is no analytical expression, which is valid for asymmetric offered load in two-way flow situation. This analysis presents two proposals, which are: (i) a relationship between the backoff timer and frame length can be expressed

by merging the Bianchi's Markov-chain model and airtime expression, (ii) the Bianchi's Markov-chain models are modified for expressing the transmission process of two-way flows with asymmetric offered load individually. Obtained analytical expressions have been verified by the comparison with simulation results. Because it is possible to obtain the throughput and delay with not only symmetric but asymmetric two-way traffics, it is expected that the analytical expressions may be applied to maximum capacity derivation of VoIP, the TCP flow analysis, and more complicated network topology analyses.

These results enhance understanding for the essence of WMHNs. It is expected that the results in this thesis contribute to various applications, such as system optimization, network control and protocol design.

7.2 Future Problems

There are continuous research topics, which should be addressed in the future. The following topics are suggested for future works.

1. General analytical expressions for multi-hop network

In this thesis, the string-topology multi-hop network is considered. As mentioned before, the string-topology network is fundamental and important network topology. However, For achieving the analytical model with high generality, it is necessary to extend to analysis model without dependence on network topology. By applying graph theory, that may be obtained.

2. Analytical expressions for multi-hop network with TCP flow

This thesis focuses on multi-hop network with UDP flow. In this thesis, the properties of MAC with respect to each node were modeled in detail. These expressions were related by using the modeling of the property in Network layer. By using this approach, analysis model with high accuracy and versatility could be obtained. By modeling the property

of Transport layer based on the proposed approach, general analytical expressions for multi-hop network taking into account the TCP flow may be obtained.

I would like to keep carrying out researches and contribute to multi-hop network analysis.

List of Related Papers by The Author

Journal Papers

[1] Kosuke Sanada, Hiroo Sekiya, Nobuyoshi Komuro and Shiro Sakata "Backoff-stage synchronization in three-hop string-topology wireless networks with hidden nodes," *IEICE Nonlinear Theory and Its Applications,* vol. 3, no. 2, pp. 200–214, Apr. 2012.

[2] Ryo Manzoku, Hiroo Sekiya, Jing Ma, Kosuke and Shiro Sakata "A control-channel type multi-channel MAC protocol applying pulse/tone exchange in ad-hoc networks," *IEICE Transactions on Communications,* vol. J97-B, no. 4, pp. 344–353, Apr. 2014. (in Japanese)

[3] Kosuke Sanada, Jin Shi, Nobuyoshi Komuro and Hiroo Sekiya, "End-to-end delay analysis for IEEE 802.11 string-topology multi-hop networks," *IEICE Transactions on Communications,* vol. E98-B, no. 7, pp. 1284-1293, July. 2015.

[4] Yuta Shimoyamada, Kosuke Sanada, Nobuyoshi Komuro, and Hiroo Sekiya, "End-to-end throughput analysis for IEEE 802.11e EDCA string-topology wireless multi-hop networks," *IEICE Nonlinear Theory and Its Applications,* vol. E6-N, no. 3, pp. –, July. 2015 (to be published).

International Conferences

[1] Kosuke Sanada, Hiroo Sekiya, Nobuyoshi Komuroy and Shiro Sakata, "Coupling effect in IEEE 802.11 DCF wireless multi-hop networks," *2011 International Symposium on Nonlinear Theory and its Applications (NOLTA2011),* pp. 248–251, Sept 2011.

[2] Kosuke Sanada, Hiroo Sekiya, Nobuyoshi Komuroy and Shiro Sakata, "Analytical method of maximum UDP throughput for one-way wireless multi-Hop networks using markov chain model," *2012 International Workshop on Nonlinear Circuits, Communications and Signal Processing (NCSP2012),* pp. 125–128, Mar. 2012.

[3] Sho Motegi, Hiroo Sekiya, Jing Ma, Kosuke Sanada and Shiro Sakata, "A directional MAC protocol with the DATA-frame fragmentation and short busy advertisement signal for mitigating the directional hidden node problem," *2012 IEEE 23rd International Symposium on Personal, Indoor and Mobile Radio Communications (PIMRC2012),* pp. 409–414, Sept. 2012.

[4] Ryo Manzoku, Hiroo Sekiya, Jing Ma, Kosuke Sanada and Shiro Sakata, "An asynchronous multi-channel MAC protocol with Pulse/Tone exchange for RTS collision avoidance, " *1st IEEE International Symposium on Telecommunication Technologies (ISTT2012),* Nov. 2012.

[5] Yuta Shimoyamada, Kosuke Sanada, and Hiroo Sekiya, "Non-saturated and Saturated Throughput Analysis for IEEE 802.11e EDCA Multi-hop Networks, " *The 16th International Symposium on Wireless Personal Multimedia Communications (WPMC),* Apr. 2013.

[6] Kosuke Sanada, Hiroo Sekiya, Nobuyoshi Komuro, and Shiro Sakata, "Maximum throughput analysis for IEEE 802.11 string topology wireless multi-hop networks tak-

ing into account hidden nodes using Markov-chain model, " *2014 International Workshop on Nonlinear Circuits, Communications and Signal Processing (NCSP'14),* pp.77-80, Mar. 2014.

[7] Minh Huy Bui, Kosuse Sanada, Nobuyoshi Komuro, Shigeo Shioda, Shiro Sakata, Kazunori Miyoshi, Tutomu Murase, and Hiroo Sekiya, "Throughput analysis of wireless networks with Tethering function, " *2015 IEEE Wireless communications and networking conference (WCNC2015),* Mar. 2015.

[8] Kosuse Sanada, Nobuyoshi Komuro and Hiroo Sekiya, "End-to-end throughput analysis for IEEE 802.11 string-topology multi-hop networks with two-way flows, " *The 11th International Conference on Multimedia Information Technology and Applications (MITA2015),* June. 2015.

[9] Kosuse Sanada, Nobuyoshi Komuro and Hiroo Sekiya, "End-to-end throughput and delay analysis for IEEE 802.11 string topology multi-hop network using markov-chain model, " *The 2015 IEEE 25th International Symposium on Personal, Indoor and Mobile Radio Communications - (PIMRC),* Aug. 2015.

[10] Kosuse Sanada, Nobuyoshi Komuro and Hiroo Sekiya, "Throughput and delay analysis of IEEE802.11 string-topology multi-Hop networks, " *The 2015 International Symposium on Nonlinear Theory & its Applications (NOLTA 2015),* Dec. 2015.

Technical Reports and Other Presentations

[1] Kosuke Sanada, Hiroo Sekiya, Nobuyoshi Komuro and Shiro Sakata, "Coupling effect in IEEE 802.11 DCF wireless multi-hop networks," *IEICE Technical Report,* NS2011-111, no.8, pp.49–54, Apr. 2011. (in Japanese)

[2] Kosuke Sanada, Hiroo Sekiya, Nobuyoshi Komuro and Shiro Sakata, "Analysis for wireless ad-hoc networks with frame drop," *IEICE Technical Report,* NLP2011-106, no, 106, pp.35–40, June 2011. (in Japanese)

[3] Kosuke Sanada, Hiroo Sekiya, Nobuyoshi Komuro and Shiro Sakata, "Back-off stage synchronization in the wireless multi-hop networks and discussion," *IEICE Technical Committee on Complex Communication Sciences* vol. CCS2012-006, pp.29–35, Aug. 2012. . (in Japanese)

[4] Kosuke Sanada, Hiroo Sekiya, and Shiro Sakata, "Non-saturated and maximum throughput analysis for string topology wireless multi-hop networks " *IEICE Technical Report,* vol. 112, no. 350, NS2012-132, pp.91–95, Dec. 2012. (in Japanese)

[5] Ryo Manzoku, Hiroo Sekiya, Jing Ma, Kosuke Sanada, and Shiro Sakata "A multi-channel MAC protocol with pulse/tone exchange for RTS collision avoidance," *IEICE Technical Report,* vol. 112, no. 351, RCS2012-194, pp. 65–69, Dec. 2012. (in Japanese)

[6] Sho Manzoku, Hiroo Sekiya, Jing Ma, Kosuke Sanada, and Shiro Sakata, "A directional MAC protocol the DATA-frame fragmentation and short busy advertisement signal for mitigating the directional hidden node problem," *IEICE Technical Report,* vol. 112, no. 351, RCS2012-194, pp. 59–64, Dec. 2012. (in Japanese)

[7] Yuta Shimoyamada, Kosuke Sanada, Jin Shi and Hiroo Sekiya, "Non-saturated and saturated throughput analysis for IEEE 802.11e EDCA string topology wireless

multi-hop networks ," *IEICE Technical Report,* vol. 113, no. 129, NS2013-59, pp. 131–136, July. 2013. (in Japanese)

[8] Kosuke Sanada, Yuta Shimoyamada, Yuji Ikeda, Nobuyoshi Komuro and Hiroo Sekiya, "Generalized analytical expressions for throughput and transmission delay of IEEE 802.11 string topology networks," *IEICE Technical Report,* vol. 114, no. 163, NS2014-76, pp. 155–160, July. 2014. (in Japanese)

[9] Hire Sekiya and Kosuke Sanada "Throughput and delay analyses for wireless multi-hop networks,"
textitIEICE Technical Report, vol. 114, no. 418, ASN2014-151, pp. 225–229, Jan. 2015. (in Japanese)

[10] MinhHuy BUI, Kosuke Sanada, Nobuyoshi Komuro †, Shiro Sakata †, Shigeo Shioda, Kazunori Miyoshi, Tutomu Murase, and Hiroo Sekiya "Throughput analysis of wireless networks with tethering function,"
textitIEICE Technical Report, vol. 114, no. 418, ASN2014-152, pp. 231–236, Jan. 2015. (in Japanese)

[11] Tetsuro Okazawa, Nobuyoshi Komuro, Jing Ma, Kosuke Sanada, and Hiroo Sekiya "A MAC Protocol for mitigating exposed node problem in MIMO ad hoc networks,"
textitIEICE Technical Report, vol. 114, no. 480, ASN2014-156, pp. 1–6, Mar. 2015. (in Japanese)